**Cell Adhesion Molecules in Human Hair Follicle Morphogenesis**

by

**Elizabeth Danford Kaplan**

A dissertation submitted in partial fulfillment
of the requirements for the degree of

**Doctor of Philosophy**

**University of Washington**

**1996**

Approved by _____
(Chairperson of Supervisory Committee)

Program Authorized
to Offer Degree Biological Structure

Date June 28, 1996

**Doctoral Dissertation**

In presenting this dissertation in partial fulfillment of the requirements for the Doctoral degree at the University of Washington, I agree that the Library shall make its copies freely available for inspection. I further agree that extensive copying of this dissertation is allowable only for scholarly purposes, consistent with "fair use" as prescribed in the U.S. Copyright Law. Requests for copying or reproduction of this dissertation may be referred to University Microfilms, 1490 Eisenhower Place, P.O. Box 975, Ann Arbor, MI 48106, to whom the author has granted "the right to reproduce and sell (a) copies of the manuscript in microform and/or (b) printed copies of the manuscript made from microform."

Signature 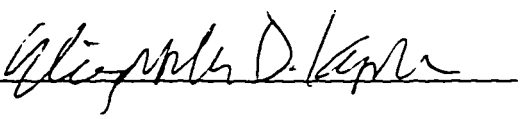

Date 6-23-96

University of Washington

Abstract

**Cell Adhesion Molecules in Human Hair Follicle Morphogenesis**

By Elizabeth Danford Kaplan

Chairperson of the Supervisory Committee: Professor Thomas A. Reh
Department of Biological Structure

Hair follicle formation in fetal development is characterized morphologically by invagination and elongation into the dermis of an epidermal cell collective in association with a follicle-specific population of mesenchymal cells. The process is thought to involve cell proliferation and migration, mediated by molecules such as NCAM and E-cadherin, which govern intercellular adhesion, and the extracellular matrix molecules tenascin-C (TN-C) and chondroitin sulfate proteoglycan, which affect cell-substrate adhesion. In research presented here, immunohistochemical analysis was used to examine their distribution patterns, along with those of the adhesion modulating molecules ICAM-1, alpha-2 beta-1 integrin, hyaluronan, versican and perlecan, in relation to human hair follicle morphogenesis. Alternative splicing of a central domain of TN-C has differential effects on cell adhesion and is associated with increased cell proliferation, so molecular probes were developed and used with isoform-specific antibodies for molecular and biochemical analyses of TN-C expression in relation to cell proliferation.

Initiation of hair follicle morphogenesis was distinguished by discrete placodes of a small TN-C isoform which lacked the alternatively spliced domain, and which were present at the dermal-epidermal interface. The alternatively spliced domain was detected later in follicle development, and was distributed in the follicle epithelium, basement membrane, and the extracellular matrix of the follicle-specific mesenchyme. Northern and Western blot analysis resolved three mRNA transcripts of 6, 7, and 8 kb in length, and three protein isoforms of approximately $220 \times 10^3$, $250 \times 10^3$ and $280\text{-}300 \times 10^3$ kD. These showed temporally distinct expression patterns, and initiation was marked by maximal levels of the 6 kb mRNA at the same time as TN-C transcript was detected by *in situ* hybridization in collections of epidermal cells. Mesenchymal cell expression was not detected until later stages of development.

Invagination was characterized by the transient presence of ICAM-1 on follicle epithelial cells, and by the overlapping distribution of TN-C, versican and hyaluronan in the basement membrane and follicle-associated mesenchyme, where cells were enriched in NCAM immunostaining. TN-C expression was associated with proliferation of epithelial and mesenchymal cells at the periphery of the developing appendage, while the core and base of the developing structure formed a non-proliferative zone. The distributions of versican and hyaluronan, although more widespread than that of TN-C, overlapped with TN-C in the proliferative region, and the three molecules were diminished or absent from the mitotically inactive regions. Preliminary observations included here suggest that TN-C and versican interact *in vitro* and may imparting a macromolecular organization to the follicle-specific extracellular matrix *in vivo*.

## TABLE OF CONTENTS

## LIST OF FIGURES

## LIST OF TABLES

## ACKNOWLEDGMENTS

I would like to acknowledge the assistance and support received from various sources, particularly to Drs. Tom Wight, Karen Holbrook, Tom Reh, John Clark and Sylvia Pollack, who collectively formed the supervisory committee which helped to guide my research. Dr. Karen Holbrook deserves enormous thanks for introducing me to the subject of hair follicle morphogenesis, and members of her past laboratory were extremely helpful at the start of this project. I am especially grateful to Bob Underwood, not only for fundamental education in all aspects of immunohistochemistry, but particularly for his patient training in photomicroscopy, and more recently, in digital imaging techniques. I would also like to acknowledge Dr. John Clark, for his long-standing confidence and support, and my sincere appreciation goes to Dr. Tom Reh, for good-naturedly shouldering the administrative duties of committee chairperson, and to Roger Williams in that laboratory, for his unending assistance in various matters.

I owe an enormous debt of gratitude to Dr. Tom Wight, my mentor for the past three years. His scientific insight and steady encouragement enabled me to complete this project while I developed a broader understanding of, and interest in, the importance of cell-matrix interactions in general. I am equally indebted to members of his laboratory, who fostered and encouraged the matrix biologist in me. I have no doubt that their friendly advice and helpful suggestions, invaluable up to now, will continue to guide me in the future.

Thanks are also due to the Department of Biological Structure for financial and material support, and to members of that department for valuable assistance at every stage of this program. Their individual interest in my project and my progress was always greatly appreciated. The Dermatology Training Grant and the Molecular and Cellular Biology Training Grant provided additional financial support, for which I am thankful. In addition, I owe a special thank-you to Julie Mason and Melissa Eisenhauer in the Human Embryology Laboratory, for their diligent collection of tissue specimens used in this research, and for their enormous co-operation in accommodating special requirements, without which some of the more difficult experiments could not have been completed.

I would also like to acknowledge the enormous support provided by extended family and friends, with special thanks to my in-laws, Joan and John Kaplan, who cheerfully traveled from Florida on a moment's notice, and without whose loving childcare, this dissertation would not have been written. Additional heartfelt thanks to Keely Bumsted, who was instrumental in the final stages of manuscript preparation.

With great love and gratitude, I dedicate this dissertation to my parents, Bill and Jean Danford, who instilled and nurtured in me a quest for knowledge, to my husband, John, who has tirelessly supported me and encouraged me in fulfilling that quest, and to our daughter Maria, who has been a wonderful inspiration to finish this project.

# CHAPTER I

# INTRODUCTION TO HAIR FOLLICLE MORPHOGENESIS

## *Overview*

The word morphogenesis is derived from the Greek words *morphe* (μορπηε), meaning form, and *genesis* (γενεσισ), meaning origin, and is defined as "the embryological development of the structure of an organism or part" (Morris, 1969). People have long been fascinated and entranced by the complicated processes and unknown mechanisms which conspire during development to generate the mature form or structure of a given organism, a form which allows the organism to function in its environment such that it can reproduce and thus preserve the genetic information it carries. In vertebrates, the histological structure of a number of organs, glandular tissues and epidermal derivatives arises from reciprocal interactions of adjacent epithelial and mesenchymal tissues during development, (reviewed in Thesleff et al., 1995). These epithelial-mesenchymal interactions contribute to the morphogenesis of hair follicles, teeth, mammary glands, nails and scales, and organs such as kidney, lung, and intestine, to identify just a few.

Hair follicles are specialized derivatives of the mammalian epidermis which produce keratinized hair fibers in a regionally specific manner, (reviewed in Sengel, 1976), contributing to the animal's vitality in a number of ways. Fibers from pelage follicles form the hair coat, or fur, which protects the animal, maintains thermal homeostasis, and aids in non-verbal communication important to mating and territorial dominance behavior. Follicles and hair fibers also relay information to and from the animal's surroundings by serving as conduits for neuroendocrine secretions from follicle-associated glands, and by transducing important spatial information about the external environment through highly specialized sensory follicles (e.g. vibrissae follicles).

## *Hair Follicle Morphogenesis*

The hair follicle, or pilosebaceous apparatus, is derived from and continuous with the epidermis, and like the epidermis, it is separated from the dermis by a basement membrane. The precise timing and molecular composition of events leading to follicle formation are unknown, but initiation of follicle morphogenesis is recognized

histologically and defined as the formation of a cluster of elongated epidermal cells (epidermal placode or follicle pre-germ) which displaces the basement membrane toward the adjacent dermis (illustrated in Figure 1.1a), (and reviewed in Holbrook et al., 1988; 1993). Recombination experiments pairing separated murine epidermal and dermal tissues from heterologous developmental ages and anatomical regions have demonstrated that, although these morphological changes are observed in the epidermis, they occur in response to an instructive signal (or signals) from the dermis (reviewed in Sengel, 1976 and Hardy, 1992). Recombination experiments have demonstrated further that this is not an inherent property of the dermis, but rather is induced early in skin histogenesis as a result of proximity to the primitive epidermis or surface ectoderm (reviewed by (Sengel, 1990)).

Follicle morphogenesis proceeds with invagination of the cluster of elongated epidermal cells into the dermis, forming the hair germ, while a collection of mesenchymal cells coalesces on the opposite side of the basement membrane, forming the mesenchymal or dermal condensation (Figure 1.1b). Tissue recombination studies have also suggested that the mesenchymal condensation, visible subsequent to follicle invagination, forms in response to a signal originating from the epidermal appendage. The developing follicle elongates deeper into the dermis (hair peg), maintaining a close association with the mesenchymal condensation at the distal terminus, while additional mesenchymal cells condense along its length (Figure 1.1c). Subsequent morphogenetic movements are marked by a widening of the follicle terminus into a bulbous shape (bulbous hair peg), and invagination of the follicle base toward the epidermis (differentiating hair follicle), such that the mesenchymal condensation is partially enclosed by the bulb of the follicle to form the dermal papilla (Figure 1.1d). The morphogenetic process is complete when production of a primary hair fiber and formation of follicle adnexae such as the sebaceous gland are observed (Figure 1.1e) (Holbrook et al., 1988). Although hair follicle morphogenesis has been well characterized histologically, the cellular and molecular mediators which comprise the developmental program, from induction, which is the modulation of dermal phenotype by the primitive epidermis, through initiation, invagination, elongation to differentiation of the functional appendage, are not at all understood.

***Characteristics of Differentiated Hair Follicles***

In adult skin, the fully differentiated follicle projects deep into the dermis of the skin and consists of several epithelial-derived cell layers arranged concentrically around the hair shaft. Cells positioned at the most distal portion of the follicle, where the invaginated follicle base surrounds the dermal papilla, differentiate under the influence of the dermal papilla to form the hair fiber, and the population is replenished by cell replication in the contiguous layer of the adjacent follicle wall (Sengel, 1976). Although the dermal papilla is topographically isolated, its base is continuous with a specialized compartment investing the dermal aspect of the follicle, the follicle sheath, formed from the mesenchymal cells which condensed during follicle elongation. This zone is composed of a fibrous extracellular matrix which is synthesized by the centripetally-oriented follicle sheath cells, and is biochemically distinct from that of the interstitial dermis (Messenger et al., 1991; Holbrook et al., 1993). Specialized regenerative properties unique to cells of the dermal papilla and the distal one-third of the follicle sheath have been demonstrated in the hooded rat, where these cells induce *de novo* follicle formation *in vivo* from normally hairless epidermis (Oliver, 1967; Oliver, 1968; Kollar, 1970; Jahoda et al., 1984).

Hair follicles in the adult animal cycle between a hair fiber-producing phase (anagen) and a quiescent resting phase (telogen). The morphology of the telogen follicle is radically different from that of the anagen follicle, with the follicle epithelium retracted toward the epidermal surface such that the follicle bulb is eliminated and the dermal papilla is exposed. Despite its displacement toward the epidermis in conjunction with the follicle base, the cohesion of the dermal papilla is largely maintained in telogen. Re-entry into anagen is triggered by the dermal papilla, and is characterized by the joint downward migration of the papilla and follicle base, and the restoration of their histologic relationships in a process reminiscent of follicle morphogenesis (reviewed in Sengel, 1976). Thus, the controlled development and periodic resumption of follicle function involves not only the precisely coordinated movements of two distinct cell populations, but depends upon their dynamic interplay as well. The over-arching question, then, is how is this accomplished?

***Background***

Replication and migration are primary cellular processes which are essential for vertebrate development. An abundant literature surrounding feather follicle morphogenesis reflects the extent to which these processes have been examined in

developing avian skin, while relatively little is known about their respective contributions to appendage morphogenesis in mammalian skin, (reviewed in Sengel, 1976). A seminal study by Wessells and Roessner (1965), examining cell proliferation in fetal mouse skin, revealed mitotic activity in the follicle epithelium, and not in the mesenchymal condensation. Based on these observations, the authors proposed that follicle elongation is driven by cell proliferation, while formation and growth of the mesenchymal condensation results from migration of cells from the interstitial dermis (Wessells and Roessner, 1965). Moreover, formation of the epidermal placode is marked by a dramatic change in cell morphology, and does not appear to involve cell proliferation (Wessells and Roessner, 1965), suggesting that yet another mechanism is involved in morphogenetic intitiation. Thus, factors affecting cell proliferation, migration or morphology are likely to be important in hair follicle morphogenesis.

Molecules in the extracellular environment, whether integrated into the extracellular matrix, embedded in the membrane of a neighboring cell, or diffusing freely in the extracellular space, potentially affect the processes of migration and proliferation by binding to specific membrane-associated molecules on the cell surface. Transmembrane proteins with ligands in the extracellular matrix, such as the integrin family of receptors, are referred to as substrate adhesion molecules, and mediate cell attachment to the extracellular matrix (Hynes, 1987; Hynes, 1992). These molecules, and their respective binding partners, are important regulators of cell shape, migration and proliferation . Transmembrane proteins which bind surface molecules on adjacent cells are classified as cell adhesion molecules, an example of which is the neural cell adhesion molecule, NCAM (reviewed in Edelman, 1984). By mediating cell-cell interactions, cell adhesion molecules contribute to the segregation of cells into tissue-specific populations during development (reviewed in Edelman, 1984). Cell and surface adhesion molecules, then, because of their ability to affect cell morphology and cell activity, may be candidates for mediating the process of hair follicle morphogenesis.

The overall objective of the research presented here was to select morphogenetically relevant cell and substrate adhesion molecules and examine their expression patterns in relation to hair follicles developing in fetal human skin. Over the next several chapters, these molecules will be introduced, analyzed and discussed, and specific molecules which may be involved in the developmental process of human hair follicle morphogenesis will be identified.

**Figure 1.1** **Morphogenetic stages of hair follicle development in fetal human skin (drawn by K. A. Holbrook).**

A) **Initiation** of hair follicles between 10 and 11 weeks EGA in trunk skin, is recognized by clusters of basal epidermal cells which elongate and invaginate into the dermis forming the follicle **pre-germ**. Mesenchymally-derived dermal cells accumulate on the opposite side of the basement membrane, forming the mesenchymal or dermal condensation.
B) Follicle **invagination** into the dermis continues, and the follicle **hair germ** is identified between 11 and 12 weeks EGA. This is closely associated with the mesenchymal condensation.
C) **Elongation** of the hair germ between 12 and 14 weeks EGA generates a solid cord of epidermally-derived cells, termed the follicle **hair peg**. The developing follicle is polarized in orientation and elongates at an angle relative to the plane of the epidermis such that the acute angle formed with the epidermis is defined as the anterior aspect of the follicle. The mesenchymal condensation (not drawn in full) is associated with the distal tip of the appendage, and mesenchymal cells condense along the follicle length as well, forming the mesenchymal or follicle sheath.
D) **Differentiation** of the follicle hair peg into the **bulbous hair peg** is marked by a widening of the distal terminus to form the follicle bulb, flattening and then invagination of the follicle base toward the epidermis, formation of sebaceous gland primordia on the posterior aspect of the follicle and the formation of the hair canal (open space traversing epidermis), and occurs between approximately 15 and 18 weeks EGA.
E) Completion of morphogenesis, after 18 to 20 weeks EGA in trunk skin, is characterized by the formation of the dermal papilla (enclosed by the follicle bulb), and hair fiber production in the lanugo follicle of fetal human skin.

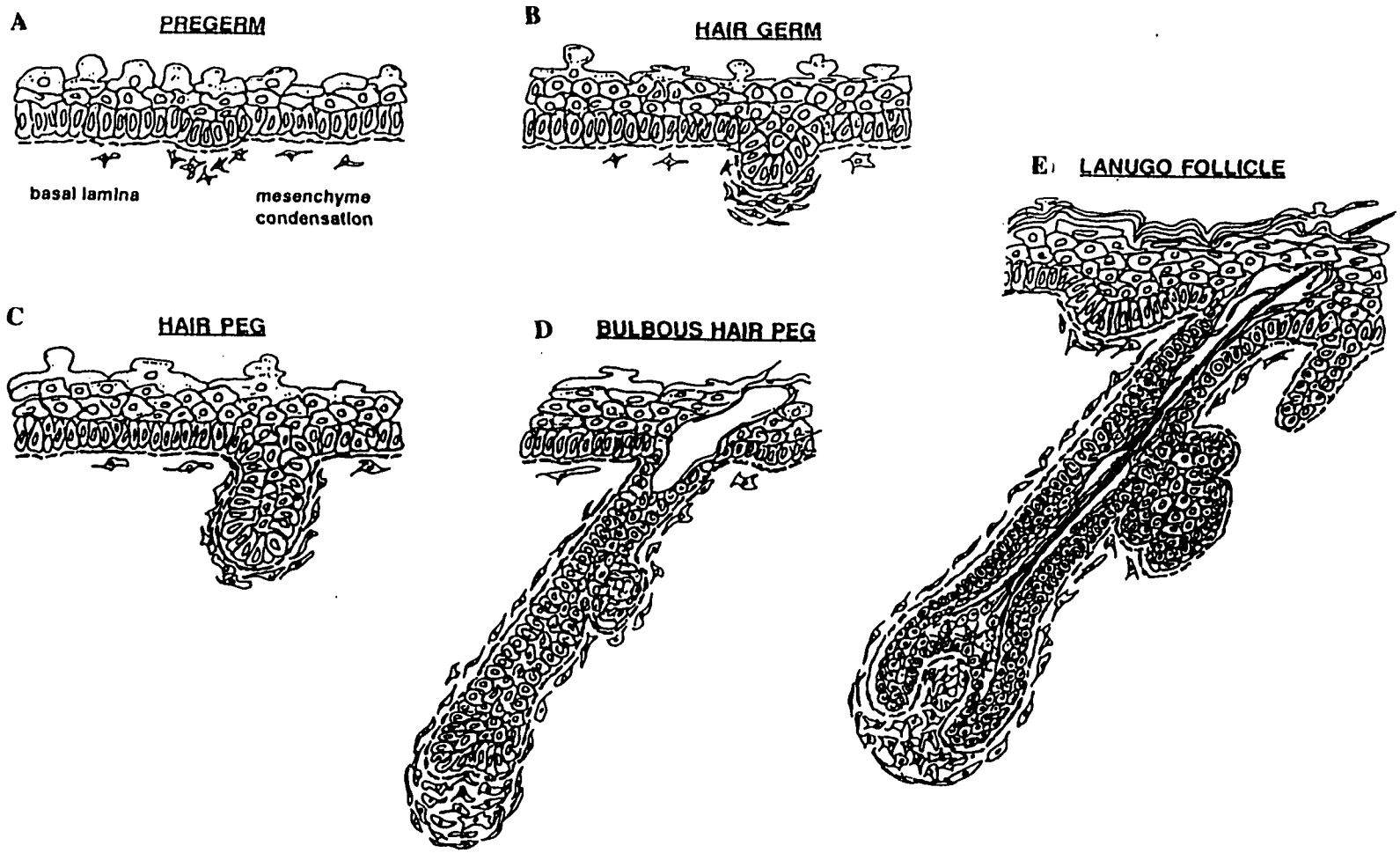
A
PREGERM
basal lamina
mesenchyme condensation
B
HAIR GERM
C
HAIR PEG
D
BULBOUS HAIR PEG
E
LANUGO FOLLICLE

(K. A. Holbrook)

## CHAPTER II

# DYNAMIC EXPRESSION PATTERNS OF TENASCIN-C, PROTEOGLYCANS AND CELL ADHESION MOLECULES DURING HUMAN HAIR FOLLICLE MORPHOGENESIS

Published in: *Developmental Dynamics* (1994) 190: 141-155

## INTRODUCTION

During embryonic development, the histogenesis of many organs depends upon cellular interactions within and between epithelial and mesenchymal tissues. Both tissues are essential for the morphogenesis and patterning of specialized derivatives of the vertebrate skin, such as hair, feathers, nails, scales, mammary and sweat glands (reviewed in Sengel, 1983). The embryonic epidermis and underlying mesenchyme exchange signals resulting in clusters of elongated basal epidermal cells, the follicle pre-germs, opposite which mesenchymal cells aggregate to form dermal condensations (reviewed in Holbrook et al., 1993). Epidermal and mesenchymal components presumably continue to interact, maintaining a close association during subsequent morphogenetic stages of hair follicle development. This mutual influence is thought to be mediated, in part, by cell adhesion molecules (CAMs) and extracellular matrix (ECM) molecules which facilitate cell-cell and cell-substrate interactions.

The calcium-dependent cell adhesion molecule E-cadherin (also known as uvomorulin, Cell-CAM 120/80, LCAM) and the calcium-independent neural cell adhesion molecule (NCAM) mediate intercellular adhesion through homotypic binding. Both show developmentally-specific localization during murine hair morphogenesis and chick feather and scale formation, and their roles in appendage formation are inferred from *in vitro* perturbation experiments (Chuong and Edelman, 1985; Gallin et al., 1986; Hirai et al., 1989; Chuong and Chen, 1991; Shames et al., 1991; Jiang and Chuong, 1992).

Tenascin-C (TN-C), also known as hexabrachion, brachionectin, cytotactin, myotendinous antigen or glioma mesenchymal extracellular matrix antigen (GMEM) is a hexameric glycoprotein which is present in the extracellular matrixextracellular matrix. It is expressed at the epithelial-mesenchymal interface during the histogenesis of many organs, and, based on *in vitro* studies, it is presumed to influence cell-substrate

interactions (reviewed in Erickson and Bourdon, 1989; Chiquet-Ehrismann, 1990; Chuong, 1990). TN-C expression has been examined in the morphogenesis of mouse hair follicles and avian feathers and scales (Chuong and Chen, 1991; Shames et al., 1991; Jiang and Chuong, 1992). Cell-substrate interactions also may be affected by proteoglycans in the extracellular milieu and on cell surfaces of interacting epithelial and mesenchymal cells (reviewed in Goetinck, 1991). Heparan sulfate proteoglycan (HSPG) is reported to co-purify with NCAM and bind NCAM *in vitro* (Cole and Glaser, 1986; Cole and Burg, 1989). Chondroitin sulfate proteoglycan (CSPG) is uniquely associated with the basement membrane of developing rat hair follicles (Couchman et al., 1990) and inhibition of glycosaminoglycan synthesis disrupted feather follicle patterning in embryonic chick skin (Goetinck and Carlone, 1988). CSPG also co-distributes with TN-C *in vivo* and binds TN-C *in vitro* (Chiquet and Fambrough, 1984; Hoffman et al., 1988).

Cumulative evidence from many studies of developmental systems has led to the proposal that epidermal appendage morphogenesis is mediated in part by these CAMs and ECM molecules. Nevertheless, their developmental distributions relative to the histogenesis of a single type of epidermal appendage has not been characterized. Thus, the goal of the present study was to systematically evaluate by immunochemistry, the spatial and temporal distribution of NCAM, TN-C, E-cadherin, CSPG and the large HSPG, perlecan, during the morphogenesis of hair follicles. The cell adhesion molecule ICAM-1 (CD-54) was included as a non-specific CAM, presumably not involved in hair follicle morphogenesis. Post-translational modification of NCAM with polysialic acid (PSA), and alternative RNA splicing of NCAM and TN-C have been demonstrated to generate tissue-specific, developmentally-regulated forms of these two molecules (reviewed in Cunningham et al., 1987 (NCAM), and Erickson and Bourdon, 1989 (TN-C)) which are thought to differentially affect cell adhesion. This study was extended to investigate the isoforms of TN-C and NCAM present in fetal human skin.

## EXPERIMENTAL PROCEDURES

*Tissue sources*

93 specimens of human embryonic and fetal trunk or thigh skin, ranging in age from 6 to 22 weeks estimated gestational age (EGA), were obtained from the Central Laboratory for Human Embryology at the University of Washington through the courtesy of Drs. Thomas Shepard and Alan Fantel, and in accord with University of Washington

Institutional Review Board and DHEW policies. EGA was determined from maternal histories, fetal measurements (crown rump and foot length) (Shepard, 1975; Mercer et al., 1987), and comparative histological appearance of epidermis (Holbrook, 1979). A minimum of two specimens per EGA was evaluated. Normal human adult skin was obtained from the upper arm of volunteers using a 2 mm biopsy punch.

*Tissue processing*

Tissue samples for cryosectioning were oriented in OCT-TissueTek (Miles Inc., Elkhart, IN) and frozen in a bath of ethanol/solid carbon dioxide. Some samples were separated into epidermal and dermal components by agitating skin pieces (4 $mm^2$) in 2M NaBr at 37°C for 30-60 minutes (Banks-Schlegel, 1982). Samples were transferred to cold phosphate buffered saline (PBS), pH 7.4, and separated into epidermal and dermal components using forceps. Separated tissues were either frozen for cryosectioning or extracted for gel electrophoresis and subsequent immunoblotting. For immunodetection of TN-C, intact or separated tissue samples were homogenized on ice (Aufderheide and Ekblom, 1988), using a 2.5-fold excess (volume : wet weight of tissue) of 3-[cyclohexylamino]-1-propane sulfonic acid (CAPS) buffer (pH 11.0) containing 0.02% aprotinin. After centrifugation (20 minutes at 20°C), supernatants were neutralized with $NaH_2PO_4$ and stored at -20°C until use. For NCAM analysis, samples were homogenized in 5-fold excess lysis buffer (50 mM Tris (pH 8.0), 150 mM NaCl, 0.02% sodium azide, 0.01% nonidet-P-40, 0.58 mM phenylmethylsulfonyl fluoride (PMSF) and 0.1% aprotinin), and centrifuged as described above. Supernatants were stored at -20°C until use.

*Antibodies and reagents*

Monoclonal antibodies (Mabs) were the generous gifts of the investigators indicated, or were purchased: F9A5 against TN-C (W. Carter, Fred Hutchinson Cancer Research Center, Seattle, WA); NKI-nb1-1 against NCAM (BioDesign, Inc., Kennebunkport, ME; (Moolenaar et al., 1990)); 5B8 against NCAM (from the Developmental Studies Hybridoma Bank, maintained by the Department of Pharmacology and Molecular Sciences, Johns Hopkins University School of Medicine, Baltimore, MD, and the Department of Biological Sciences, University of Iowa, Iowa City, IA, under contract N01-HD-6-2915 from the NICHD); E9 against E-cadherin (C. Damsky, University of California, San Francisco, CA; (Wheelock et al., 1987)); 3B3 and 2B6 against antibodies against chondroitin sulfate (ICN Biomedicals, Costa Mesa, CA;

(Couchman et al., 1984)); 938 against CSPG (T. Wight, University of Washington, Seattle, WA; (Lark et al., 1988; Yeo et al., 1992)); C11L1 against perlecan (J. Couchman, University of Alabama, Birmingham, AL; (Couchman and Ljubimov, 1989)); LB-2 against ICAM-1, and 60.3 against the β-subunit of LFA-1 (E. Clark, University of Washington, Seattle, WA; (Clark et al., 1986; Prieto et al., 1988)). The epitopes for the so-called "stub" antibodies (3B3 and 2B6) were revealed by treatment of tissue with chondroitinase ABC, which digests chondroitin sulfate glycosaminoglycan. Mab 3B3 is mono-specific for the terminal disaccharide containing a uronic acid residue linked to N-acetylgalactosamine sulfated on the sixth carbon, while Mab 2B6 is specific for the terminal disaccharide containing a uronic or iduronic acid residue linked to N-acetylgalactosamine with a sulfate in the fourth position (for review and discussion, see Caterson et al., 1987). Mab 938 identified intact CS-GAG chains which contain a higher proportion of 6-sulfated to 4-sulfated disaccharides (Lark et al., 1988; Yeo et al., 1992). Chondroitinase digestion of tissue sections eradicated the 938 epitope. The antigens are referred to as 3B3-CSPG, 2B6-CSPG and 938-CSPG, respectively, although it should be noted that these epitopes may be found on more than one protein core. Mab LB-2 was used to detect ICAM-1; two additional Mabs to ICAM-1 were used to confirm LB-2 immunostaining. Because Mab NKI-nb1-1 did not recognize NCAM in Western blot analysis, the hybridoma supernatant 5B8 was obtained from the Developmental Studies Hybridoma Bank for use in immunoblotting and for immunohistochemical staining for NCAM.

Biotinylated, species-specific secondary antibodies were obtained from Vector (Burlingame, CA); horseradish peroxidase (HRP)-conjugated strept-avidin was purchased from Zymed (San Francisco, CA); and bovine serum albumin (BSA), aprotinin, Tween-20, NP-40, purified chondroitin ABC lyase and neuraminidase (*C. perfringens*, Type X) were purchased from Sigma Chemical Co. (St. Louis, MO). Purified TN-C and human serum (Type AB) were purchased from Gibco BRL (Grand Island, NY).

*Immunohistochemistry*

Cryosections of 6-8 μm thickness were dried overnight (4°C) on silane coated slides prior to immunodetection using the avidin-biotin-peroxidase complex (ABC) technique (Hsu et al., 1981). Sections were rinsed in PBS, fixed for 5 minutes (0°C) in either 100% ethanol, 100% methanol, 0.1% glutaraldehyde or 100% acetone, and rinsed in Tris-buffered saline (TBS) (pH 7.6). Endogenous peroxidase activity was blocked with 0.3% hydrogen peroxide (30 minutes), and non-specific binding was blocked with a

solution of 1.3% horse serum and 0.3% goat serum (30 minutes). Primary antibodies were applied for 1 hour, followed by 3 rinses in TBS (5 minutes each), serum block (5 minutes), and incubation with the appropriate secondary antibody (30 minutes). After TBS rinses and serum block (as above), HRP-conjugated strept-avidin was applied to the sections (30 minutes). All dilutions were performed in 1% BSA in TBS. The antibody complex was visualized with 3,3-diaminobenzidine (DAB) (Nanney et al., 1990). Sections were fixed for 10 min. in 2% glutaraldehyde, and either coverslipped directly or counterstained with Meyer's hematoxylin prior to coverslipping. To control for labeling specificity, duplicate tissue sections were processed for each antibody and each specimen. To control for non-specific secondary-antibody binding, primary antibody was omitted from a third section which was processed simultaneously. Sections to be immunolabeled with Mabs 3B3 or 2B6 were treated with chondroitin ABC lyase (0.1 U/μl in 0.1 M Tris-acetate buffer, pH 8.0; 30 minutes, 37°C) to reveal the antigenic epitopes. Sections which were not enzymatically treated had no immunostaining and served as negative controls. In the case of Mab 938, chondroitinase treatment of sections provided a negative control because the epitope was eliminated by enzymatic digestion. Slides were viewed and photographed with a Zeiss standard photomicroscope equipped with panapochromatic lenses.

*Sodium Dodecyl Sulfate-Polyacrylamide Gel Electrophoresis (SDS-PAGE)*

Tissue extracts were mixed with sample loading buffer (containing 2% SDS and 5% β-mercaptoethanol), boiled (3-5 minutes) and subjected to SDS-PAGE (Laemmli, 1970) on 0.75 mm thick 7.5% acrylamide gels using a Mini Protean gel system (Bio-Rad, Hercules, CA). A constant loading volume of 35 μl per sample was used for skin extracts. Pre-stained Rainbow High Molecular Weight Standards (Amersham, Oak Brook, IL), Kaleidoscope Molecular Weight Standards (Bio-Rad, Hercules, CA) and purified bovine fibronectin (Sigma, St. Louis, MO) were used as standards for relative mobility. Gels not intended for blotting were stained with Coomassie Blue to compare sample loading. For blotting purposes, proteins separated by SDS-PAGE were transferred to nitrocellulose membranes (Towbin et al., 1979) using a semi-dry blotting apparatus (75 minutes at 10 V), or a tank transfer cell (60 minutes at 100 V) (Bio Rad, Hercules, CA). The blots were then air-dried and stored at 20°C. Blotted gels were stained with Coomassie Blue to verify transfer efficiency.

*Immunoblot analysis*

Blots were processed using the enhanced chemiluminescence detection (Amersham, Oak Brook, IL) with the following modifications: blots were first incubated in 0.3% hydrogen peroxide in TBS (90 minutes), and washed (10 minutes in 0.2% Tween-20 in TBS) before incubating (1 hour) with either 0.5% BSA + 0.2% Tween-20 + 1% PVP in TBS (TN-C immunodetection), or low-fat milk (1% milk fat) (NCAM immunodetection) as blocking solutions. For TN-C immunodetection, primary antibody and strept-avidin HRP were each diluted in 0.5% BSA + 0.2 % Tween-20, and the secondary antibody was pre-adsorbed in human serum (60 minutes at 4°C); for NCAM immunodetection, dilutions were in 1% BSA + 0.1% Tween-20; incubation with primary antibody (1 hour), secondary antibody (30 minutes), and strept-avidin-HRP (30 minutes) was followed by chemiluminescent development and exposure to X-OMAT XAR-5 X-ray film (Eastman Kodak, Rochester, NY) (5-25 minutes, 20°C). A graph of distance migrated vs. log ($M_r$) of protein standards was used to calculate relative mobilities of labeled bands. For some experiments, Mab F9A5 (diluted 1:100) was pre-adsorbed with 10 nmol purified TN-C for 16 hours at 4°C and centrifuged for 15 minutes before use.

## EXPERIMENTAL RESULTS

### *Immunohistochemical analysis*

Hair follicle morphogenesis is a continuous process that has been divided into five morphological stages. The distributions of TN-C, CSPGs, perlecan, NCAM, E-cadherin and ICAM-1 are described for each stage and are summarized in Table 2.1.

### *Pre-follicle environment (8-9 weeks EGA)*

Prior to the initiation of follicle development, the epidermis is organized into basal, intermediate and periderm cell layers. The underlying dermis is composed of mesenchymal cells organized in a loose matrix containing blood vessels and nerve elements. Tenascin-C was absent from the skin at 9 weeks EGA (Figure 2.1A) although it was detected immunohistochemically in myotendinous regions of limbs from the same specimens (data not shown). The 938-CSPG (Figure 2.1B) was prevalent in the dermis, the basement membrane zone (BMZ) at the dermal-epidermal junction (DEJ) and outlining the borders of suprabasal epidermal cells. Perlecan (Figure 2.1C) was detected in all skin basement membranes, with weak immunostaining of the compact mesenchyme subjacent to the DEJ. Both 3B3-CSPG and 2B6-CSPG were diffusely associated with the DEJ (not

shown). The 3B3-CSPG immunostaining extended from the DEJ through the compact mesenchyme, as has been reported previously (Fine and Couchman, 1988).

NCAM immunolabeling was present throughout the dermis and was enhanced on cells of the compact mesenchyme (Figure 2.1D). It was absent from the epidermis. E-cadherin immunostaining (Figure 2.1E) was present on all borders of intermediate cells of the epidermis. E-cadherin immunolabeling of basal cells was weak or absent, and E-cadherin was not detected on dermal cells. ICAM-1 immunoreactivity was associated with dermal vessels and inconsistently with the amniotic surfaces of periderm cells (data not shown). No immunostaining was observed on any sections which were reacted with the anti-mouse secondary antibody only, a representative micrograph of which is shown in Figure 2.1F.

***Follicle initiation: the pre-germ (10-11 weeks EGA)***

Tenascin-C immunoreactivity in skin was visible initially as focal deposits on the mesenchymal side of the DEJ (Figure 2.2A). Concentrated immunostaining was detected in trunk skin of approximately 10 weeks EGA, prior to morphologic signs of follicle formation. In other regions of the body (e.g. thigh skin), preliminary data indicated that at a similar developmental age, TN-C was expressed first as a continuous band at the DEJ, becoming restricted focally (data not shown) in the manner noted for trunk skin. In both regions, follicle pre-germs developed subsequently at sites where TN-C was intensely immunopositive (Figure 2.2B). The expression patterns of 3B3-, 2B6-, 938-CSPG, perlecan, NCAM (Figure 2.2C), E-cadherin or ICAM-1 were unchanged from the previous stage.

***Follicle invagination: the hair germ (11-12 weeks EGA)***

TN-C immunolabeling remained intense at the BMZ underlying hair germs in trunk and thigh skin at 11 weeks EGA (Figure 2.3A), but immunoreactivity decreased in the interfollicular regions. The extracellular matrix surrounding mesenchymal cells associated with the hair germ was also strongly immunopositive for TN-C. Weak TN-C immunostaining was detected on keratinocytes in the core of the hair germ and on the apical surfaces of outer layer follicle epithelial cells. Immunolabeling for 3B3-CSPG (Figure 2.3B) and 938-CSPG (data not shown) was accentuated in the follicular BMZ and diminished in the interfollicular BMZ, similar in pattern to TN-C. Basal epidermal cells

were inconsistently immunopositive for 3B3-CSPG. No 3B3-CSPG immunostaining was observed in the absence of chondroitinase treatment (Figure 2.3C).

Hair germ formation was accompanied by a re-distribution in the expression patterns of NCAM, E-cadherin, and by the onset of ICAM-1 expression by specific populations of epithelial cells. NCAM immunolabeling (Figure 2.3D) was strong on cells of the dermal condensation, and weaker in the interfollicular dermis. Hair germ cells were weakly E-cadherin immunopositive (Figure 2.3E), in contrast to strong immunolabeling associated with cells of the suprabasal epidermal layers. ICAM-1 expression was detected transiently on outer cells of the germ (Figure 2.3F) and on amniotic surfaces of periderm cells; the characteristic distribution of ICAM-1 on endothelial cells of the dermal microvasculature was retained (data not shown). Two additional antibodies recognizing different epitopes of ICAM-1 also immunolocalized to hair germ cells, confirming the identity and specificity of antigen in the hair germ (results not shown). This unexpected finding prompted an examination of the distribution of the $\beta_2$-integrin, LFA-1 (also known as $\alpha_L\beta_2$ or CD11a/CD18), which is a counter-receptor for ICAM-1 (Makgoba et al., 1988). Single cells which were LFA-1 immunopositive were distributed in the dermis and occasionally in the epidermis, however, they were not evident at the site of the ICAM-1 staining in hair germs (data not shown).

***Follicle elongation: the hair peg (12-15 weeks EGA)***

The BMZ of the hair peg was strongly immunopositive for TN-C at 14 weeks EGA (Figure 4A), while immunolabeling of the interfollicular BMZ was weak. TN-C was situated on the dermal side of the BMZ, as determined from immunolabeling of separated epidermis and dermis (data not shown), and was distributed asymmetrically, with staining on the anterior aspect of the hair peg extending farther into the interfollicular dermis than on the posterior side. A proximal-distal gradient of TN-C was evident in the follicle sheath, with strong immunolabeling near the epidermis and very little TN-C immunoreactivity associated with the dermal condensation (Figure 2.4A). Immunostaining for 938-CSPG (Figure 2.4B) and 3B3-CSPG (Figure 2.4C) delineated the BMZ of the hair peg, in contrast to that of interfollicular regions; the follicle sheath was strongly immunoreactive for both markers (Figure 2.4B,C). The BMZs of the hair peg and interfollicular regions were weakly positive for 2B6-CSPG (Figure 2.4D); the follicle sheath and the dermal papilla failed to react with the antibody, but the dermis was weakly

immunopositive and contained strongly labeled vasculature (Figure 2.4D). Epithelial cells in the interior of the hair peg were moderately immunoreactive for TN-C and 938-CSPG (Figure 2.4A, B).

A gradient of NCAM immunostaining was present at 14 weeks EGA. Cells of the dermal condensation were intensely immunopositive, but immunolabeling of follicle sheath cells diminished toward the epidermis (using Mab NKI-nb1-1); this pattern was reciprocal to the TN-C gradient (compare Figure 2.4E, A). NCAM immunostaining was cell-surface associated, as determined by immuno-electron microscopy (data not shown). Immunolabeling with a different NCAM antibody (5B8), recognizing the cytoplasmic portion of the cell adhesion molecule, identified cells of the dermal condensation only (Figure 2.4F), while follicle sheath cells were not labeled. E-cadherin immunoreactivity (Figure 2.4G) within the hair peg was strongest on the central cord of cells, derived from the intermediate layer of the epidermis (also strongly reactive for E-cadherin). The follicle cells adjacent to the BMZ were moderately immunopositive for E-cadherin, except at the terminus of the hair peg, where the cells were very weakly labeled. Cells of the hair peg no longer expressed ICAM-1, although periderm and endothelial cells remained immunopositive (Figure 2.4H).

***Follicle differentiation: the bulbous hair peg (15-18 weeks EGA)***

At approximately 15 weeks EGA, the hair peg begins to differentiate. The dermal condensation is partially enclosed by the widened follicle base, forming the dermal papilla and the hair bulb, respectively. Tenascin-C (Figure 2.5A), 938-CSPG (Figure 2.5B) and 3B3-CSPG (not shown) immunolocalized to the follicle BMZ and were diminished in interfollicular regions, as noted previously. Tenascin-C and 3B3-CSPG co-localized in the follicle sheath extracellular matrix, but the dermal papilla showed differential distributions of these molecules. The cells were immunopositive for TN-C and immunonegative for 3B3-CSPG (data not shown). The TN-C antibody no longer labeled follicle epithelial cells. Weak 938-CSPG immunostaining was associated with all cells of the follicle epithelium, except the presumptive hair matrix cells opposite the dermal condensation (Figure 2.5B). Immunoreactivity for 2B6-CSPG (Figure 2.5C) was weakly associated with the BMZ of the bulbous hair peg and the interfollicular BMZ. The 2B6-CSPG remained absent from the follicle sheath but strongly present in the interfollicular dermis and vasculature. Perlecan immunostaining (Figure 2.5D) was intense in all basement

membranes of skin and in the center of the dermal papilla. It was weakly present in the extracellular matrix of the follicle sheath. The distribution of cell adhesion molecules was similar to that seen at earlier developmental stages. The proximal-distal NCAM gradient persisted with intense NCAM immunolabeling of follicle sheath cells and dermal papilla cells, as detected by Mab NKI-nb1-1 (Figure 2.5E). Cells of the dermal papilla were immunopositive for hybridoma supernatant 5B8, as were follicle sheath cells (Figure 2.5F), in contrast to the distribution of 5B8-positive cells during follicle elongation (compare Figure 2.4F); weak staining of the interfollicular dermis was evident. At this stage, E-cadherin immunostaining (Figure 2.5G) delineated intercellular boundaries of all follicle epithelial cells except those of the presumptive matrix. Immunostaining was absent from sections incubated with secondary antibody only (Figure 2.5H).

***The differentiated lanugo hair follicle (18 weeks EGA to birth)***

The differentiated follicles produce hair fibers after 18 weeks EGA. Immunolabeling for TN-C was present in the follicle BMZ and the dermal papilla (compare Figs 2.4A, 2.6A), and for the first time, in the interfollicular BMZ and the sub-epidermal portion of the papillary dermis, similar to its distribution in adult skin (Lightner et al., 1990). The follicle BMZ, connective tissue sheath, and the dermal papilla were all immunoreactive for the 938-CSPG (Figure 2.6B). In contrast to earlier developmental stages, 2B6-CSPG was present in the connective tissue sheath, the follicle BMZ and the interfollicular dermis (Figure 2.6C). The BMZ of the follicle and the dermal papilla contained perlecan (Figure 2.6D), which remained concentrated in the center of the dermal papilla. The 3B3-CSPG was also present in the dermal papilla and the follicle BMZ (Figure 2.6E), consistent with immunolocalization of this antigenic epitope in adult human skin (Westgate et al., 1991). Immunostaining for 3B3-CSPG was localized at the periphery of the inner root sheath, where it could be either cell-associated or a transient, developmentally specific extracellular matrix layer separating inner root sheath cells from the outer root sheath. Cells of the follicle sheath and the dermal papilla were intensely NCAM immunoreactive (Figure 2.6F), with decreased immunostaining proximal to the epidermis where the follicle traverses the papillary dermis. This staining pattern was observed with either of the two NCAM antibodies. Immunolabeling of interfollicular dermal cells was diminished compared to follicle sheath and dermal papilla cells, and also relative to the interstitial dermal staining associated with earlier developmental stages.

***Immunoblot analysis***

Monoclonal antibody F9A5 was used for immunoblot analysis of TN-C in extracts of fetal skin. Although several bands were detected in skin extract (Figure 2.7A, left panel) F9A5 bound specifically to the two largest protein bands, and was inhibited by pre-adsorption of the antibody with purified TN-C (Figure 2.7A, center panel). The relative mobilities ($M_r$) of the two TN-C forms were approximately 240 $\times 10^3$ and 280-300 $\times 10^3$. While the size of the smaller form is similar to the $M_r$ of the antigenic species used to generate Mab F9A5 (Carter and Hakomori, 1981), it appeared slightly higher than other estimations for the smaller isoform of human TN-C (Erickson and Lightner, 1988; Taylor et al., 1989). The size of the larger TN-C form is similar to other estimates of human TN-C (Erickson and Lightner, 1988; Taylor et al., 1989; Schalkwijk et al., 1991). Other bands were present even in the absence of primary antibody, and thus, were attributed to non-specific binding of the secondary antibody (Figure 2.7A, right panel). A series of developmental ages was examined for the presence of either TN-C form (Figure 2.7B). Tenascin-C was not detected prior to hair follicle initiation (9 weeks EGA). At 10.5 weeks EGA, corresponding to follicle initiation, both TN-C forms were evident when blots were exposed for periods of time longer than shown in Figure 2.7B. A smaller protein of approximately 220 $\times 10^3$ was also present in specimens of 10.5, 12 and 13 weeks EGA, but it was similar in size to a band in the TN-C standard lane, which appeared upon storage of the purified protein (not shown). This was attributed to autodegradative activity in both the standard and the specimens, since Erickson and Lightner have reported that TN-C is relatively unstable even when stored carefully, and is particularly sensitive to hydrolyis at weakly acid pH (Erickson and Lightner, 1988). At 11 weeks EGA (not shown) and after, both larger species of TN-C were readily detected, corresponding to the initiation, invagination, elongation and differentiation stages of hair follicle development.

Monoclonal antibody 5B8 was used to detect NCAM on immunoblots of fetal skin. Since this hybridoma supernatant had not been used to recognize human antigen, it was first used in comparative immunohistochemical and immunoblot staining of human fetal brain with rat brain to establish cross-reactivity (data not shown). An extract of human fetal brain showed a polydisperse band of NCAM, with $M_r$ ranging from 175 $\times 10^3$ to 205 $\times 10^3$. Human fetal skin of 15 weeks EGA contained a single form of NCAM ($M_r$

160 $\times 10^3$) as detected by Mab 5B8 (Figure 2.8A, left panel, arrow). Treatment of fetal tissue extracts with neuraminidase, an enzyme which degrades sialic acid, did not alter the electrophoretic mobility of skin NCAM ($M_r$ 160 $\times 10^3$), although brain NCAM was shifted to a single band at $M_r$ 160 $\times 10^3$ (data not shown). Thus, as detected by Mab 5B8, NCAM in fetal skin did not appear to be modified by polysialic acid. Other protein bands detected at $M_r$ 125, 140, 180 and 205 $\times 10^3$ migrated with relative mobilities similar to NCAM isoforms, although they did not seem to be NCAM-related because similar protein species were evident when blots were incubated with a control myeloma supernatant in place of 5B8 (Figure 2.8A, middle panel), or when primary antibody incubation was omitted (Figure 2.8A, right panel). The 5B8 hybridoma supernatant was reacted with extracts of skin ranging in age from 9 weeks EGA to adult (Figure 2.8B). A protein band corresponding to the skin NCAM ($M_r$ 160 $\times 10^3$) was present at 9 (weakly visible), 11, 13, 15, and 19 weeks EGA, corresponding to stages of initiation, growth, elongation, and differentiation. This form of NCAM was absent from an extract of adult skin and from isolated fetal epidermis.

## DISCUSSION

This investigation of TN-C, NCAM, E-cadherin, ICAM-1, CSPGs and perlecan in fetal human skin revealed their selective distributions relative to developing hair follicles, providing additional evidence in support of developmental roles for TN-C, NCAM and E-cadherin, and suggesting further that the concerted actions of a diverse array of molecules may coordinate morphogenetic processes.

A striking observation was the appearance of regularly-spaced, focal concentrations of TN-C subjacent to the DEJ, coincident with the gestational age when follicle initiation is observed (Pinkus, 1958; Holbrook et al., 1988). These spatially restricted regions of TN-C correlated with BMZ-affiliated immunostaining of pre-germ follicles visible in slightly older specimens, indicating that TN-C provides an early marker for epidermal appendage morphogenesis before histologic changes are observed. During hair germ and hair peg stages, TN-C immunostaining was observed in the follicle, suggesting that epithelial-derived cells may be a source of TN-C. These observations are consistent with avian feather formation, where, just prior to initiation of feather germs, TN-C mRNA and protein are localized to discrete collections of epidermal cells (Tucker, 1991; Jiang and Chuong, 1992). During subsequent hair follicle development, TN-C

accumulates in follicle-associated mesenchyme, and is diminished in the dermal condensation, similar to the pattern associated with developing mouse vibrissae and teeth (Chiquet-Ehrismann et al., 1986; Thesleff et al., 1987).

The initial immunohistochemical detection of TN-C in fetal human skin corresponds to the appearance of two TN-C isoforms, with approximate $M_r$ of 250 $\times 10^3$ and 280-300 $\times 10^3$. Both forms were detected during hair follicle morphogenesis, which differs from normal adult skin where two species of TN-C mRNA have been reported (Borsi et al., 1993), but only the large isoform has been detected in Western blots (Lightner et al., 1989; Schalkwijk et al., 1991).

Tenascin-C has an anti-adhesive effect on cells *in vitro* (Chiquet-Ehrismann, 1991; Chiquet-Ehrismann et al., 1991), is associated with tissue reorganization and cell migration (Kaplony et al., 1991), and the large TN-C is associated with increased proliferation of adult human keratinocytes (Schalkwijk et al., 1991; Schalkwijk et al., 1991). Tenascin-C accumulation is associated with increased epithelial and mesenchymal cell proliferation during murine odontogenesis (Vainio and Thesleff, 1992). Although the proliferative activity of developing human hair follicles is not well characterized, follicle epithelial cell proliferation is associated with elongation of developing mouse hair follicles, while cells of the dermal condensation temporarily cease to incorporate $^3$H-thymidine (Wessells and Roessner, 1965). Based on the localization of TN-C to hair follicle BMZ and associated mesenchyme, as well as its absence from the dermal condensation, it appears that TN-C is well situated to influence the growth and migration of either follicle epithelial or follicle-associated dermal cells, or both. On the other hand, TN-C may not directly influence, but simply mark sites of cell proliferation and tissue reorganization, as suggested by a recent report that mice develop normally in the absence of TN-C (Saga et al., 1992).

To investigate CSPG distribution in developing skin, antibodies recognizing different carbohydrate moieties were used. The 3B3 antibody immunolabeling was enhanced in the follicle BMZ, similar to the specific immunolocalization of a basement membrane CSPG (BM-CSPG) in developing rat hair follicles (Couchman et al., 1990). It may well be that the 3B3 labeling in human skin is equivalent to that of the rat BM-CSPG. 3B3 immunolabeling of follicle BMZ coincided with accentuated TN-C immunolabeling of the same region. Together with reports demonstrating that an avian CSPG (CTB-CSPG) and TN-C co-localize *in vivo*, co-purify, and bind to each other *in vitro* (Chiquet and

Fambrough, 1984; Vaughan et al., 1987; Hoffman et al., 1988), the results showing the co-localization of 3B3 and TN-C to hair follicle BMZ suggest that these molecules may interact during human follicle morphogenesis. Immunostaining with the 2B6 antibody was noticeably absent from follicle-associated mesenchyme, while it increased ontogenetically in interfollicular dermis. The distribution of 2B6 has a similar pattern to that of fibrillar collagens I and III, which are abundant in interfollicular dermis and reduced in the follicle-associated mesenchyme (Smith et al., 1986). Biglycan and decorin are two small dermatan sulfate proteoglycans which are expressed in skin (Voss et al., 1986; Bianco et al., 1990), and which participate in the formation of interstitial collagen fibrils *in vitro* (Pog'any and Vogel, 1992). The 2B6 epitope may also be substituted with dermatan-sulfate glycosaminoglycan, rather than chondroitin sulfate glycosaminoglycan (Couchman et al., 1984), suggesting that the 2B6 antigen observed here might represent the distribution of one or both of these, and might be involved in collagen fibriollogenesis during skin histogenesis. In any case, the segregated distribution of 2B6 immunoreactivity is further evidence that, during development, the composition of glycosaminoglycan chains is carefully regulated (discussed by Couchman et al., 1984).

Unlike the "stub" antibodies, Mab 938 binds intact chondroitin sulfate glycosaminoglycan chains (Lark et al., 1988; Yeo et al., 1992). Mab 938 immunostaining of hair follicle BMZ and the follicle sheath overlapped with Mab 3B3, suggesting that these antibodies may recognize unique aspects of a common CSPG. Of the CSPG antibodies included here, only 938 labeled epidermal and follicle epithelial cells. The large extracellular matrix proteoglycan versican, and the transmembrane protein CD44, have been implicated in cell adhesion and migration, and are both expressed by adult human epidermal cells (Konter et al., 1989; Zimmermann et al., 1994). CD44 is also present on follicle epithelial cells during murine hair follicle morphogenesis, although its expression in fetal human skin is uncharacterized (Underhill, 1993). It is possible that one or both of CD44 or versican is expressed in fetal human skin and is identified by Mab 938. Taken together, the CSPG immunolabeling observed here emphasizes the need to analyze regulation of proteoglycan transcription, translation and post-translational modifications to determine if one core protein is differentially modified with distinct CS-GAGs in a regionally specific manner, or if unrelated core proteins are modified with identical CS-GAGs and subsequently co-localized during development.

All fetal human skin basement membranes contained perlecan, which was also concentrated in the dermal papilla during later stages of hair follicle morphogenesis. These results confirm and extend previous data for the HSPG (Horiguchi et al., 1989). NCAM has been shown to co-purify with an HSPG (Cole and Burg, 1989). The cDNA sequence of perlecan was obtained recently, and the protein is predicted to contain several domains resembling the immunoglobulin-like domains found in NCAM (Kallunki and Tryggvason, 1992). In fetal skin, prominent perlecan immunoreactivity centered in the dermal papilla coincided with enhanced NCAM immunostaining of dermal papilla cells. If NCAM functions as a substrate adhesion molecule, with perlecan as its ligand, these results suggest that the dermal papilla may represent a site *in vivo* where the two proteins interact to immobilize an already segregated cell population such that the cohesion of the developing structure is maintained.

During human skin development, the expression of NCAM was progressively restricted to mesenchymally-derived cells associated with the follicle. NCAM was not detected on follicle epithelial cells, unlike its transient, appendage-specific expression in mouse and chick (Chuong and Edelman, 1985; Crossin et al., 1985; Hardy et al., 1992; Jiang and Chuong, 1992). Immunoblot analysis with Mab 5B8 revealed that fetal skin contains an isoform of NCAM ($M_r$ 160 $\times 10^3$) which is not modified by PSA. This is in contrast to the abundance of PSA-modified NCAM present in developing chick skin (Chuong and Edelman, 1985). NCAM isoforms have similar extracellular domains containing PSA-modification sites, while they differ according to the presence or absence of transmembrane and cytoplasmic domains. With the transmembrane domain, NCAM is an integral membrane protein, and without it, NCAM is anchored to the cell surface via a phosphoinositol (PI) link (reviewed in Murray, 1990). The 5B8 antibody is thought to recognize the cytoplasmic portion of NCAM (J. Dodd, personal communication), thus recognizing NCAM in its transmembrane, but not PI-linked, form. The Mab NKI-nb1-1 is specific for an epitope common to both forms (Moolenaar et al., 1990). The epitope may be conformation-sensitive, as well, based on the absence of immunoreactivity in Western blots or paraffin-fixed tissue sections (data not shown). Both monoclonal antibodies immunostained developing fetal skin, with overlapping distribution in the dermal papilla but not the follicle sheath (see Figure 2.4). Thus, follicle sheath cells express PI-linked NCAM, while the transmembrane form, and perhaps the PI-linked NCAM, is expressed by dermal papilla cells, presumably affecting cell-cell interactions and signal transduction.

Although the presence of PSA on PI-linked NCAM could not be evaluated in the current study, the transmembrane form did not appear to be PSA-modified which may be significant for intercellular interactions, as has been proposed previously (Rutishauser, 1990).

At all stages of hair follicle morphogenesis, E-cadherin immunostaining was strongest on cells in the center of the appendage and weaker on cells at the follicle periphery. These results are consistent with those reported recently for E-cadherin expression in fetal human skin (Fujita et al., 1992), and are in agreement with the distribution of this CAM in developing murine hair follicles (Hirai et al., 1989). E-cadherin forms a stable association with cytoskeletal elements *in vitro* (Nelson et al., 1990), and is associated with differentiated epithelia *in vivo* (reviewed in Takeichi, 1988). Its expression pattern in developing hair follicles suggests that cells one layer removed from the follicle BMZ may shift to a more stable morphology, presumably correlated with a more differentiated status.

The highly specific, transient expression of ICAM-1 by hair germ cells remains unexplained. The identity of the hair germ-specific antigen was verified using multiple unrelated ICAM-1-specific antibodies. Although there was no correlation with expression of its ligand, LFA-1, another $\beta_2$ integrin, Mac-1, was reported recently to bind ICAM-1 (Diamond et al., 1991). Thus, the possibility that ICAM-1 expression facilitates intercellular adhesion, perhaps through Mac-1, cannot be excluded. During morphogenesis, epithelial budding and downgrowth involves cell proliferation and migration, accompanied by degradation and deposition of newly synthesized basement membrane and other extracellular matrix components. These are similar to events associated with tumorigenesis and inflammatory response during wound healing. Cytokines such as IL-1, TNF-$\alpha$, and IFN-$\gamma$, which govern the latter processes, regulate ICAM-1 expression (Dustin et al., 1988; Rothlein et al., 1988), and its expression is associated with increased cell proliferation *in vitro* (Detmar et al., 1992). The precise localization of ICAM-1 on hair germ cells may reflect a specific response elicited by inflammatory mediators which have not previously been linked to morphogenesis, but could nevertheless be present during development, promoting subsequent tissue restructuring and follicle downgrowth. At this time, one can only speculate as to the significance of ICAM-1 expression at such a precise morphogenetic stage of hair follicle development.

Based on the results obtained in this study, a model for hair follicle morphogenesis is proposed. The premise of the model is that localization of TN-C near the BMZ corresponds to sites of epidermal/follicle cell proliferation, and that TN-C is selectively maintained in the follicle BMZ through binding interactions with 3B3-CSPG. In the model, it is hypothesized that prior to follicle initiation, epidermal cells proliferate at sites where they contact focal deposits of TN-C. Constrained suprabasally and peripherally by cells which are biomechanically stabilized through E-cadherin/cytoskeletal interactions, the clusters of cells may be forced to elongate into the dermis, producing a pre-germ follicle. ICAM-1 may facilitate homo- or heterotypic cell interactions (as discussed above), thus, promoting tissue restructuring. The proximal-distal gradient of TN-C associated with developing hair follicles is oriented opposite to the expression gradient of NCAM, which mediates intercellular adhesion. Tenascin-C is proposed to influence mesenchymal cell movement through, or out of, TN-C-rich realms proximal to the epidermis, toward TN-C-poor domains opposite the follicle base or interfollicular dermis. This is similar to the role proposed for TN-C in developing intestinal villi (Aufderheide and Ekblom, 1988), and consistent with its association with cell migration and the down-regulation of focal adhesions *in vitro* (Murphy-Ullrich et al., 1991). The segregation of mesenchymal cells into follicle-associated or interfollicular dermal fibroblastic cells may be orchestrated by NCAM-mediated intercellular adhesion. The absence of E-cadherin on follicle epithelial cells permits them to maintain a flexible, undifferentiated status, thereby accommodating shape changes associated with proliferation and migration. The model suggests that the combined effects of NCAM and TN-C and E-cadherin promote epithelial and mesenchymal cell migration to form a hair peg.

The current study has systematically examined a variety of morphogenetic mediators in a single developmental system. The results demonstrate that TN-C, NCAM, E-cadherin, and proteoglycans are spatially and developmentally regulated during human hair follicle morphogenesis, and an additional cell adhesion molecule, ICAM-1 has been identified in a morphogenetic context. While these data, and the model proposed, are only fragments of a complex developmental picture, it is hoped that they will assist in directing future investigations.

**Table 2.1. Summary of Expression of TN-C, Proteoglycans, and Cell Adhesion Molecules During Human Hair Follicle Morphogenesis[a].**

| Marker | Prefollicle (Fig. 2.1) | Pre-Germ (Fig. 2.2) | Hair germ (Fig. 2.3) | Hair peg (Fig. 2.4) | Bulbous Hair peg (Fig. 2.5) | Lanugo (Fig. 2.6) |
|---|---|---|---|---|---|---|
| TN-C | – | + Focal BMZ | ↑ F-BMZ<br>+ FS<br>+ F-KCs | ↑ FS<br>~ DC | + DP<br>– F-KCs | NC |
| 938-CSPG | + (BMZ, BV, CM) | NC | ↑ F-BMZ<br>↓ IF-BMZ<br>+ F-KCs | + FS | + DP | – F-KCs |
| 3B3-CSPG | + (BMZ, BV, CM) | NC | ↑ F-BMZ<br>↓ IF-BMZ | NC | NC | + DP<br>+ IRS (?) |
| 2B6-CS/DS | + (BMZ, BV, CM) | NC | NC | – FS<br>– DP | ↑ IF-dermis | + FS<br>+ DP |
| Perlecan | + (BMZ, BV, CM) | NC | NC | NC | + DP<br>+ FS | NC |
| NCAM | + (Dermis) | NC | ↑ DC | ↑ DC | ↑ DP<br>↑ IF | NC |
| Ecadherin | + (Intermediate epidermal cells) | NC | NC | + F-KCs<br>– Matrix | NC | NC |
| ICAM-1 | + (BV, periderm) | NC | + F-KCs | – F-KCs | NC | NC |

[a]BMZ, basement membrane zone; BV, blood vessels; CM, compact mesenchyme; NC, no change; FS, follicle sheath; F, follicular; IF, interfollicular; KCs, keratinocytes; DC, dermal condensation; DP, dermal papilla; IRS, inner rooth sheath; +, present; –, absent; ↑, increased immunostaining; ↓, decreased immunostaining; ~, weakly present.

**Figure 2.1 Prior to follicle initiation (8-9 weeks EGA)**

Light micrographs of immunolabeling for tenascin-C (A), 938-CSPG (B), perlecan (C), NCAM (D), E-cadherin (E) in frozen sections of fetal human skin. Tenascin-C immunostaining is absent from skin **(A)** while 938-CSPG is present in the dermis, along the BMZ at the DEJ, and on cell-cell borders in the epidermis **(B)**, and perlecan is present in all basement membranes **(C)**. NCAM immunoreactivity is detected in the dermis **(D)**, and E-cadherin is only in suprabasal layers of the epidermis **(E)**. A control section is shown in **(F)** (primary antibody was omitted). Symbols and abbreviations: opposing arrowheads indicate the dermal-epidermal junction (DEJ); **e**, epidermis; **d**, dermis; **bv**, blood vessel. Bar, 25 μm.

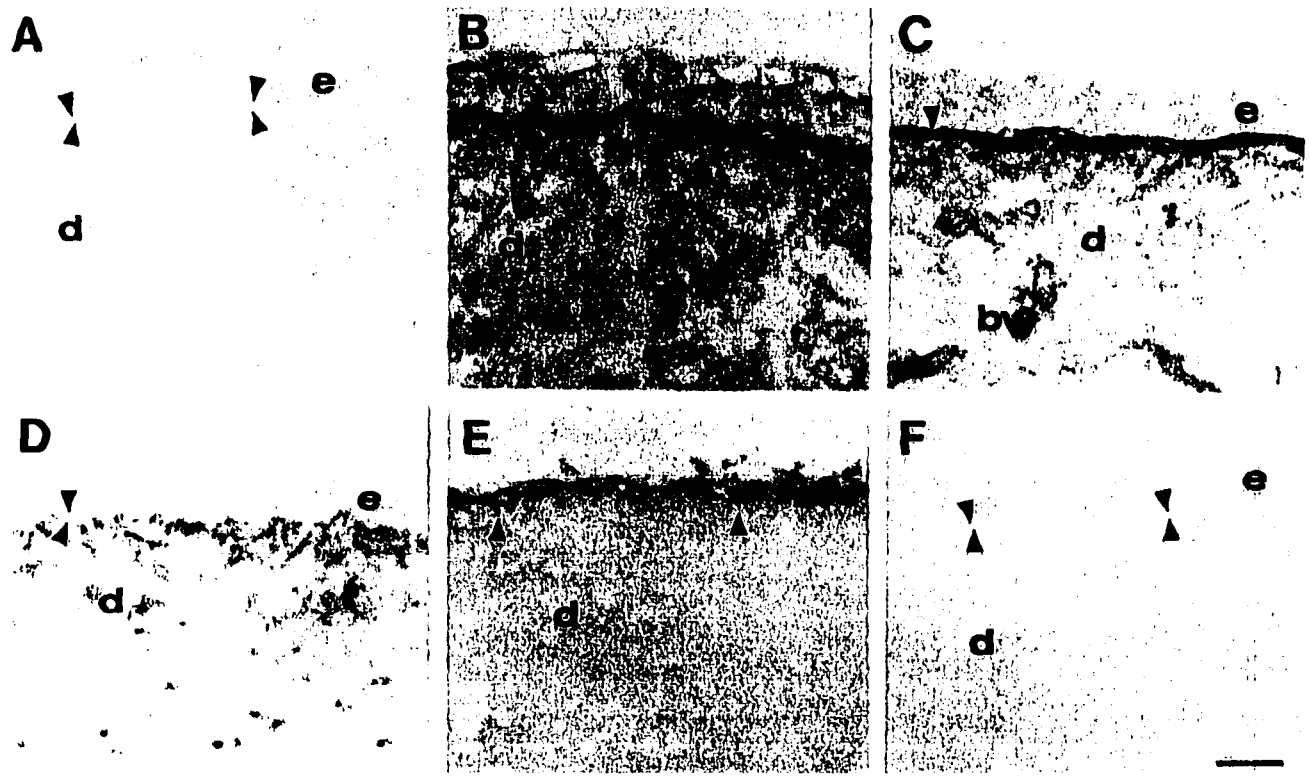
A
e
d
B
C
e
d
bv
D
e
d
E
d
F
e
d

**Figure 2.2 Follicle initiation: the pre-germ follicle (10-11 weeks EGA)**

Light micrographs of immunolabeling for TN-C (A,B) and NCAM (C). Focal immunolabeling for TN-C is present at the DEJ (arrows) before pre-germ follicles are visible (**A**) and in the BMZ underlying pre-germ follicles (**B**). NCAM immunolabeling does not change (**C**). Abbreviations: **e**, epidermis; **d**, dermis; **pg**, pre-germ. Bar, 25 μm.

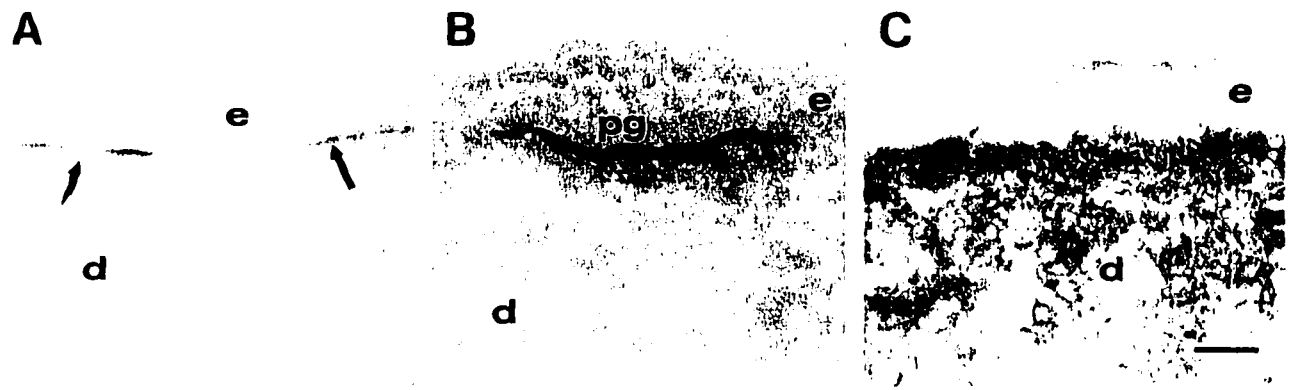
A
e
d
B
pg
e
d
C
e
d

**Figure 2.3 Follicle invagination: the hair germ (11-12 weeks EGA)**

Light micrographs showing immunodistribution of TN-C (A), 3B3-CSPG (B), NCAM (D), E-cadherin (E), and ICAM-1 (F) in the hair germ. TN-C immunostaining is concentrated in the BMZ of the hair germ, with diffuse labeling in the ECM of mesenchymal cells associated with the hair germ (*) (**A**). Mab 3B3 stains the hair germ BMZ and blood vessels (**B**); no immunostaining is observed if chondroitinase treatment is omitted (**C**). NCAM immunoreactivity is seen throughout the dermis, especially on cells of the dermal condensation (**D**). E-cadherin immunostaining is associated with intermediate layer epidermal cells (**E**). Immunolabeling for ICAM-1 is detected on cells of the hair germ and the luminal surfaces of some periderm cells (**F**). Abbreviations: **hg**, hair germ; **dc**, dermal condensation; **p**, periderm; **bv**, blood vessel. Bar, 25 μm.

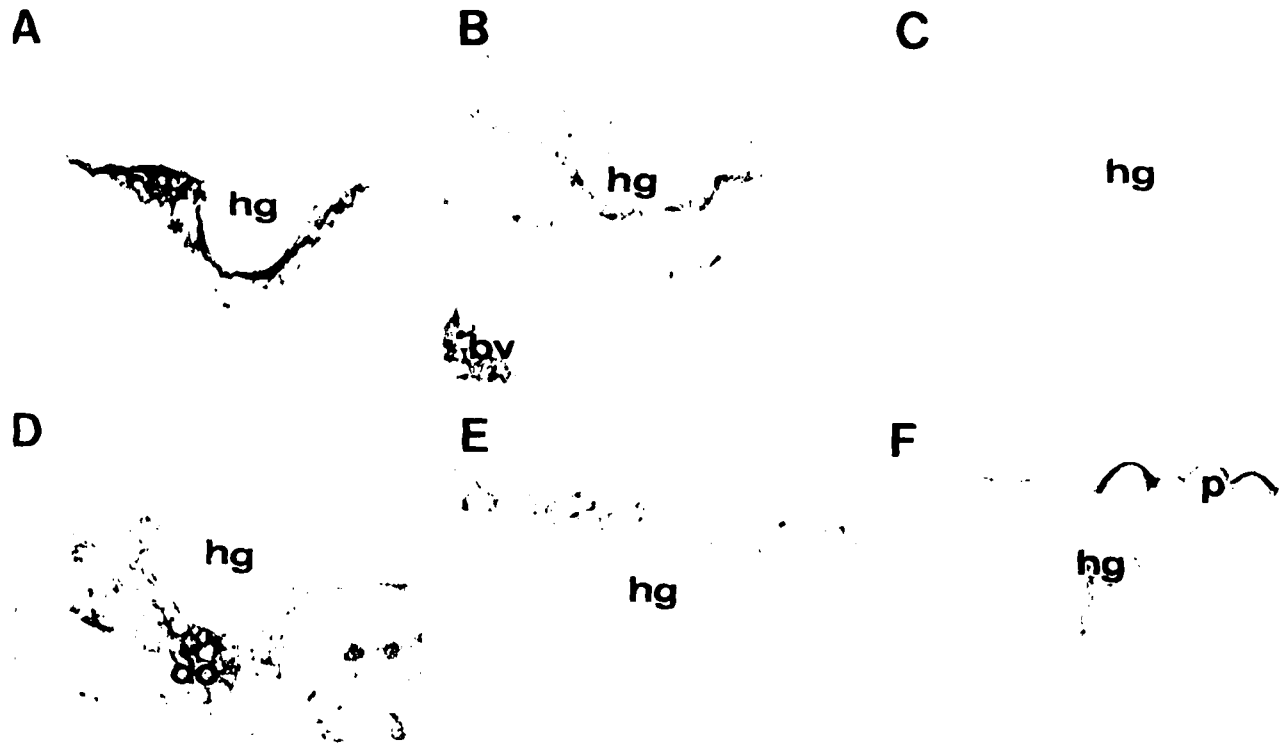
A
hg
B
hg
bv
C
hg
D
hg
do
E
hg
F
p
hg

**Figure 2.4 Follicle elongation: the hair peg (12-15 weeks EGA)**

Light micrographs of TN-C (A), 938-CSPG (B), 3B3-CSPG (C), 2B6-CSPG (D), NCAM (E,F), E-cadherin (G) and ICAM-1 (H) immunostaining. TN-C immunolabeling is intense in the BMZ and the follicle sheath, extending further into the interfollicular dermis on the anterior of the hair peg. Immunostaining is diminished in the dermal condensation (arrow), with weak labeling in the hair peg (**A**). The follicle sheath, hair peg BMZ, and hair peg are also immunopositive for 938-CSPG (**B**); 3B3-CSPG is found in the follicle BMZ (**C**). Weak immunoreactivity for 2B6-CSPG is found in hair peg BMZ and the dermis, but not in the follicle sheath (arrowheads indicate the follicle BMZ) (**D**). Immunolabeling for NCAM, using Mab NKI-nb1-1, is weak in the dermis and enhanced on follicle-associated cells, especially in the dermal condensation (**E**), while Mab 5B8 labels the dermal condensation only (**F**). E-cadherin immunoreactivity is strong on cells in the core of the hair peg, and weaker on peripherally located cells, particularly those at the tip of the follicle, the presumptive matrix of the hair follicle (*)(**G**). ICAM-1 immunostaining is present only on blood vessels and periderm cells (**H**). Abbreviations: **hp**, hair peg; **a**, anterior; **bv**, blood vessel. Bar, 50 μm.

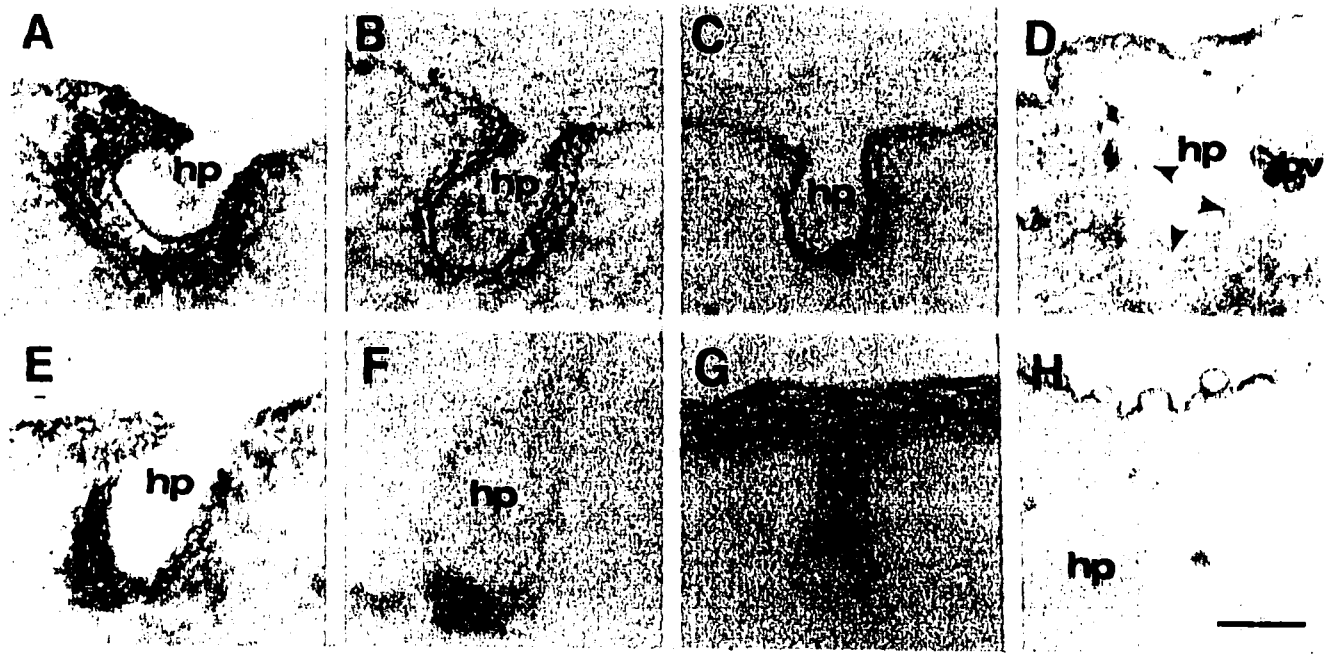
A
hp
B
hp
C
hp
D
hp
pv
E
hp
F
hp
G
H
hp

**Figure 2.5 Follicle differentiation: the bulbous hair peg (15-18 weeks EGA)**

Light micrographs of immunostaining for TN-C (A), 938-CSPG (B), 2B6-CSPG (C), perlecan (D), NCAM (E,F) and E-cadherin (G). TN immunoreactivity is concentrated in the follicle BMZ and the follicle sheath (open arrows indicate follicle sheath) and immunostaining is also present in the dermal papilla (arrow) **(A)**. The follicle BMZ is strongly immunopositive for 938-CSPG, with weaker immunolabeling of the follicle sheath, dermal papilla and cells of the bulbous hair peg **(B)**. The follicle BMZ is weakly immunoreactive for 2B6-CSPG (arrowheads), but the follicle sheath and dermal papilla are negative **(C)**. Perlecan is concentrated in the center of the dermal papilla, and the BMZ of the follicle (and all skin basement membranes) **(D)**. Mabs NKI-nb1-1 **(E)** and 5B8 **(F)** show enhanced NCAM immunolabeling in the follicle sheath and dermal papilla, with weaker immunostaining of the dermis. Intense E-cadherin immunoreactivity is present on cells in the interior of the follicle, and diminished immunostaining is present on cells adjacent to the BMZ, particularly in the bulb **(G)**. A control section shows no immunostaining (primary antibody was omitted) **(H)**. Abbreviations: **b**, bulb; **bv**, blood vessel. Bar, 50 μm.

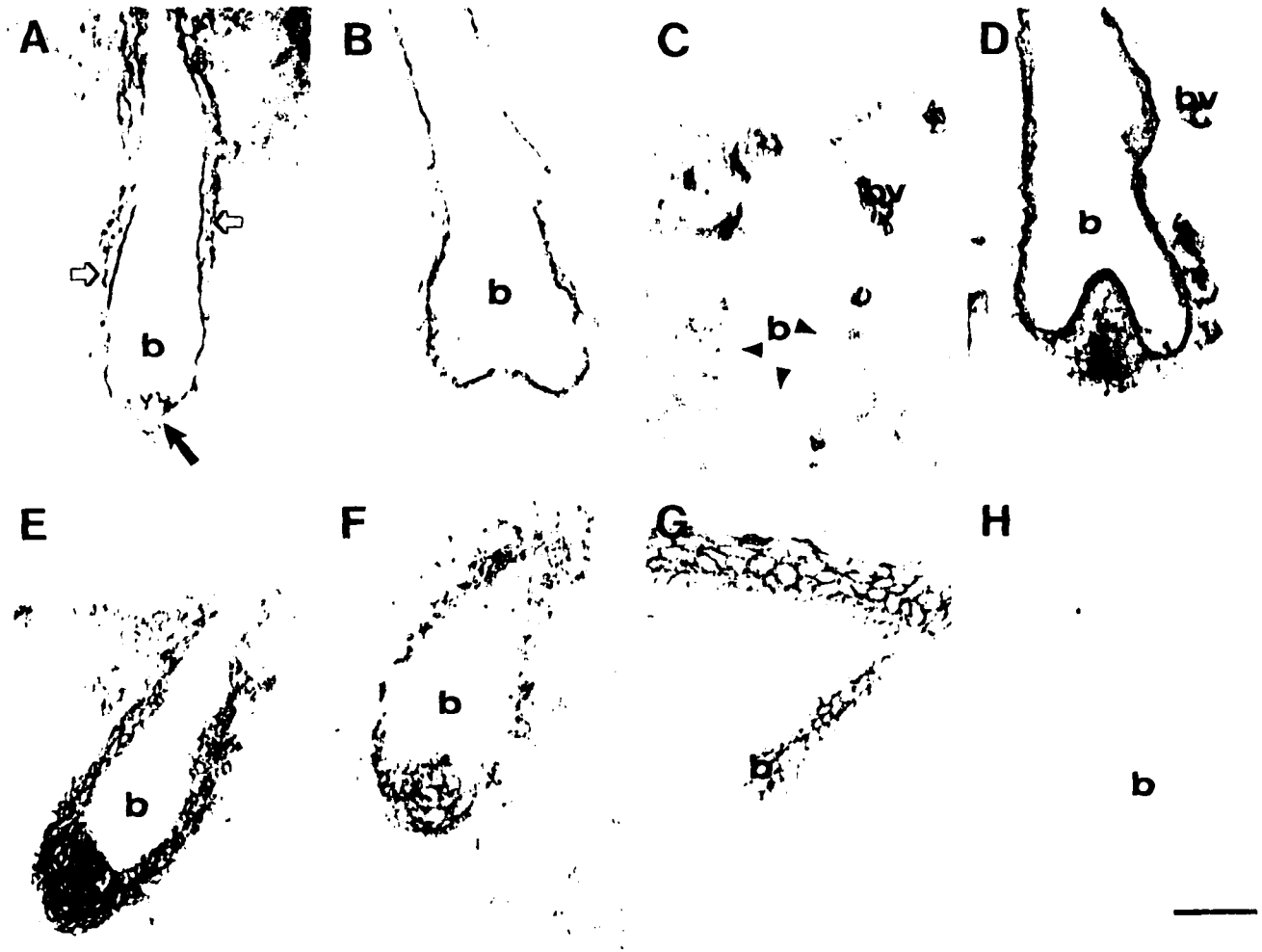
A
B
C
D
b
b
b
b
E
F
G
H
b
b
b

**Figure 2.6 The differentiated hair follicle (18 weeks EGA and older)**

Immunodistribution of TN-C (A), 938-CSPG (B), 2B6-CSPG (C), perlecan (D), 3B3-CSPG (E), and NCAM (F) in fetal human skin containing differentiated hair follicles, sectioned tangentially. TN-c immunostaining is found in the dermal papilla (arrow), the sub-epidermal mesenchyme of the papillary dermis, and the follicle BMZ **(A)**. The dermal papilla (arrow) and follicle BMZ are positive for 938-CSPG, as is the entire dermis **(B)**. Immunolabeling for 2B6-CSPG is found in the dermal papilla (arrow), follicle BMZ, and dermis **(C)**. Perlecan immunolabeling is concentrated in the dermal papilla (arrow) and the basement membranes of the follicle, blood vessels and DEJ **(D)**. The 3B3-CSPG is detected in follicle BMZ, and at the junction of the inner and outer root sheaths (arrowheads) **(E)**. NCAM immunolabeling is intense on cells of the dermal papilla (arrow, inset) and the follicle sheath, with weaker immunoreactivity in the interfollicular dermis **(F)**. Abbreviations: **f**, hair follicle; **bv**, blood vessel. Bar, 100 μm.

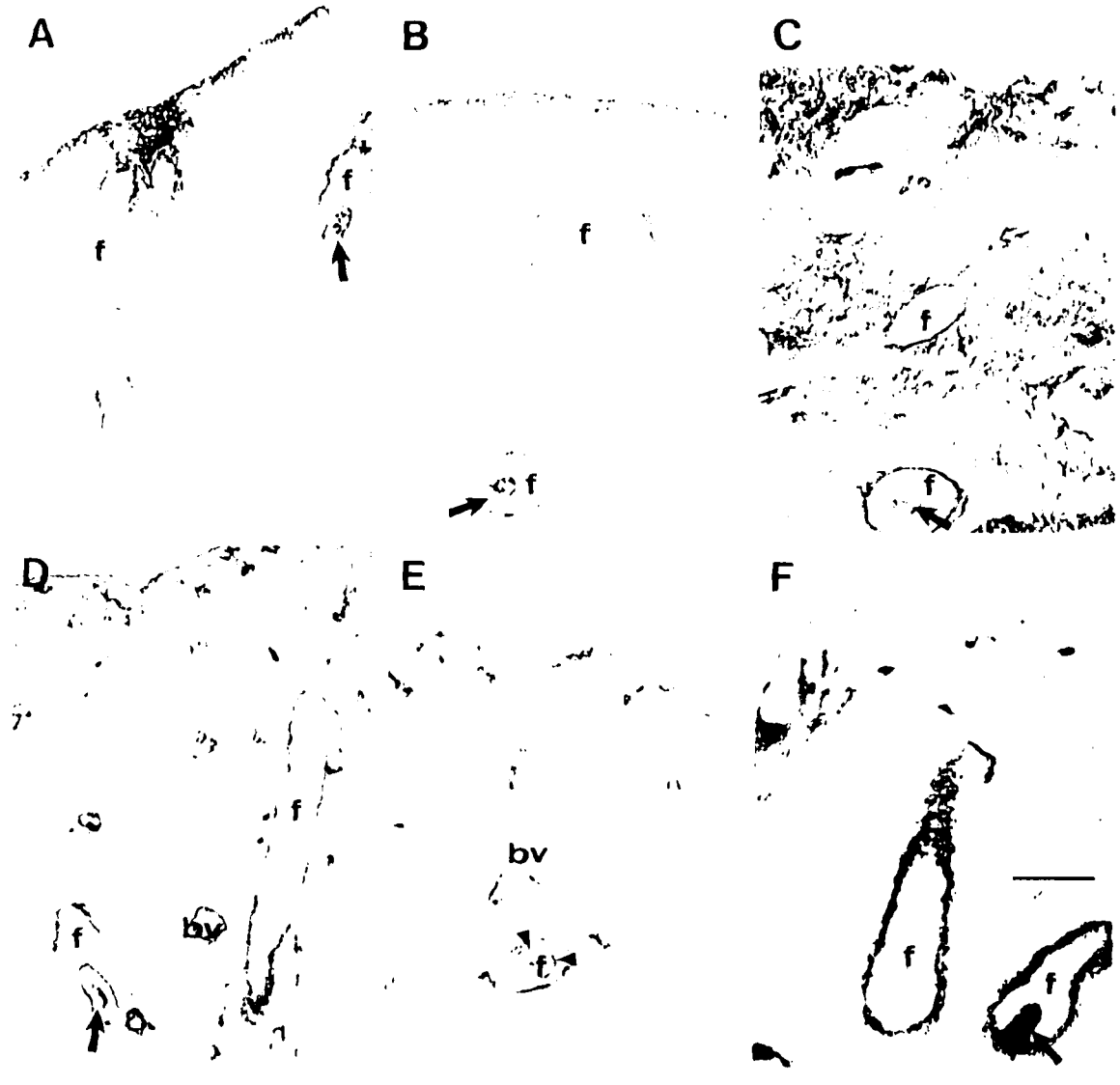
A
f
f
B
f
f
C
f
f
D
f
bv
f
E
bv
f
F
f
f

**Figure 2.7 Western blot detection of TN-C in fetal human skin extracts**

**A)** An extract of 14 week EGA fetal skin (sk) and 200 ng of purified TN-C (TN) were separated on 7.5% SDS-polyacrylamide gels and immunoblotted using Mab F9A5 (left panel), Mab F9A5 pre-adsorbed with purified TN-C (center panel), and no primary antibody (right panel). Antibody binding to purified TN-C and to two fetal skin proteins of $300 \times 10^3$ and $250 \times 10^3$ $M_r$ (arrows) is eliminated after pre-adsorption of F9A5. Other bands are due to non-specific binding of secondary antibody. **B)** Total skin from 9, 10.5, 12, 12.5, 14, 17, and 19 weeks EGA was extracted and electrophoretically separated on 7.5% SDS-polyacrylamide gels. Immunoblot detection reveals specific protein bands of $300 \times 10^3$ and $250 \times 10^3$ $M_r$ (arrows) are present in samples between 12 and 19 weeks EGA. Molecular weight markers are shown on the left.

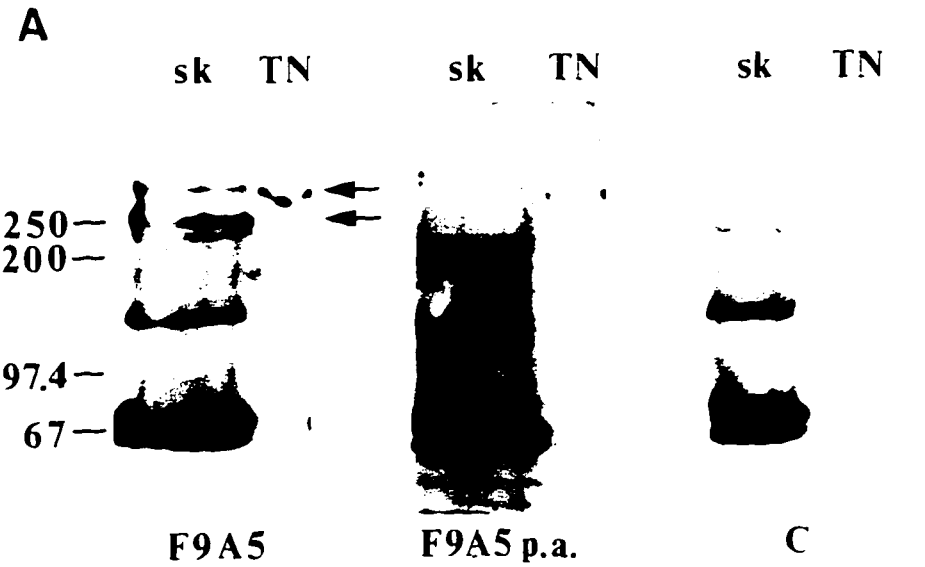
A
sk TN
sk TN
sk TN
250—
200—
97.4—
67—
F9A5
F9A5 p.a.
C

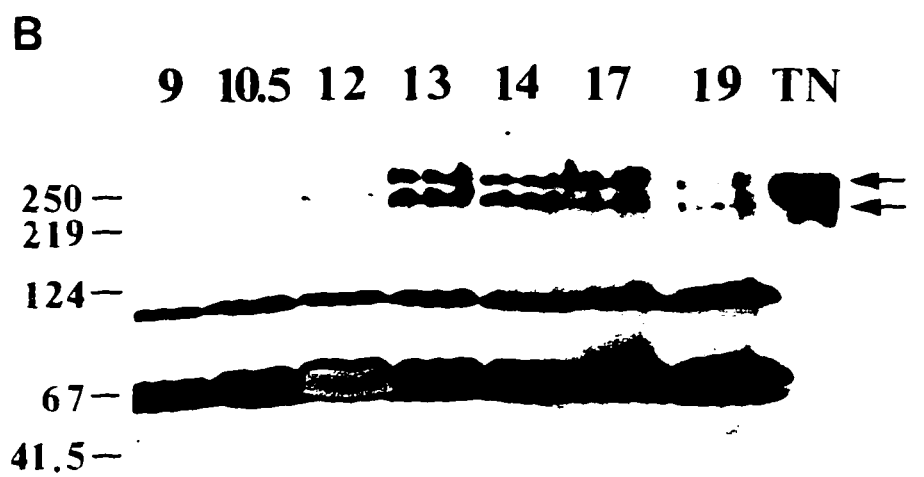
B
9 10.5 12 13 14 17 19 TN
250—
219—
124—
67—
41.5—

F9A5

**Figure 2.8 Western blots detection of NCAM in fetal human skin extracts**

**A)** Extracts of 15 week EGA fetal skin (sk) and brain (br) were separated on 7.5% SDS-polyacrylamide gels and immunoblotted using hybridoma supernatant 5B8 to NCAM (left panel), myeloma supernatant NS-1 (center panel) and no primary antibody (right panel). Human fetal skin contains a protein band of $160 \times 10^3$ $M_r$ (arrow), which is detected with 5B8 but not with NS-1, or in the absence of primary antibody. Immunoreactive bands of $140 \times 10^3$, $180 \times 10^3$, and $205 \times 10^3$ $M_r$ are evident with 5B8, NS-1 and in the absence of primary antibody. Molecular weight markers are shown on the right. **B)** Extracts from 9, 11, 13, 15, 19 weeks EGA fetal skin, adult skin (ad), and isolated 13 week EGA fetal epidermis (epi) were separated as in (A) and immunoblotted using hybridoma supernatant 5B8. The skin NCAM (arrow) is present from 9 to 19 weeks EGA, but absent from adult skin and isolated fetal epidermis. Molecular weight markers are shown on the right.

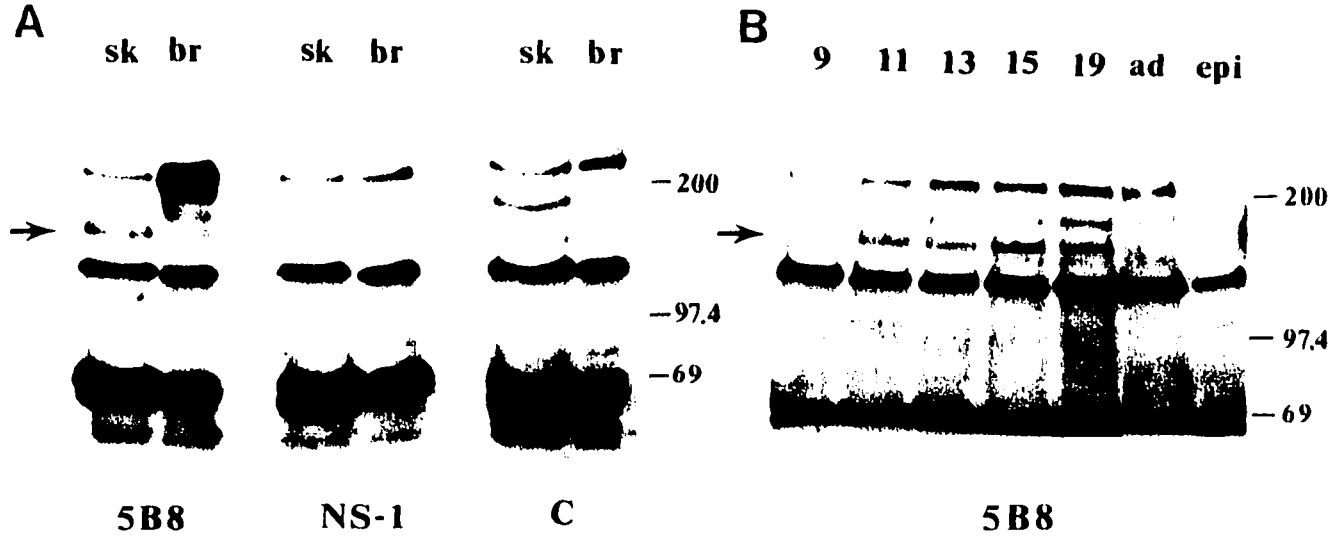
A
sk br
sk br
sk br
200
97.4
69
5B8
NS-1
C
B
9 11 13 15 19 ad epi
200
97.4
69
5B8

# CHAPTER III

# ANALYSIS OF TENASCIN-C ISOFORM EXPRESSION AND CELL PROLIFERATION DURING HUMAN HAIR FOLLICLE DEVELOPMENT

## INTRODUCTION

Reciprocal signaling between adjacent epithelial and mesenchymal cell layers is necessary for the histogenesis of hair follicles and other vertebrate epidermal appenages, such as feathers, nails, teeth and sweat glands, (reviewed in Sengel, 1976). Although the identity of the initiation signal(s) is unknown, the cellular response is evident histologically, first as clusters of elongated epidermal cells opposed by condensations of mesenchymal cells, and later as a cord of epidermal cells projecting and extending into the dermis, in continued close association with a condensed dermal cell population (reviewed in Holbrook et al., 1988). Thus, factors which influence the primary processes of cell shape, proliferation and migration may directly or indirectly govern the morphogenesis of epidermal derivatives. One such molecule is the hexameric extracelluar matrix protein tenascin-C (TN-C), which has anti-adhesive and adhesive effects on cells *in vitro*, and is associated with changes in cell replication *in vitro* (Chiquet-Ehrismann et al., 1986; Crossin, 1991; End et al., 1992). *In vivo*, TN-C is expressed in the rapidly proliferating mesenchymal condensations associated with murine odontogenesis and lung and mammary gland histogenesis (Inaguma et al., 1988; Vainio and Thesleff, 1992; Young et al., 1994). Mitotically active regions of avian feather primordia and the human placenta are sites of elevated TN-C expression as well (Chuong, 1990; Castellucci et al., 1991; Chuong et al., 1991), and evidence is accumulating that TN-C expression is correlated with cell proliferation during wound healing and pathogenesis (Mackie, 1988; Gatchalian et al., 1989; Castellucci et al., 1991; Schalkwijk et al., 1991; Schalkwijk et al., 1991; Kanno and Fukuda, 1994; Mackie, 1994; Zagzag et al., 1995).

The diverse functions of tenascin-C are attributed to its modular structure shown schematically in Figure 3.1, which consists of a unique N-terminal sequence, repeated domains similar to the epidermal growth factor (EGF repeats), a stretch of between 8 and 16 repeated units identified as fibronectin Type III repeats (FN-III repeats) due to their similarity to the cell-binding domain of fibronectin, and a C-terminal sequence with

homology to fibrinogen (Nies et al., 1991; Siri et al., 1991). Of particular interest are the central eight FN-III repeats, which have been collectively termed the alternatively spliced domain (ASD) (Siri et al., 1991). Alternative processing of primary TN mRNA transcripts causes these units to be retained or removed, generally as a cassette, generating large and small protein isoforms of TN-C (Jones et al., 1989; Saga et al., 1991; Weller et al., 1991). The large TN-C isoform has been suggested to mediate neural crest cell migration into the developing avian cornea, and its selective upregulation in tumorigenesis and *in vitro*, in response to cytokine-stimulation, are taken as additional evidence that the ASD has functional significance (Kaplony et al., 1991; Borsi et al., 1994; LaFleur et al., 1994; Rettig et al., 1994). This idea is supported by experiments demonstrating that the alternatively spliced domain disrupts focal adhesion contacts *in vitro* (Murphy-Ullrich et al., 1991).

Results from the previous chapter demonstrated that TN-C is deposited at the dermal-epidermal interface, coincident with the initiation of hair follicle morphogenesis, and TN-C is present in the follicle-specific mesenchyme and basement membrane zone during the morphogenetic process. Western blotting revealed the presence of two forms of TN-C which appeared to be developmentally regulated during follicle development. The distribution patterns and potential functions of these isoforms in fetal human skin is unknown, however, and thus, the goal of the present study was to examine the patterns of expression of TN-C transcripts and protein isoforms during hair follicle morphogenesis.

## EXPERIMENTAL PROCEDURES

*Tissue Processing*

Fetal human trunk skin from specimens age 9-15 weeks estimated gestational age (EGA) was collected by the Human Embryology Laboratory at the University of Washington and in accordance with DHEW policies. For each specimen, 3 pieces of skin were collected for subsequent processing. To minimize degradation of tissue RNA, one piece of tissue was immediately placed into 4% Paraformaldehyde fixative (for use in *in situ* hybridization), and a second piece for RNA extraction was snap-frozen in liquid nitrogen and stored at -80°C. A third piece of tissue was placed in Hank's Buffered Saline Solution and maintained on ice for not more than 5 hours, until it could be processed for immunocytochemical analysis as described in Chapter II.

*Antibodies Sources and Immunohistochemical Procedures*

Monoclonal antibodies BC-4 and BC-2 were the generous gifts of Dr. Luciano Zardi (Genoa, Italy). These were diluted 1:500 and 1:10, respectively, for single label immunostaining as described (Chapter II). Monoclonal antibody MIB-1 (Dako Corporation) recognizing cell-cycle associated antigen Ki-67 (Schluter et al., 1993) was diluted 1:50 for use in the same protocol. The same basic immunostaining protocol was used for whole mount immunostaining of separated epidermal sheets, the only difference being that all buffers contained 0.1% saponin for optimal antibody penetration. The procedure was modified slightly for double immunolabeling with monoclonal antibodies MIB-1 and BC-2, or MIB-1 and BC-4. Briefly, MIB-1 immunodetection through horseradish peroxidase conjugated to avidin-biotin complex (ABC-HRP) was performed first and visualized using nickel-enhanced diaminobenzidine (Ni-DAB) as a substrate, generating a black precipitate wherever MIB-1 was bound. Sections were washed extensively, incubated with monoclonal antibody BC-2 or BC-4, and processed using the ABC-HRP technique again, this time with DAB as a substrate, yielding a brownish-gold precipitate. Some sections were also counterstained with Methyl Green, dehydrated and coverslipped with permanent mounting medium.

*Western Blotting*

Fetal skin specimens were extracted in CAPS buffer, subjected to SDS-PAGE, transferred to nitrocellulose membranes and incubated with Mab BC-2 (diluted 1:10) or Mab F9A5 as described in Chapter II, except that streptavidin-alkaline phosphatase (Zymed, San Francisco, CA) was substituted in place of streptavidin-horseradish peroxidase in order to use an even more sensitive chemiluminescent substrate (Tropix, Bedford, MA).

*PCR cloning*

Total RNA isolated from human dermal fibroblast strain A8496 was used for RT-PCR and was the generous gift of Dr. Terry LaBell (LaBell, 1995). Random hexanucleotide primers and AMV-RT (Promega, Madison, WI) were used to generate cDNA from 10 μg total RNA A8496, as described (Willing et al., 1988). Probes specific for TN-C were generated by polymerase chain reaction (PCR) and are diagrammed in Figure 3.1. A 494-bp segment of the alternatively spliced domain (TNA3B) was obtained using A8496 cDNA for a template with the oligonucleotide pimer pair 5'-ACTCCTTACACAGTCACCCTGC-3' and 5'-TATTCCACAGTCTCCAGCAACC-3'. Oligonucleotides 5'-TACAATGTCCTCCTGACAGCCG-3' and 5'-

AAGCCCTTCATGGCGATGATGC-3' flanking the splice junction were used to generate a 299-bp segment (TN56). A third probe, corresponding to a 280 bp sequence within the EGF-like region (TNEGF) was amplified with the primers 5'-TTTCTTGCTTTCCTTGCCCTCG-3' and 5'-GCGATGTGTGAAGACAATCTGG-3'. Reaction mixes of 100 µl volume contained 50 ng template cDNA, 5 mM KCl, 10 mM Tris, pH 8.3, 1.5 mM $MgCl_2$, 10 mM dithiothriotol (DTT), 0.01% (w/v) gelatin, 250 mM each deoxynucleoside triphosphate, 50 pM each oligonucleotide primer and 1 unit Taq polymerase (Stratagene, LaJolla, CA). Reaction mixes were placed in a programmable thermal cycler (MJ Research, Watertown, MA) and incubated for 1 min. at 94° C, 1 min. at 60° C and 30 sec. at 72° C, cycled 35 times and held for 7 min. at 72° C. A 5 µl aliquot of each reaction was run on a 1% non-denaturing flatbed agarose gel and stained with ethidium bromide for comparison of amplifed DNA with DRIgest III DNA standards (Pharmacia, Piscataway, NJ). Ligation of PCR products into the plasmid PCR-II, subsequent transformation into INV-α cells and blue/white colony screening was accomplished using the TA-cloning kit (Invitrogen, San Diego, CA) according to supplier's instructions. White colonies were selected and grown up for isolation of plasmid DNA and subsequent screening by restriction mapping and excision digestion (Sambrook et al., 1989). To confirm insert identity, hydrolyzed plasmid DNA was used for double-stranded DNA sequencing with the Sequenase Version 2.0 kit (U. S. Biochemical, Cleveland, OH) and oligonucleotide primers flanking the multiple cloning site. Two clones carrying the TN56 insert in opposite orientations were identified as TN56x and TN56z.

*Synthesis of radiolabeled cDNA probes*

Cloned TN fragments were released from plasmid DNA by Eco RI digestion, separated on a 1% agarose gel and viewed after ethidium bromide staining. The insert-containing band was excised and electroeluted using the Elutrap (Schleicher & Schuell). Purified insert was labeled with [α-$^{32}$P]dCTP (DuPont, NEN Division, Boston, MA) using a random prime labeling kit (Gibco Life Technologies, Gaithersburg, MD) and separated from unincorporated nucleotides by elution from a 2 ml G-50 Sephadex column using standard methods (Sambrook et al., 1989).

*RNA isolation and Northern analysis*

Total RNA was isolated from fetal skin specimens following the acid-guanidinium-phenol-chloroform technique (Chomczynski and Saachi, 1987), using a ten-fold excess

volume Solution D to wet weight of tissue. For each sample, 10 μg total RNA was loaded onto a 0.8% agarose-formaldehyde gel and separated by electrophoresis, after which RNA was transferred by capillary elution (Sambrook et al., 1989) and immobilized on Zetaprobe membrane (BioRad, Hercules, CA). Hybridization was carried out for 16 hours at 42°C in 6X SSPE (Sambrook et al., 1989), 5X Denhardt's reagent, 0.1% SDS, 50% deionized formamide, 100 μg/ml sonicated salmon sperm DNA, and approximately 1 x $10^6$ cpm probe/ml hybridization buffer. Blots were washed at 42°C in three changes of 3X SSPE, 0.1% SDS, followed by two high stringency washes at 65°C in 0.1X SSPE, 0.1% SDS (20 min. each wash). Hybridized probe was visualized by standard autoradiograpic techniques and NIH Image software was used to normalize transcript signal relative to the 28S ribosomal RNA band detected on the corresponding ethidium bromide negative image.

*Additional plasmid constructs*

The plasmid construct pCN-I, containing a 500 bp insert corresponding to the alpha-2 chain of Type I Collagen, was the generous gift of Dr. Terry LaBell (LaBell, 1995). Other plasmid constructs already available in the laboratory were used for a comparative study of *in vitro* transcription of digoxigenin-labeled cRNA probes and are summarized in Table 3.1.

*RNA Transcription*

For conventional transcription reactions, RNA polymerases (final concentration of 45 U/μl) and RNasin from Gibco Life Technologies were used, with nucleotides from Boehringer-Mannheim Corporation (Indianapolis, IN). High yield reaction components were supplied with the AmpliScribe High Yield Transcription Kit (Epicentre Technologies, Madison WI), except for digoxigenin-11-UTP (Boehringer-Mannheim Corporation) which was used in all reactions. Transcription reaction mixes were assembled in the order listed in Table 3.2. In the High Yield B reaction, the first five components were diluted into RNase-free water and pre-heated to 42°C for 5 min. before adding remaining ingredients. At the termination of each reaction, RNase-free DNase I (Gibco Life Technologies) was added (final concentration of 0.02 μg /μl), and incubated for 10 min. at 37°C, after which 0.1 vol. TE buffer (10 mM Tris, 1 mM EDTA) was added.

*Purification, Quantitation and Analysis of digoxigenin-cRNA Transcripts*

Except for one experiment (shown in Figure 3.8B) when 5 M ammonium acetate precipitation was used, digoxigenin-cRNA transcripts (dig-cRNA) were typically purified using RNase-free Select-D columns (5 Prime-3 Prime, Boulder CO) followed by ethanol precipitation. RNA was recovered by centrifugation at 12000 ×g for 30 min. at 4°C and was resuspended in DEPC-treated $H_2O$. Quantitation of digoxigenin-cRNA was based on absorbance measurements, using a Beckman Model DU-70 spectrophotometer, and also by dot blot comparison of dig-cRNA with digoxigenin-labeled standards (Boehringer-Mannheim). For qualitative analysis, 0.5 µg of transcript (calculated from absorbance measurements) was loaded onto a 1.2% agarose gel, separated under denaturing conditions and transferred to nitrocellulose for detection using alkaline-phosphatase-conjugated anti-digoxigenin (AP-anti-dig, Boehringer-Mannheim). Nitrocellulose membranes containing dotted or transferred cRNA probes were incubated first with 2% BSA diluted in PBS for 30 min. and then blocked for 30 min. in the same buffer containing 20% heat-inactivated lamb serum. AP-anti-dig was diluted into blocking buffer (1:2000, vol:vol) and membranes were incubated from 45 to 60 min. After equilibration for 5-15 min. in alkaline phosphatase buffer (AP-buffer: 50 mM Tris, pH 9.5, 15 mM NaCl, 25 mM $MgCl_2$), membranes were transferred to AP-buffer containing 0.3375 mg/ml Nitro-Blue-Tetrazolium (NBT) and 0.175 mg/ml 5-Bromo-4-chloro-indolyl-phosphate (BCIP) and monitored for color development (usually complete within 3 to 5 min.).

*In Situ Hybridization*

Tissue *in situ* hybridization was carried out as described in by Schaeren-Wiemers and Gerfin-Moser (1993), with slight modifications. Tissue specimens were immersion-fixed for 16-24 hours in 4% paraformaldehyde, rinsed in phosphate buffered saline (PBS) and cryo-protected by successive immersion in 10%, 15% and 20% sucrose solutions before cryo-embedding in TissueTek OCT Compound (Miles Inc., Elkhardt IN). Cryo-sections of 8-10 µm thickness were collected on SuperFrost Plus slides (VWR, Philadelphia PA), air-dried for 30-60 min. and either used immediately for *in situ* hybridization, or stored at -80°C for later use. At the start of the *in situ* protocol, slides were incubated in PBS for 5 min., fixed in 4% paraformaldehyde for 10 min., and rinsed in PBS (three changes of 5 min. each), after which sections were covered with 150-200 µl hybridization buffer containing 50% deionized formamide (Amresco), 5X SSC, 5X Denhardt's solution (5 Prime-3 Prime), 250 µg /ml yeast tRNA (Boehringer-Mannheim), and 500 µg /ml salmon sperm DNA (Sigma) and incubated for 1-3 hours at room

temperature. Digoxigenin-labeled cRNA probes were diluted into fresh hybridization buffer to final concentrations of 150 ng/ml or 500 ng/ml (optimal concentration varied for each probe), heated for 10 min. at 85°C and cooled for 5 min. on ice. Slides were immersed in hybridization mix in RNase-free 5-slide slide mailers (Baxter Scientific McGaw Park, IL) and incubated for 16 hours at 72°C. Post-hybridization washes at 72°C consisted of 5 min. in 5X SSC, 5 min. in 0.2X SSC and 60 min. in 0.2X SSC, after which slide mailers were equilibrated to room temperature for 30-45 min. Slides were incubated for 5 min. in buffer B1 (0.1 M maleic acid, 150 mM NaCl, pH 7.5), blocked for 60 min. in 1% Blocking Reagent (Boehringer-Mannheim) diluted in buffer B1, and incubated for 60 min. with AP-anti-dig diluted 1:500 in blocking buffer. Slides were washed two times for 30 min. each in B1 and then equilibrated for 5-15 min. in AP-buffer. Each section was covered with 200 µl of AP-buffer containing NBT, BCIP and 1 mM levamisole (Sigma), and slides were placed in humidified chambers for color development, which was monitored with a dissecting microscope (detection time ranged from 10 min. to 60 hours, depending on target mRNA abundance.) Slides were immersed 5 min. in each of TE buffer and PBS, followed by 10 min. in 4% paraformaldehyde before coverslipping in Glycergel aqueous mounting medium, (DAKO Corp., Carpenteria, CA). For double-label analysis of TN-C *in situ* hybridization with MIB-1 immunostaining, sections were not coverslipped, but rather placed in PBS overnight at 4°C. Sections were immunolabeled with the MIB-1 antibody in the standard protocol, the only difference being that the peroxidase substrate amino-ethylcarbonate was used in place of DAB.

## EXPERIMENTAL RESULTS

Isoforms of TN-C which are differentially regulated in development and pathogenesis may have functionally distinct roles in modulating cell migration and cell proliferation. Results obtained previously (Chapter II) point to temporal regulation of TN-C isoform expression in morphogenetically active fetal human skin. To examine the spatial patterning of TN-C protein forms and transcripts in relation to hair follicle morphogenesis in more detail, an array of isoform-specific probes, antibody and molecular, was assembled for use in immunocytochemical and molecular analysis. These are summarized in Table 3.3.

### *TN-C immunoreactivity in epidermis*

TN-C is typically associated with the stroma of mesenchymal tissues during development, and in some of these, its expression in the mesenchyme is induced by epithelial contact (Aufderheide et al., 1987; Inaguma et al., 1988; Ekblom and Aufderheide, 1989). Human hair follicle morphogenesis is likewise characterized by intense TN-C immunostaining in the extracellular matrix of the condensed mesenchyme associated with the developing appendage. Weak immunoreactivity was regularly observed in the follicle epithelium, however (see Figure 2.4A), raising the interesting possibility that TN-C protein is present in follicle epithelial cells of fetal human skin. An alternative, although unlikely, explanation is that immunolabeling within the follicle epithelium is due to diffusion of DAB precipitate from the adjacent condensed mesenchyme, or perhaps to sectioning artifact. To examine these possibilities more carefully, separated fetal human epidermis was sectioned and immunostained for TN-C. Immunoreactivity for TN-C was detected within the follicle epithelium and not in the interfollicular epidermis. Tenascin-C immunolabeling was localized near the apices of the outermost or basal layer cells in follicle pre-germs and hair germs at 11 weeks EGA (Figure 3.2) and older (not shown). This observation suggests that TN-C is present in the epithelium of developing hair follicles, as well as in the associated mesenchyme. While this is consistent with the epithelial expression of TN-C during feather follicle morphogenesis (Tucker, 1991; Jiang and Chuong, 1992), and during lung morphogenesis (Koch et al., 1991) it nevertheless puts TN-C in a new perspective and raises the possibility that the extracellular matrix protein may function in the follicle epithelium and in the condensed mesenchyme. Indeed, the identification of epithelia as sources of TN-C, and the implications of epithelial expression of TN-C, have recently been attracting significant attention (Linnala et al., 1993; Sakai et al., 1993; Lightner et al., 1994; Jones et al., 1995).

***Patterned distribution of TN-C in whole epidermis***

Prior to follicle initiation, TN-C is distributed discontinuously at the DEJ in sections of fetal skin, and the spacing of TN-C-positive regions appears to correspond approximately to follicle pre-germs (results presented in Chapter II). To better examine the patterning of TN-C expression, and thus to evaluate whether it is indicative of follicle initiation, histological sections and intact epidermal sheets from specimens of approximately 10 and 11 weeks gestation were immunostained for TN-C and viewed *en*

*face* (Figure 3.3). Tenascin-C immunolabeling was observed in discrete, irregularly spaced circular deposits in a specimen of 10 weeks EGA (Figure 3.3A). Placodes of TN-C were present at the dermal-epidermal interface in the same specimen in section, but no follicle primordia were detected (not shown). A specimen of 11 weeks EGA contained hexagonally arranged foci of TN-C which corresponded to developing follicles, some of which were seen projecting out of the focal plane (Figure 3.3B). These observations suggest that TN-C immunostaining at the dermal-epidermal interface predicts sites of follicle initiation. The initiation of hair follicle morphogenesis progresses along cranial-caudal and dorsal-ventral axes in fetal human skin. In older specimens, follicles of different morphogenetic stages can be distinguished within the same histological section, suggesting that initiation occurs in temporally distinct waves, although the timing and patterning of such waves is not at all understood (Pinkus, 1958; Holbrook et al., 1988). The irregularly spaced foci of TN-C at 10 weeks may reflect a first wave of follicle formation, while the regular array at 11 weeks, containing hair germ follicles and pre-initiation foci of TN-C, presumably reflects the passing of more than one wave. In this sense, TN-C expression may be a useful marker for deciphering the regionally specific timing and patterning of hair follicle initiation.

***TN-$C_S$ is specifically associated with morphogenetic initiation***

To determine if the alternatively spliced domain of TN-C is uniquely distributed in relation to developing hair follicles, the monoclonal antibodies BC-4 and BC-2 were used for comparative immunoanalysis. Monoclonal antibody BC-4 binds within the EGF-like region of TN-C (see Figure 3.1), recognizing all TN-C molecular forms, while Mab BC-2 binds to two FN-III units within the ASD (repeats A1 and A3, see Figure 3.1), and is specific for TN-$C_L$ (Balza et al., 1993). Specimens of initiation age contained discrete foci of BC-4 immunoreactivity at the dermal-epidermal interface, although no morphological changes were observed in epidermal cells. No immunolabeling was detected in adjacent sections of the same specimens immunostained with Mab BC-2. Representative micrographs are pictured in Figure 3.4A and B. Expression of the ASD, indicated by Mab BC-2 immunostaining, was delayed by about 1 week, and was detected at approximately 11-12 weeks EGA in the BMZ and in the condensed mesenchyme associated with elongating follicles (Figure 3.4C and D). The pattern of immunostaining was indistinguishable from that of Mab BC-4. At subsequent developmental stages, both

antibodies showed the same immunolabeling pattern already described for Mab F9A5 (data not shown). These immunohistochemical data support the Western blot data already presented (Figure 2.7). Taken together, these results suggest that TN-C isoforms are temporally regulated, with TN-$C_S$ expressed specifically at the dermal epidermal interface prior to follicle initiation, and both TN-$C_S$ and TN-$C_L$ expressed in association with follicle elongation. The expression of TN-$C_L$ did not appear to be restricted spatially relative to BC-4 immunostaining of TN-C. While the possibility exists that TN-$C_S$ expression is limited topographically, it cannot be examined at this time because probes which bind TN-$C_S$ specifically are not available.

***Western blot characterization of TN-C Isoforms***

Western blot analysis using Mab F9A5 and fetal human skin extracts demonstrated a developmental shift in TN-C expression, with immunoreactive species of approximately 250 kD and 300-350 kD appearing at 10.5 to 11 weeks EGA (Figure 2.7C). This observation was supported and extended by results presented in the preceding section in which comparative immunohistochemistry suggested that the ASD was absent from an initiation-specific form of TN-C, and the ASD-containing TN-$C_L$ form was upregulated later in development. To verify these observations, as well as to determine which of the molecular forms identified by Mab F9A5 contains the ASD, identical Western blots were generated from tissue extracts of skin specimens previously characterized for follicle development and TN-C immunostaining, and these were probed in parallel with Mabs F9A5 and BC-2. The resulting immunoblot with Mab F9A5 (shown in Figure 3.5A) revealed a distinct signal corresponding to a protein of approximately 250 kD migrating the same distance as purified TN-C. This protein was present at all ages examined. A minor protein of approximately 220 kD was detected in a 9.5 week EGA specimen and was seen more readily in specimens older than approximately 11 weeks EGA. Also detected at 11 weeks EGA, and subsequent ages, was a third, larger protein, with relative mobility of roughly 300 kD. The 250 kD and 300 kD proteins correspond to the sizes reported previously. The smallest form, 220 kD, was easily detected in every specimen here, suggesting that, although it may represent a degradation product, it was dismissed incorrectly in the previous chapter. The ontogeny of the 300 kD isoform corresponded roughly to that shown in Figure 2.7. The 220 kD and 250 kD forms, on the other hand, both of which were detected prior to follicle inititation in a specimen of 9.5 weeks EGA in

the current experiment, were not detected prior to follicle initiation previously (Figure 2.7). Although it is possible that expression of the two forms is turned on between 9 and 9.5 weeks EGA, a more likely explanation is that the current blot was developed with a much more sensitive alkaline phosphatase-based chemiluminescent detection method, as opposed to the horse-radish peroxidase system used earlier.

An identical blot probed with Mab BC-2 is shown in Figure 3.5B. A single reactive band with relative mobility of approximately 250 kD migrated the same distance as purified TN-C and corresponded to the intermediate sized band identified by Mab F9A5. This was observed in all specimens examined, and was interpreted as the ASD-containing isoform, TN-$C_L$. This is interpreted to mean that the 250 kD protein detected with Mab F9A5 corresponds to TN-$C_L$and contains a BC-2 binding site within the ASD, while the 220 kD form is presumed to lack part or all of the ASD, and correspond to TN-$C_S$. These sizes and tentative molecular identities are in agreement with published observations (Natali et al., 1990; Carnemolla et al., 1992). The presence of the 300 kD F9A5-immunoreactive species, while consistent with the previous Western blot (Figure 2.7), is nevertheless intriguing because it was not recognized by Mab BC-2, and yet its appearance at 11 weeks EGA coincides with the first detection of BC-2 immunostaining of tissue sections. While it may represent an uncharacterized TN-C isoform, identified here as TN-$C_{XL}$, which is larger and yet lacks the ASD, it may instead correspond to some novel form of TN-$C_L$ which is recognized by Mab BC-2 in tissue sections, but which loses its antigenicity during the process of Western blotting. Western blot analysis using Mab BC-4 was expected to assist in identifying the 220 kD and 300 kD bands, but was unsuccessful because the antibody did not even bind purified TN-C (results not shown).

***Cloning and characterization of TN-C probes***

In the previous sections, immunohistochemical staining and Western blot analysis using a comparison of universal and ASD-specific antibodies only partially resolved the expression patterns of TN-C isoforms in relation to human hair follicle morphogenesis. Thus, a molecular probe designed to identify all TN-C mRNA transcripts (TNEGF), and probes intended to distinguish transcripts lacking the ASD (TN56), from those containing FN-III repeats A3, A4 and B within the ASD (TNA3B) (see Figure 3.1), were developed for use in Northern blot and *in situ* hybridization analysis. This section describes the

cloning strategy employed and the molecular characterization of the probes TNEGF, TN56 and TNA3B.

The cDNA sequence for human TN-C, available through GenBank (Siri et al., 1991) was used to select oligonucleotide primers for PCR cloning of TNEGF, TN56, and TNA3B from the human dermal fibroblast strain A8496 (Willing et al., 1988). Positive clones were screened by restriction mapping, and one clone of each construct was chosen for sequence verification (data not shown).

A 6 kb transcript for TN-C is expressed almost exclusively in most adult human tissues, with low levels of a larger 8 kb transcript detected in some tissues (Siri et al., 1991). Although adult skin reportedly contains nearly equivalent levels of the two TN-C transcripts (Siri et al., 1991), the pattern of transcript expression in fetal skin is unknown. In order to characterize the cloned TN-C segments in Northern blot analysis, a control tissue expressing the large TN-C transcript was needed. Since TN-$C_L$ is upregulated in tumorigenesis, RNA extracted from normal myometrium and from the smooth muscle cell tumor leiomyoma was included for analysis, along with RNA isolated from cultured A8496 cells, 11 week EGA fetal skin, and from the human smooth muscle cell strain RR392. Using either TNEGF or TN56, a transcript of approximately 6.8 was detected in myometrial RNA (Figure 3.6A). A faint signal corresponding to a transcript of roughly 7.8 kb was also detected with both probes. The same transcripts were present with approximately equal intensity in the leiomyoma RNA, suggesting that the larger mRNA is upregulated in the smooth muscle tumor, consistent with numerous reports of increased TN-$C_L$ expression under tumorigenic conditions (Nicolo et al., 1990; Borsi et al., 1992; Carnemolla et al., 1992; Ventimiglia et al., 1992; Chiquet-Ehrismann, 1993; Leprini et al., 1994; Mackie, 1994). The same blot was stripped and probed with TNA3B but yielded no signal, most likely because immobilized RNA had been removed by repeated cycles of hybridization and stripping prior to TNA3B hybridization (not shown).

A strong hybridization signal corresponding to transcript sizes of 6 and 7 kb in total RNA extracted from human skin fibroblasts and human smooth muscle cells was detected using either TNEGF or TN56 probes (Figure 3.6A). Transcripts of the same size were observed in a fetal skin specimen of 11 weeks EGA, but only after extended exposure times of longer than 1 week. When TNA3B was used to probe a duplicate blot, only the larger size transcript was detected, indicating the presence of the ASD in this variant. It was anticipated that TNEGF would hybridize to multiple transcripts, while

TN56 and TNA3B would bind with mutual exclusivity to uniquely sized transcripts. As shown in Figure 3.6A, this was not the case for TN56, which identified the same size transcripts in tissue and cell culture extracts as did TNEGF. The TN56 probe corresponds to sequence within FN-III units 5 and 6, and under the appropriate conditions it could conceivably hybridize to less homologous sequences from other FN-III repeats. This possibility was tested directly using replicate blots onto which had been dotted 1, 0.1, and 0.01 ng of TNA3B, TN56, and CN-I insert cDNA. Blots were probed with random-prime labeled TNA3B or TN56, and subjected to increasingly stringent post-hybridization washes. Results are shown in Figure 3.6B. When TNA3B was immobilized on the blot and probed with TN56, stable hybrids were only washed off at 65°C in 0.05X SSPE and 0.1% SDS. Similarly, if TN56 was immobilized, TNA3B hybridized to 1 ng of either TN56 or CN-I and washed off at 65°C in 0.05X SSPE and 0.1% SDS, conditions which also caused a reduction in the intensity of the specific signal. Thus, despite its sequence which spans the splice junction of TN-C and was expected to confer isoform specificity, TN56 cross-hybridizes to TNA3B and is only eliminated with the most stringent washing, resulting in a decrease in specific signal. The extent to which the TN56 probe might cross-hybridize to other FN-III segments under the less controlled conditions of a tissue RNA blot is unpredictable, bringing its utility in Northern analysis into question. The probes TNEGF and TNA3B were chosen for subsequent Northern blot analysis.

***Three TN-C transcripts are detected in fetal human skin***

Total RNA extracted from the same specimens used in earlier Western blot and immunohistochemical analyses was used for Northern blot hybridization with TNEGF and TNA3B. Two transcripts with estimated sizes of 6 and 7 kb were detected in each specimen, from 9.5 to 15 weeks EGA (Figure 3.7A). A weak signal from a third, larger transcript of approximately 8 kb was transiently expressed, and was detected in some specimens, but not all, between approximately 10 and 11 weeks EGA. Transcript signal intensity was normalized to the ethidium bromide-stained 28S ribosomal RNA signal and relative amounts of 6 and 7 kb transcripts were calculated for each specimen and expressed as a ratio (Figure 3.7B). The amount of small relative to large transcript ranged from 0.75, in a specimen of 9.5 weeks EGA, to 2.34 for a specimen of 11 weeks EGA. Based on immunohistochemical screening of tissue sections, specimens were grouped according to immuno-morphological criteria, and the ratios of 6 kb to 7 kb were averaged

for each developmental group. Initiation of follicle morphogenesis occurs between 10 and 11 weeks EGA in human trunk skin, and thus, specimens of less than 10 weeks EGA were categorized as pre-initiation. Specimens between the ages of 10 and 11 weeks EGA fell into two populations: a group in which no immunostaining for TN-C was detected, and a second group which contained placodes of BC-4 immunostaining characteristic of follicle initiation, but lacked morphologically identifiable hair follicle primordia. Samples older than 11 weeks EGA all contained elongating hair follicles at the hair germ stage or beyond, and these were grouped according to morphological stage (hair germ and hair peg follicles). The results are graphed in Figure 3.7C and show a developmental shift in transcript levels. Fetal skin of less than 10 weeks EGA contained nearly equivalent amounts of the 6 and 7 kb TN-C transcripts. In specimens older than 10 weeks EGA, the 6 kb message increased relative to the 7 kb transcript, and was maximal in specimens which contained initiating follicles marked by foci of BC-4 immunostaining. Subsequent to initiation, the relative amount of 6 kb transcript declined, and nearly equivalent levels of 6 and 7 kb transcripts were present in specimens which contained differentiating hair peg follicles. These data suggest that two transcripts, 6 and 7 kb in size, are expressed constitutively in fetal human skin, and that initiation of follicle morphogenesis is characterized by a temporary increase in the relative amount of the 6 kb message. This shift is accompanied by the transient expression of a third, 8 kb TN-C transcript.

***Optimization of digoxigenin-labeled RNA transcription: quantitative comparsion of two in vitro transcription reaction protocols***

Tenascin-C is a protein with a variety of cell modulating activities *in vitro* (Chiquet-Ehrismann, 1990; Chiquet-Ehrismann, 1991; Sage and Bornstein, 1991; Hoffman et al., 1994). Its precisely timed and discretely localized deposition at the dermal-epidermal interface suggests that it could be a signaling molecule, originating from cells of either of the adjacent tissues. To gain a better insight into this possibility, it was decided to use *in situ* hybridization to determine which cells, epithelial or mesenchymal, or both, contain TN-C mRNA. The restricted distribution of TN-C protein suggested that only a few cells of either tissue might express TN-C mRNA at follicle initiation. Moreover, since the highly sensitive chemiluminescent technique was necessary to detect TN-C protein in Western blots of fetal skin extracts, and long exposure times were required to visualize mRNA transcript in Northern analysis, a low abundance transcript was expected. It was

important, then, to use an *in situ* hybridization technique with excellent sensitivity and spatial resolution for optimal detection of TN-C transcripts in fetal human skin. The non-radioactive *in situ* hybridization method described by Schaeren-Wiemers et al. (Schaeren-Wiemers and Gerfin-Moser, 1993) and modified by Lindsell (personal communication) offered precise cellular localization with excellent sensitivity. Large amounts of digoxigenin-labeled cRNA probes are needed, however, because hybridization is accomplished by slide immersion, rather than by the coverslip method. Consequently, it was critical to optimize *in vitro* transcriptional yields of digoxigenin-labeled cRNA probes. This section presents a comparison between transcription yields obtained with a conventional reaction protocol and a commercial high yield transcription system. This is accompanied by a brief discussion of parameters which were found to further enhance the yield of digoxigenin-labeled cRNA.

In addition to the TN-C clones described earlier, several plasmid constructs available in the laboratory (identified numerically in Table 3.1) were included for transcription with the conventional and high yield (AmpliScribe) reaction protocols outlined in Table 3.2. With the exception of pCN-I, transcription using AmpliScribe reactions consistently generated more dig-cRNA per μg DNA template than did conventional transcription reactions (Figure 3.8A). AmpliScribe reactions using T7 or T3 RNA polymerase transcribed between 4.2 and 102 μg RNA per μg DNA, approximately 1.2 to 18.1 times the yield from the comparable conventional transcription reactions. When transcripts were generated using SP6 RNA polymerase (as in the pCN-I reaction), similar amounts of dig-cRNA were obtained from either reaction protocol. It was suspected that this might be due either to an inhibitory effect of dig-UTP (Heer et al., 1994), or to secondary structure of the pCRII plasmid construct. To address these possibilities, the construct pTNEGF was included for analysis, and pCN-I and pTNEGF were transcribed using a ratio of dig-UTP:UTP of 1:3 (in High Yield B, and conventional reaction mixes). Under these conditions, the AmpliScribe SP6 polymerase generated 2.6 and 4.1 times the amount of dig-cRNA for pCN-I and pTNEGF, respectively, as did conventional reactions. These results suggest that digoxigenin-11-UTP has an inhibitory effect on the AmpliScribe SP6 polymerase, and better yields are obtained with a lower concentration of dig-UTP.

***Optimization of digoxigenin-labeled RNA transcription: qualitative comparison of two transcription reaction protocols***

A qualitative comparison of dig-cRNA, purified from the two reaction protocols by either spin-column chromatography or ammonium acetate precipitation, is shown in Figure 3.8B. The predominant transcripts for pCN-I and pTNEGF (500 bp and 300 bp, respectively) were enriched in either reaction protocol and either purification scheme. Conventional reactions contained a transcript of approximately 3-4 kb found in either purification scheme but not in AmpliScribe reactions. An additional transcript of intermediate size was also detected in the conventional reaction using pTNEGF. These bands likely result from non-specific transcription initiation. Their absence in the high yield reactions suggests greater fidelity of the AmpliScribe polymerases, and thus, greater purity of transcribed cRNA probes. In either reaction protocol, samples purified by ammonium acetate precipitation were enriched in a band migrating at a size slightly larger than anticipated, perhaps due to anomolous behavior of ammonium acetate-precipitated samples on denaturing agarose gels. Based on the comparison presented here, the commercial high yield kit was selected for additional transcription reactions.

***Optimization of digoxigenin-labeled RNA transcription: effect of digoxigen concentration and incubation temperature on transcriptional yield***

Having found that a decreased digoxigenin concentration improved the AmpliScribe SP6 transcriptional yield, it was necessary to use the same conditions to synthesize the opposite strand cRNA (for use as a control in *in situ* hybridization). To enhance the transcription reaction further, reaction temperature was increased to 42° C. The results for pCN-I and pTNEGF, in which T7 and SP6 reactions were conducted using High Yield A and B conditions (Table 3.2) are shown in Figure 3.9. Transcription from pCN-I with either AmpliScribe T7 or SP6 RNA polymerases gave greater yields with the lower concentration of dig-UTP (roughly 10 times the dig-cRNA using T7 when the dig-UTP:UTP ratio was 1:3, compared to a ratio of 1:1.6). Although transcription from pTNEGF with T7 RNA polymerase showed the opposite trend (lower yield at a lower concentration of digoxigenin), the 20% decrease still constituted an abundant yield of riboprobe.

These data indicate that poor transcriptional yields may be improved by decreasing the digoxigenin-11-UTP concentration and increasing the incubation temperature (as with

pCN-I), while exceptional yields may already be maximal. Although T3 transcription was not included in this experiment, previous results suggest that transcription with T3 RNA polymerase is similar to, or even slightly better than, T7 RNA polymerase (see Figure 3.8A).

***In situ hybridization with Type I Collagen probe***

In order to be confident of *in situ* hybridization results obtained with TN-C probes and the anticipated low copy mRNA in fetal human skin, it was decided that an unrelated probe specific for an abundant mRNA should be included for comparison. Type I collagen appeared to be an appropriate molecule. This extracellular matrix protein constitutes a major component of adult and fetal human dermis. Type I collagen is present well in advance of follicle initiation, and its distribution in relation to developing hair follicles has been described carefully (Smith et al., 1986). As anticipated, hybridization with the anti-sense strand dig-cRNA probe yielded an intense signal in the cytoplasm of mesenchymal cells in fetal skin of approximately 10 weeks EGA (Figure 3.10A). The signal appeared somewhat attenuated in cells of the presumptive papillary dermis, proximal to the dermal-epidermal interface, although this region is enriched in immunostaining for Type I collagen (Smith et al., 1986). The hybridization signal for Type I collagen was also somewhat reduced in mesenchymal cells associated specifically with the the hair follicle as it elongated into the dermis (Figure 3.10B), corresponding to a region of diminished collagen immunostaining as well (Smith et al., 1986). The strand-specific probe for Type I collagen hybridized weakly to follicle epithelial cells situated at the base of the developing structure (Figure 3.10C). Within the intrafollicular dermis, the intense collagen hybridization signal remained relatively unchanged through 15 weeks EGA, the oldest specimen examined (Figure 3.10D). No signal was detected when the sense strand probe was used (Figure 3.10E).

***TN-C mRNA is present in follicle-specific epithelial and mesenchymal cells***

In skin histogenesis, a signal (or signals) to initiate appendage morphogenesis originates in the dermal tissue, triggering a morphogenetic response by basal epidermal cells and a cascade of reciprocal interactions beween mesenchyme and epidermis (Sengel, 1976; Sengel, 1983). The precise timing and discrete localization of TN-$C_S$ immunostaining at the dermal-epidermal interface prior to morphogenetic rearrangements

suggests that TN-$C_S$ might mediate a dermal initiation signal, or might be part of the morphogenetic response by the epidermis. It was anticipated that determining the cellular origin(s) of TN-$C_S$ with *in situ* hybridization analysis of fetal human skin might allow these two possibilities to be distinguished, leading to the identification of a potential role for TN-$C_S$ in follicle morphogenesis.

Tissue *in situ* hybridization for TN-C transcripts was tested initially using digoxigenin-labeled cRNA anti-sense and sense probes transcribed from the three plasmid constructs described earlier (pTN56, pTNA3B, and pTNEGF). The strongest signal was obtained using pTN56, despite, or perhaps due to, its potential cross-hybridization with TNA3B and similar sequences (see Figure 3.7). Consequently, a complete developmental study was conducted using digoxigenin-labeled TN56 anti-sense and sense probes. The pattern of TN56 hybridization must be interpreted cautiously, however, and is taken to indicate the presence of any TN-C splice variant, and not just TN-$C_S$ since the probe may hybridize to other TN-C transcripts besides TN-$C_S$.

Figure 3.11 illustrates results obtained with the TN56 probes. Fetal skin sections of initiation age (10.5 to 11 weeks EGA) contained clusters of epidermal cells which were positive for TN-C transcript but were otherwise undistinguished by any morphologic changes (Figure 3.11A). No signal was observed in adjacent mesenchymal cells. This suggests that the placodes of TN-$C_S$ protein at the dermal-epidermal interface originate from epidermal cells. A pre-germ follicle is shown in Figure 3.11B, where appendage-specific epithelial cells and associated mesenchymal cells alike hybridized with the TN-C anti-sense probe. While epithelial cells of follicle pre-germs and hair germs were generally positive for TN-C mRNA, an intense hybridization signal was detected in cells situated at the junction of follicular and interfollicular epithelium (Figure 3.11C, D). A weaker signal was observed in cells of the mesenchymal condensation at these stages, while interstitial mesenchymal cells were negative. No hybridization signal was evident in sections incubated with the sense strand control (Figure 3.11G).

TN-C transcript was abundant in the cytoplasm of cells of the outermost layer of the follicle epithelium during elongation stages of morphogenesis, pictured in Figure 3.11E and F. In striking contrast, little or no hybridization signal was observed in cells positioned at either the center or flattened base of the follicle. Cells of the dermal condensation were positive for TN-C mRNA, exhibiting a relatively weaker signal than the

follicle epithelium. Mesenchymal cells ensheathing the follicle were weaker yet, but contained TN-C transcript.

These *in situ* hybridization results suggest that TN-C is expressed specifically by epidermal cell clusters at morphogenetic initiation, and the onset of mesenchymal expression of TN-C occurs during subsequent morphogenetic stages. The presence of TN-C-positive cells in the outer epithelial layer and in the mesenchyme ensheathing the elongating follicle suggests that cells of both types contribute to the accumulation of TN-C in the BMZ and the extracellular matrix of the follicle sheath.

***Compartments of mitotic activity and inactivity in developing human hair follicles***

TN-C expression has been linked to increased cell proliferation, notably in hyperproliferative epidermal disorders (Schalkwijk et al., 1991; Schalkwijk et al., 1991). Its presence in the BMZ of developing hair follicles, as well as in the extracellular matrix of the condensed mesenchyme, suggests it could be associated with increased proliferation in either compartment. While the mitotic activity of developing murine and avian epidermal appendages has been studied thoroughly (Wessells, 1965; Wessells and Roessner, 1965), data for fetal human skin are limited to a single analysis of a specimen of 18 weeks EGA (Gerstein, 1971). The monoclonal antibody MIB-1 recognizes a proliferation-associated nuclear protein (Ki-67 antigen) which accumulates during the G1, S, and G2 phases of the cell cycle, and is turned over rapidly after the M phase (within 24 hours *in vitro*) (Schluter et al., 1993). Because its utility in estimating the mitotic index for pathological specimens is comparable to that obtained with either $^{3}$H-thymidine or bromo-deoxyuridine (BrdU) incorporation (Limas et al., 1993; van Weerden et al., 1993), this antibody was chosen for analysis of cell proliferation in fetal human skin.

A double-label immunostaining technique was developed using MIB-1 and TN-C antibodies, so that the patterns of epithelial and mesenchymal cell proliferation could be examined in relation to TN-C expression and hair follicle morphogenesis in fetal human skin. Results are shown in Figure 3.12, where recent mitotic activity is indicated by a dark brown precipitate, restricted to cell nuclei and corresponding to MIB-1 binding, and TN-C immunostaining is marked by a golden-brown precipitate distributed in the extracellular matrix. MIB-1 immunoreactivity was observed in the nuclei of cells in the basal and intermediate epidermal layers in a pre-initiation specimen of 10 weeks EGA, and MIB-1-positive cells were scattered throughout the mesenchyme (Figure 3.12A). Follicle

initiation, marked by the appearance of TN-C at the DEJ, was not accompanied by any obvious change in the pattern of MIB-1-positive cells in either epidermis or mesenchyme, with labeled cells distributed randomly in both tissues (Figure 3.12B). At the follicle pre-germ stage of development, however, shown in Figure 3.12C, MIB-1 immunoreactive cells were detected at the edges of the follicle epithelium, at the transition to the basal layer of the epidermis, similar in pattern to the *in situ* hybridization signal obtained for TN-C transcript. Cells in the same location in more advanced hair germ follicles (Figure 3.12D) were labeled with MIB-1, although the rest of the follicle epithelium also contained mitotically active cells. Very few cells of the mesenchymal condensation were immunoreactive for MIB-1, suggesting that proliferative activity in this population is arrested or suspended. Immunolabeled cells were detected in interstitial regions of the dermis, indicating that not all mesenchymally-derived cells are growth arrested. This is consistent with the report by Wessells and Roessner, who observed a cessation of $^{3}$H-thymidine incorporation in the dermal condensation associated with vibrissae and pelage follicle development in murine skin (Wessells and Roessner, 1965). Elongation of the appendage into the dermis, at the hair peg stage of follicle development, showed the outermost layer of follicle epithelium to be enriched in MIB-1 immunoreactive cells (Figure 3.12E). Immunolabeled cells were rarely observed at the flattened follicle base, or in the central cord of cells. The dermal condensation was also immunonegative for the proliferation antigen at the hair peg stage, while a few labeled cells were detected in the condensed mesenchyme investing the follicle. This trend continued, and was perhaps even more pronounced, with follicle differentiation (Figure 3.12F). Prominent labeling of the outer layer of follicle epithelial cells was observed, with no MIB-1 immunoreactivity detected in cells at the center or base of the follicle. Some proliferation of follicle sheath cells was indicated by MIB-1 immunostaining in this compartment, while a striking absence of immunolabeled cells in all but the periphery of the dermal condensation suggests these cells remain in a growth arrested state.

***Cells in proliferative zone are TN-C positive***

Results obtained separately with the MIB-1 antibody to Ki-67 proliferation antigen and *in situ* hybridization for TN-C suggested that the proliferative compartments of the developing follicle contained cells positive for TN-C transcript. To determine if the same cells expressing TN-C mRNA were also mitotically active, a double-labeling protocol was

developed where sections of fetal human skin were first subjected to non-radioactive *in situ* hybridization detection of TN-C transcript, after which the same sections were immunostained with MIB-1 antibody. The detection methods result in a reddish-brown cytoplasmic signal, corresponding to TN56 hybridization, and a magenta-colored nuclear stain corresponding to the binding of the MIB-1 antibody. Representative results are pictured in Figure 3.13.

Cells of the pre-germ follicle all contained TN-C transcript, and a few of these were also weakly MIB-1 positive (Figure 3.13A). Double-labeled cells were readily detected in a hair germ follicle in the same field, while the adjacent condensed mesenchyme was single-labeled with TN56 probe. In the early stages of follicle elongation, double-labeled cells were found almost exculsively in the outer layer of the follicle epithelium (Figure 3.12B). This pattern was even more pronounced in the more elongated hair peg follicle where weak TN-C hybridization signal was detected in cells at the center of the developing appendage but there was a striking absence of MIB-1 labeling in the same region (Figure 3.13C). The associated mesenchymal condensation consisted of single-labeled cells containing TN-C transcript at this stage. As the follicle differentiated, some cells of the mesenchymally-derived follicle sheath were double-labeled, as were cells of the external layer of the follicle epithelium (not shown). Cells single-labeled for MIB-1 were not detected in the follicle epithelium or associated mesenchyme at any developmental stage examined, although such profiles were observed in the interstitial demis. The results described here suggest that during follicle morphogenesis, a positive correlation exists beween TN-C expression and proliferation in cells of the follicle epithelium. The two events are not correlated in follicle-specific mesenchymal cells, as interpreted from the predominance of single-labeled cells containing TN-C transcript in this population.

## DISCUSSION

The developmental regulation of TN-C isoform expression during human hair follicle morphogenesis was suggested by results obtained in Chapter II. The current study reveals part of an emerging picture illustrating the highly specific regulation of this extracellular matrix molecule in the morphogenetic process. Of particular interest was the immunohistochemical observation that morphogenetic initiation is distinguished by the spatially restricted and selective expression of TN-$C_S$, the small TN-C isoform which lacks

the alternatively spliced domain of FN-III repeats. Expression of a second isoform containing the alternatively spliced domain was associated with the elongation and differentiation stages of follicle development, apparently lagging that of TN-Cs somewhat. Northern and Western blot analysis supported these observations in part, resolving not only two, but three mRNA transcripts and three protein isoforms which appeared to have temporally distinct expression patterns. Adding to the overall picture of TN-C expression, *in situ* hybridization with a TN-C probe showed that collections of epidermal cells express TN-C first around initiation, while follicle-specific cells of epithelial and mesenchymal origin alike are potential sources of TN-C during follicle invagination and elongation stages.

Tissue recombination experiments have demonstrated that the developing dermis directs the patterning and timing of appendage formation, while the epidermis dictates appendage specificity (reviewed in Sengel, 1976). This information is exchanged in a series of reciprocal intracellular interactions or signals by unidentified factors, which result in tissue restructuring and morphogenesis involving cell migration and proliferation. The spatial, temporal, and molecular specificity of TN-Cs expression at the epithelial-mesenchymal interface, together with the purported association of TN-C with cell proliferation and migration, indicate that TN-Cs is part of this exchange. TN-C mRNA was present in epidermal cell clusters before it was expressed in mesenchymal cells, indicating that it is not conveyed from the dermis to the epidermis as an initiation signal, but rather constitutes part of an epidermal response to a morphogenetic initiation signal from the dermis. The cluster of epidermal cells expressing TN-C mRNA corresponds temporally and spatially to the pattern of TN-Cs protein distribution at the dermal-epidermal interface, suggesting that the transcript detected by *in situ* hybridization was TN-Cs, although the inability to identifiy it conclusively as such was one shortcoming of the present study.

The functional significance of TN-Cs expression at follicle initiation remains unclear. This isoform is incorporated preferentially into insoluble extracellular matrix *in vitro*, however, while the large isoform is diffuses more freely into the culture medium (Linnala et al., 1993). This suggests that in fetal human skin, the selective expression of TN-Cs by a topographically limited group of epidermal cells ensures that the glycoprotein remains close to its source, and implies further that spatial specificity of function is important. Although it was not correlated with cell proliferation at this stage, it is possible

that TN-$C_S$ acts in an autocrine fashion to modulate other aspects of the epidermal cells which secrete it, perhaps by disrupting cell-cell or cell-substrate adhesion and altering the morphology of a select population of basal epidermal cells, thereby promoting invagination of the initiating follicle epithelium. Indeed, initiation of hair follicle morphogenesis is similar in some respects to the morphological changes associated with gastrulation during embryogenesis, where a spatially related group of ectoderm cells elongates and invaginates into the blastula. Not only do sea urchin embryos contain a tenascin-like molecule at gastrulation, (Anstrom et al., 1990), but exogenous TN-C disrupted amphibian gastrulation (Riou et al., 1990), suggesting that TN-C may be part of a wider, evolutionarily and developmentally conserved mechanism for modulating morphology of ectodermally-derived cells and mediating the invagination of a cell collective.

The observation that TN-$C_S$ is expressed selectively at follicle initiation is a novel finding and it offers a tangible starting point from which to investigate the molecular nature of developmentally earlier inter- and intracellular signaling interactions by analyzing factors which regulate TN-$C_S$ expression. In this regard, it is surprising that while TN-$C_S$ is present constitutively in adult human tissues (Borsi et al., 1993), no evidence exists for its selective induction. This is despite abundant evidence suggesting the transcriptional control of TN-$C_L$ by cytokines *in vitro*, and by pathogenic and inflammatory mediators *in vivo* (Mackie, 1988; Borsi et al., 1992; Mackie et al., 1992; Ventimiglia et al., 1992; LaFleur et al., 1994; Mackie, 1994; Rettig et al., 1994). Indeed, Borsi and colleagues speculated that expression of TN-C isoforms is not regulated specifically, but that TN-$C_S$ is expressed as part of a default transcription program, and the upregulation of TN-C in neoplastic and hyperproliferative disorders saturates the spliceosome machinery responsible for alternative processing of pre-mRNA transcripts, resulting in the accumulation of TN-$C_L$ transcripts and the apparent selective induction of TN-$C_L$ (Borsi et al., 1994). The current report, on the other hand, demonstrated an increase of the 6 kb relative to the 7 kb TN-C mRNA at follicle initiation, which suggests that in fetal human skin at least, expression of TN-$C_S$ is regulated specifically, perhaps through post-transcriptional mechanisms such as mRNA stability, for example.

If TN-$C_S$ expression is regulated transcriptionally in developing hair follicles, an appropriate place to start searching for control points might be with the transcription factors AP-2 and *Krox-20*, binding sites for both of which have been identified in the five-

prime region of the human TN-C gene, and both of which have roles in initiating developmentally specific transcription (Gherzi et al., 1995). On the other hand, the apparent patterning of TN-$C_S$ expression at hair follicle initiation points toward the involvement of members of the homeobox family, transcription factors which govern pattern formation in vertebrate and invertebrate development (Wolpert, 1994). Indeed, the avian TN-C gene has a binding site for the homeobox protein *evx-1*, and the TN-C promoter region can be activated experimentally by murine *evx-1* in co-transfection experiments (Jones et al., 1992). Moreover, although no link has yet been made experimentally, the patterned expression of TN-C in epidermal placodes of embryonic chick skin prior to initiation of feather follicle morphogenesis correlates with the expression of homebox proteins *Msx-1* and *Msx-2*, suggesting that TN-C could be under the control of either of these homeobox proteins (Tucker, 1991; Edelman and Jones, 1992; Chuong, 1993; Noveen et al., 1995). Future investigations should include an examination of the potential involvement of this path in human hair follicle morphogenesis well.

The developmental expression of TN-C isoforms was analyzed by Northern and Western blotting techniques, yielding results which were intriguing in several respects. First, extracts of fetal human skin contained three TN-C RNA transcripts, apparently corresponding to three TN-C protein forms detected by Western blotting with Mab F9A5. This is not altogether surprising, since as many as sixteen TN-C splice variants are predicted from cDNA library screening and from PCR analysis (Siri et al., 1991; Sriramarao and Bourdon, 1993). Only two message sizes have been reported in Northern blot analysis of human RNA (Siri et al., 1991), however, and thus the observation that multiple transcripts are present at detectable levels in tissue RNA blots represents a novel finding. The selective binding of ASD-specific cDNA and antibody probes to the 7 kb transcript and to the 250 kD protein, respectively, but not to the 6 kb mRNA and the 220 kD protein, suggests that the intermediate-sized transcript and protein correspond to TN-$C_L$, and the smallest transcript and protein correspond to TN-$C_S$. The identities of the largest 8 kb transcript and the 300 kD protein remain to be determined.

Expression of this third RNA transcript and the largest protein, identified here as TN-$C_{XL}$, coincided with initiation of follicle morphogenesis, and also corresponded temporally to expression of the large isoform detected in Chapter II (Figure 2.7). Their relative sizes and temporal expression suggest that TN-$C_{XL}$ may be the translational

product of the 8 kb transcript. It is perplexing that the BC-2 antibody did not recognize this protein, however, because the timing and size correlate with the appearance of BC-2 immunostaining in tissue sections, and in addition, the TNA3B cDNA probe hybridized weakly to the 8 kb transcript. It is possible that TN-$C_{XL}$ represents a novel form of TN-C, or that it is a genetically distinct but related protein such as TN-X (reviewed in Erickson, 1993; Chiquet-Ehrismann et al., 1994). The latter possibility is highly unlikely, given that a 500 kD TN-X protein has been characterized in mice, and the human TN-X transcript is roughly 13 kb in size and predicts a protein in excess of 400 kD (Bristow et al., 1993; Matsumoto et al., 1994). There are several additional explanations for the lack of BC-2 recognition, many of which could be attributed to variable splicing of the FN-III repeats within the ASD. Splicing of the primary transcript such that one or both of the A1 and A3 FN-III repeats which bind BC-2 is omitted, might either eliminate or disrupt BC-2 binding to the protein but still permit recognition by TNA3B probe through cross-hybridization to related sequences. It is also conceivable that the 250 kD form (positive for BC-2) does not contain the entire ASD, but only carries some combination of A1 or A3, and inclusion of all eight FN-III repeats of the ASD, causes a conformational change and abrogates BC-2 binding. In any case, it will be important to confirm the identities of all three transcripts by RT-PCR analysis using primer combinations specific for FN-III repeats within and flanking the ASD. Furthermore, elucidation of the transcript composition should be accompanied by thorough Western blot analysis with a panel of antibodies specific for individual FN-III repeats, as has been developed by Balza and colleagues (Balza et al., 1993).

Another finding to emerge from the Western blot analysis in this chapter is that pre-initiation specimens, sections of which were immunohistochemically negative for TN-C, and similarly, specimens which were immuno-positive for TN-$C_S$ but not TN-$C_L$ in section, contained TN-$C_L$ in immunoblot detection. This discrepancy could be due to the increased sensitivity of the alkaline-phosphatase chemiluminescent substrate as compared to the horse-radish peroxidase method used in immunohistochemical staining and in Figure 2.7. It is possible, also, that skin specimens used for extraction were contaminated by subcutaneous tissue which is often positive for TN-C immunostaining. As a rule, care was taken to eliminate this possibility by the partition of each skin sample into two portions--one for cryoembedding and immunohistochemical analysis, and the other for protein extraction and immunoblotting. Specimens found by histological examination to contain

subcutaneous tissue were not included in either Western or Northern blot analyses, but it nevertheless remains a remote possibility. Alternatively, it is possible that TN-$C_L$ and TN-$C_S$ isoforms are transcribed and translated, and yet are masked or otherwise unavailable for antibody binding in tissue sections until after follicle initiation. Although this does not seem particularly likely, the ever-increasing list of proteins demonstrated to bind TN-C, many of which bind within the ASD, suggests that it is not an unrealistic possibility.

Included in the group of proteins which bind TN-C are the matrix metalloproteinases MMP-2 (also known as Gelatinase A), MMP-3 (Stromelysin 1), and MMP-7 (Matrilysin) (Nagase, 1994; Siri et al., 1995). Although MMP-7 cleaves TN-C at a site proximal to the amino terminus and common to all TN-C isoforms, the ASD is cleaved by MMP-2 and MMP-3 in addition to MMP-7, making TN-$C_L$ uniquely susceptible to degradation by MMP-2 and MMP-3 (Siri et al., 1995). The expression of MMP-2 and MMP-3 is uncharacterized in fetal human skin, but MMP-7 is present in the follicle epithelium during human hair follicle morphogenesis, where it is postulated to contribute to basement membrane degradation during follicle elongation (Karelina et al., 1994). If any one of the metalloproteases does in fact bind TN-C in fetal human skin, obscuring the BC-2 epitope prior to follicle intiation, binding must occur without enzymatic activation since the integrity of the 250 kD band was not compromised, and the degradative products of 120, 170, and 190 kD were not observed.

An alternative, and perhaps more attractive, approach for resolving the apparent discrepancy between Western and immunohistological data will be to conduct a detailed comparative analysis employing a panel of TN-C antibodies specific for individual FN-III repeats, as has been done for the metalloproteinase analysis (Siri et al., 1995), in conjunction with *in situ* hybridization with splice-junction specific end-labeled oligonucleotides, or *in situ* PCR to detect individual splice variants with specificity and confidence. The development of an antibody or antibody panel with specificity for uniquely spliced combinations of ASD FN-III repeats will be exceedingly useful in future studies as well.

Results obtained from analysis of cell proliferation in relation to TN-C expression suggested that there was no clear association between cell proliferation and TN-C immunostaining or mRNA expression at follicle initiation, effectively negating the initiation stage of the morphogenetic model proposed at the end of Chapter II. There was, however, a positive correlation between proliferation of follicle epithelial cells and TN-C

expression at later morphogenetic stages. In particular, follicle elongation was characterized by the striking presence of proliferative and non-proliferative zones in the follicle epithelium, and the same cells of the outer layer of the follicle which contained TN-C transcript were also labeled by the proliferation-specific antibody MIB-1. In contrast, follicle epithelial cells situated at the base and in the center of the follicle appeared to be growth arrested, as were cells of the dermal condensation. The quiescent appearance of the dermal condensation is similar to what Wessells and Roessner reported for murine follicle morphogenesis, and seems to suggest that growth of this specialized cell population is achieved through migration or recruitment of cells from the adjacent mesenchyme and not by replication (Wessells and Roessner, 1965). The delineation of a non-proliferating compartment in the follicle epithelium, contiguous with the growth arrested dermal condensation, represents a new observation. Moreover, although Wessells and Roessner (1965) and Gerstein (1971) separately observed mitotic activity within developing mouse and human follicle epithelia, the clearly compartmentalized pattern of replication reported here indicates there is a delicate balance between proliferating and non-proliferating regions of the follicle. Indeed, the juxtaposition of these two populations, and the maintenance of this organization during the elongation and differentiation stages of morphogenesis, suggests a mechanism for appendage elongation wherein cell replication in the outer layer of the follicle drives non-replicating epithelial and mesenchymal populations further and further into the dermis.

**Figure 3.1 Schematic diagram of TN-C structure**

Tenascin monomers are disulfide-crosslinked into homo-hexamers through the unique N-terminal region. This is followed by 14.5 EGF-like repeats in humans. The distal portion of the molecule contains between 8 and 15 repeated sequences similar to the cell- and heparin-binding Type III region of fibronectin (FN-III), terminating in a globular domain similar to the beta and gamma portions of fibrinogen. Stippling represents FN-III domains which are alternatively spliced. The approximate antigenic regions for monoclonal antibodies BC-4 and BC-2 are indicated. Oligonucleotide primer pairs used for PCR cloning are diagrammed, as well as the corresponding region and length of amplified DNA.

# TENASCIN-C

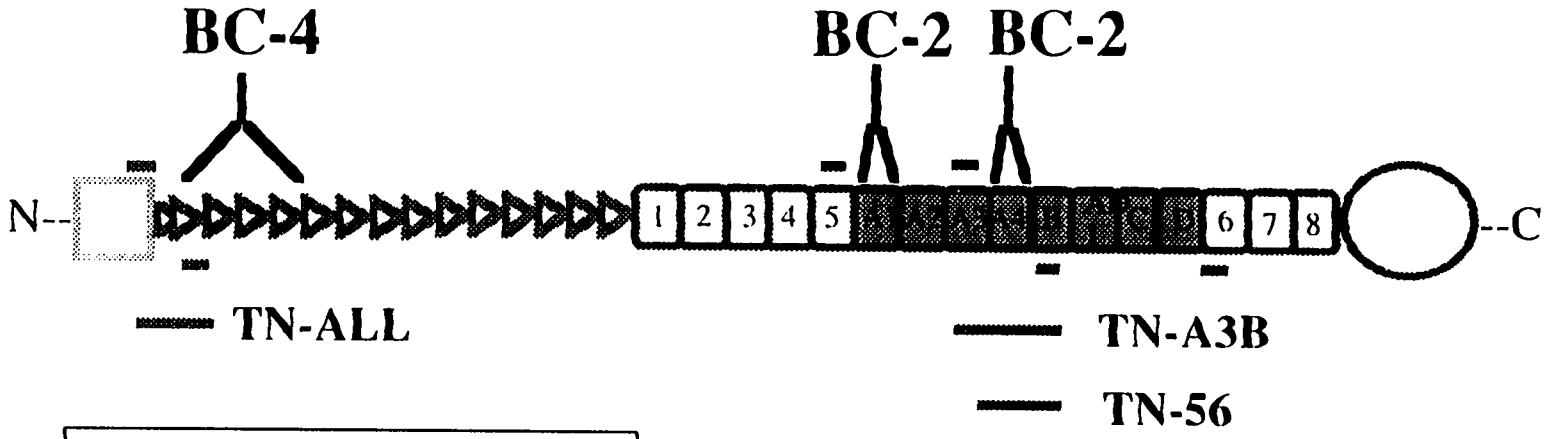
BC-4
BC-2
BC-2
N--
1
2
3
4
5
6
7
8
--C
TN-ALL
TN-A3B
TN-56
EGF-like
FN-III-like
Spliced domain
Fibrinogen-like

**Table 3.1. Plasmid Constructs**

| Construct | Vector | Insert size (kb) | Rest. Enz. | Polymerase |
|---|---|---|---|---|
| pTNEGF | pCR-II | 0.3 | Spe I | T7 |
| pTNEGF | pCR-II | 0.3 | Not I | SP6 |
| pTN56x | pCR-II | 0.5 | Hind III | T7 |
| pTN56z | pCR-II | 0.5 | Hind III | T7 |
| pTNA3B | pCR-II | 0.5 | Hind III | T7 |
| pTNA3B | pCR-II | 0.5 | Xho I | SP6 |
| pCN-I | pCR-II | 0.5 | Bam HI | T7 |
| pCN-I | pCR-II | 0.5 | Not I | SP6 |
| 1 | pBluescript[a] | 1 | Bam HI | T7 |
| 1 | pBluescript | 1 | Sal I | T3 |
| 2 | pBluescript | 1.1 | Bam HI | T7 |
| 2 | pBluescript | 1.1 | Hind III | T3 |

[a]pBluescript SK(-) from Stratagene (LaJolla, CA)

**Table 3.2. Reaction Conditions for Conventional and High Yield RNA Transcription**

| Component | Conventional | High Yield A | High Yield B |
|---|---|---|---|
| GTP | 1 mM | 7.5 mM | 7.5 mM |
| ATP | 1 mM | 7.5 mM | 7.5 mM |
| CTP | 1 mM | 7.5 mM | 7.5 mM |
| UTP | 0.325 mM | 5 mM | 6 mM |
| DTT | 10 mM | 10 mM | 10 mM |
| RNasin | 0.2 U/ µl | ---- | ---- |
| dig-11-UTP | 0.175 mM | 3 mM | 2 mM |
| DNA template | 0.05 µg/µl | 0.05 µg/µl | 0.05 µg/µl |
| Polymerase | 45 U/µl | * | * |
| Volume | 50 µl | 20 µl | 20 µl |
| Inc Time/Temp | 2 hours @ 37°C | 2 hours @ 37°C | 2 hours @ 42°C |

*AmpliScribe polymerases were used according to kit instructions.

**Table 3.3. Summary of reagents and probes**

| Antibody | TN-C Isoform | $M_r$ (kDa) | Construct | Probe | Transcript (kb) |
|---|---|---|---|---|---|
| BC-2 | TN-$C_L$ | 250 kDa | pTNA3B | TNA3B | 7, 8 kb |
| --- | | 220 kDa | pTN56 | TN56 | 6, 7, 8 kb |
| BC-4, F9A5 | all forms TN-C | 300, 250, 220 kDa | pTNEGF | TNEGF | 6, 7, 8 kb |

**Figure 3.2 TN-C immunostaining of separated epidermis**

Light micrograph of separated 11 week EGA epidermis immunostained for TN-C. Bracket indicates hair germ (**hg**). Bar, 40 μm.

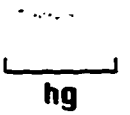
hg

**Figure 3.3 Whole-mount TN-C immunostaining of separated epidermis**
Light micrograph of separated epidermis immunostained for TN-C and viewed *en face*. Arrowheads in (A) indicate placodes of TN-C immunostaining which were irregularly distributed at 10 weeks (**A**), and arranged in an hexagonal array at 11 weeks EGA (**B**), where the placodes were associated with hair germ follicles (arrow). Bar, 40 μm.

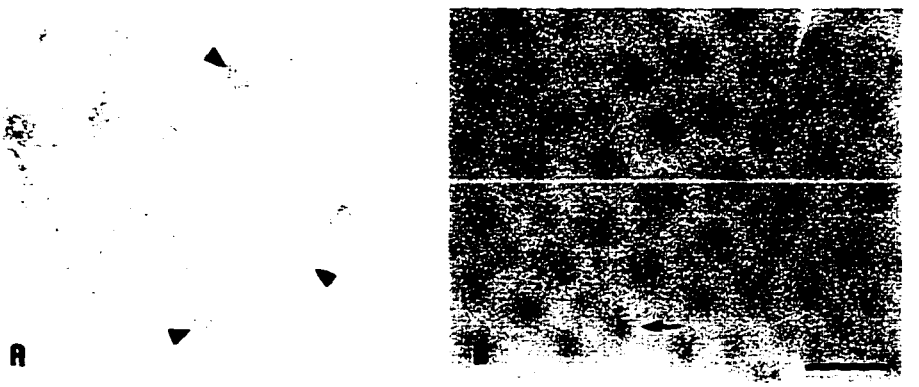
A

**Figure 3.4 A comparison of TN-C immunostaining using monoclonal antibodies BC-4 and BC-2**

Light micrographs of TN-C immunostaining detected with Mab BC-4 (**A**,**C**) and Mab BC-2 (**B**,**D**) at 10.5 week EGA (A, C) and 11.5 weeks EGA (B, D). Arrowheads indicate a placode of TN-C at the dermal-epidermal interface (A), and none in an adjacent section stained with the ASD-specific antibody, BC-2 (B). At 11.5 weeks EGA, immunostaining with BC-4 and BC-2 was nearly identical in the condensed mesenchyme and follicle BMZ (C, D). Bar, 45 μm.

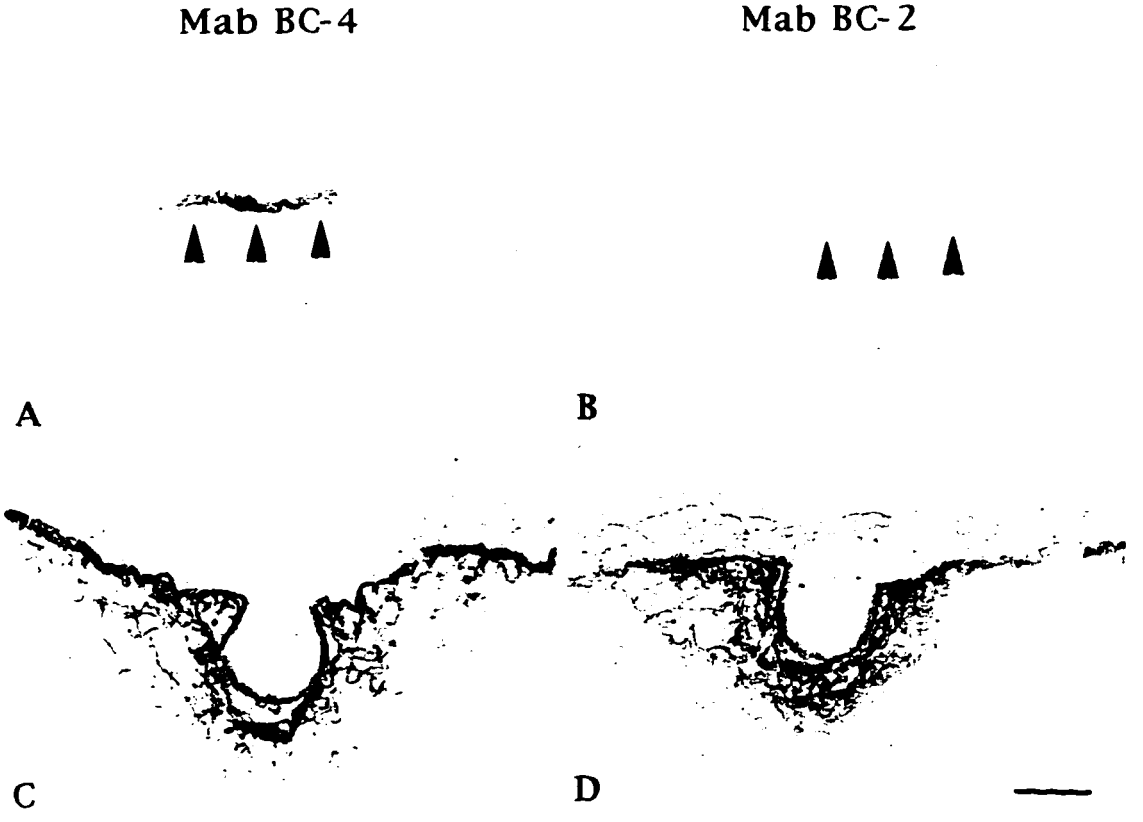
Mab BC-4
Mab BC-2
A
B
C
D

**Figure 3.5 Western blot detection with 2 different antibodies to TN-C**

**A)** Total skin from 9.5, 10, 10.5, 11, 11.5, 12, 13, and 15 weeks EGA was extracted and electrophoretically separated on 7.5% SDS-polyacrylamide gels. Immunoblot detection with Mab F9A5 revealed specific protein bands of $220 \times 10^3$ and $250 \times 10^3$ $M_r$ present in all specimens, while a protein species of approximately $300 \times 10^3$ $M_r$ was detected in specimens of 10 to 10.5 weeks EGA and older (arrows). **B)** A duplicate blot probed with Mab BC-2 shows the presence of a single $250 \times 10^3$ $M_r$ species in all specimens. Purified human TN-C was used as a standard (TN).

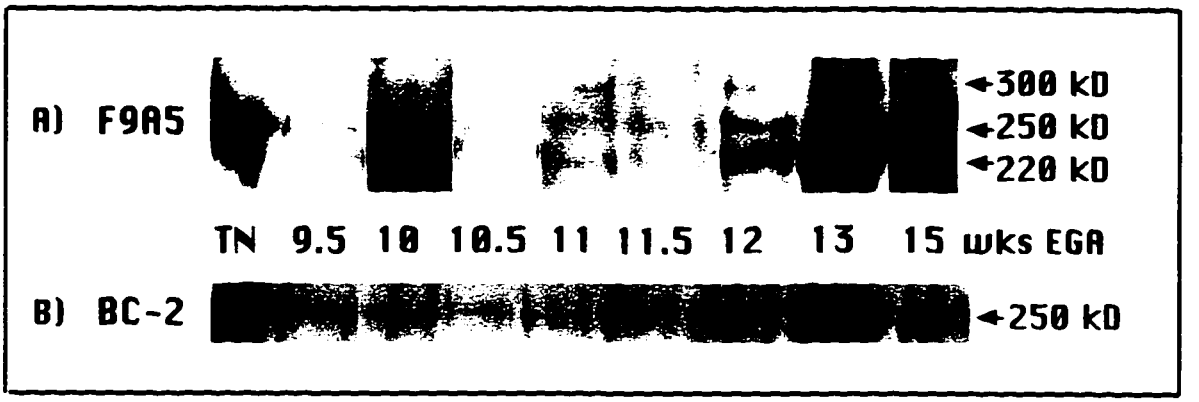
A) F9A5
300 kD
250 kD
220 kD
TN 9.5 10 10.5 11 11.5 12 13 15 wks EGA
B) BC-2
250 kD

**Figure 3.6 Northern blot characterization of TN-C cDNA probes**

Ten micrograms of total RNA from various sources was separated on a 1% (top two panels) or 0.8% (bottom panels) denaturing agarose gel and blotted to nylon membrane for hybridization with radio-labeled TNEGF, TN56 or TNA3B cDNA probes. Transcripts of 6.8 and 7.8 kb were detected in RNA from normal adult myometrium (**M**) and leiomyoma (**L**). Transcripts of 6 and 7 kb were detected with TNEGF and TN56 in RNA from cultured human skin fibroblasts (**hSF**), 11 week EGA fetal skin (**sk**) and cultured human smooth muscle cells (**hSMC**).

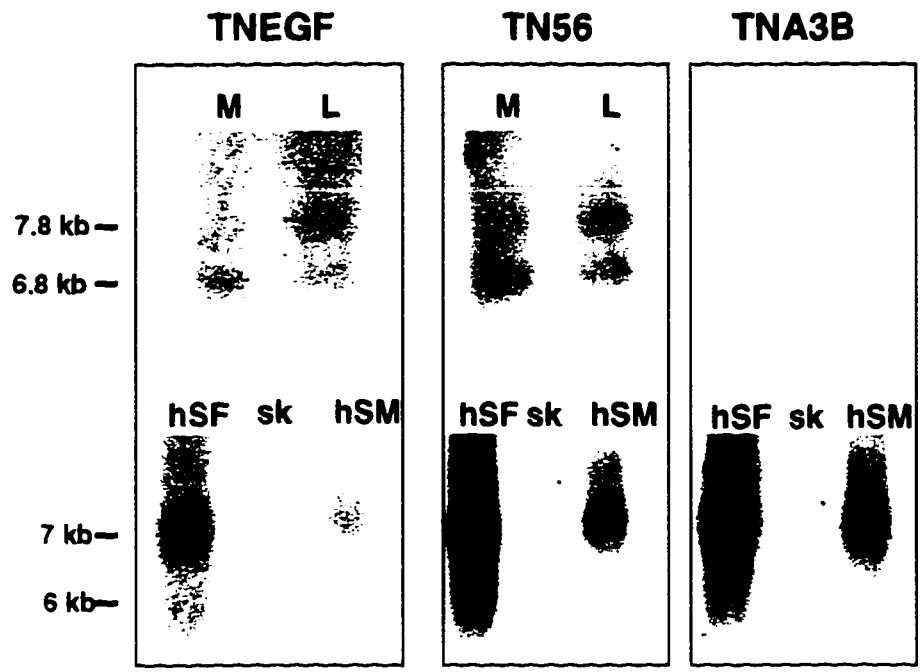
TNEGF
TN56
TNA3B
M
L
M
L
7.8 kb
6.8 kb
hSF
sk
hSM
hSF
sk
hSM
hSF
sk
hSM
7 kb
6 kb

**Figure 3.6 (Continued) Dot blot characterization of TN-C cDNA probes**
1, 0.1, and 0.01 ng of purified insert DNA corresponding to CN-I, TN56, and TNA3B was dotted onto nylon membrane, hybridized with radio-labeled TN56 or TNA3B and washed at 65°C and 0.1 % SDS at the indicated concentration of SSPE.

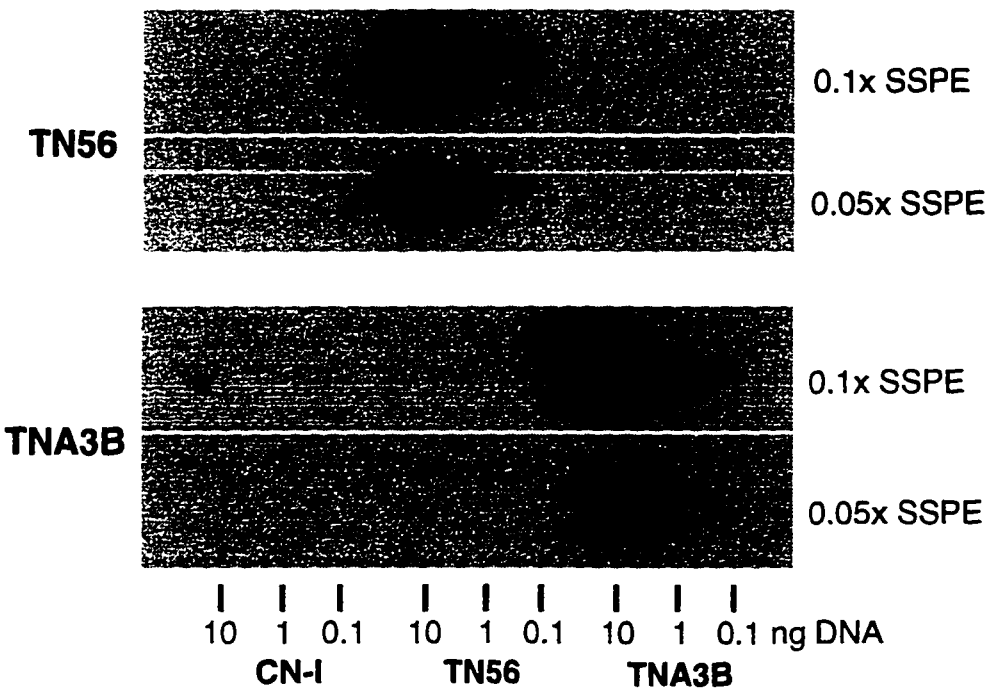
TN56
0.1x SSPE
0.05x SSPE
TNA3B
0.1x SSPE
0.05x SSPE
10 1 0.1 10 1 0.1 10 1 0.1 ng DNA
CN-I
TN56
TNA3B

**Figure 3.7 Northern blot analysis of TN-C transcripts in fetal skin extracts**
Ten micrograms of total RNA from specimens of 9.5 to 15 weeks EGA, (identified individually as A1 to E4) was separated on a 0.8% denaturing agarose gel and transferred to nitrocellulose membrane for hybridization with radio-labeled TNEGF probe. Transcripts of 6 and 7 kb were present in all specimens, and lanes marked with * indicate specimens in which a third, 8 kb transcript was detected. The immunohistochemical staining characteristics, together with morphologic and ontologic information are summarized in the chart below the blot.

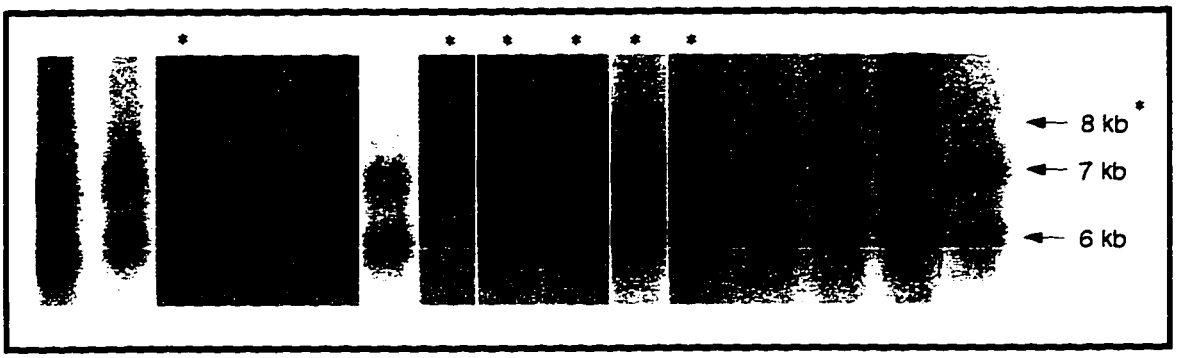


| | | | | | |
|---|---|---|---|---|---|
| – | – | + | + | + | BC-4 |
| – | – | – | + | + | BC-2 |
| pre | init | init | hg | hair peg | Stage |
| <10 wks | 10-11 wks | 10-11 wks | 11-12 | >12 wks | EGA |

**Figure 3.7 (Continued) Ratio of 6 kb TN-C transcript relative to 7 kb transcript**

The relative amounts of 6 kb and 7 kb transcripts detected in Figure 3.7A, graphed as a ratio after normalization to 28S ribosomal RNA on the ethidium-bromide stained negative image.

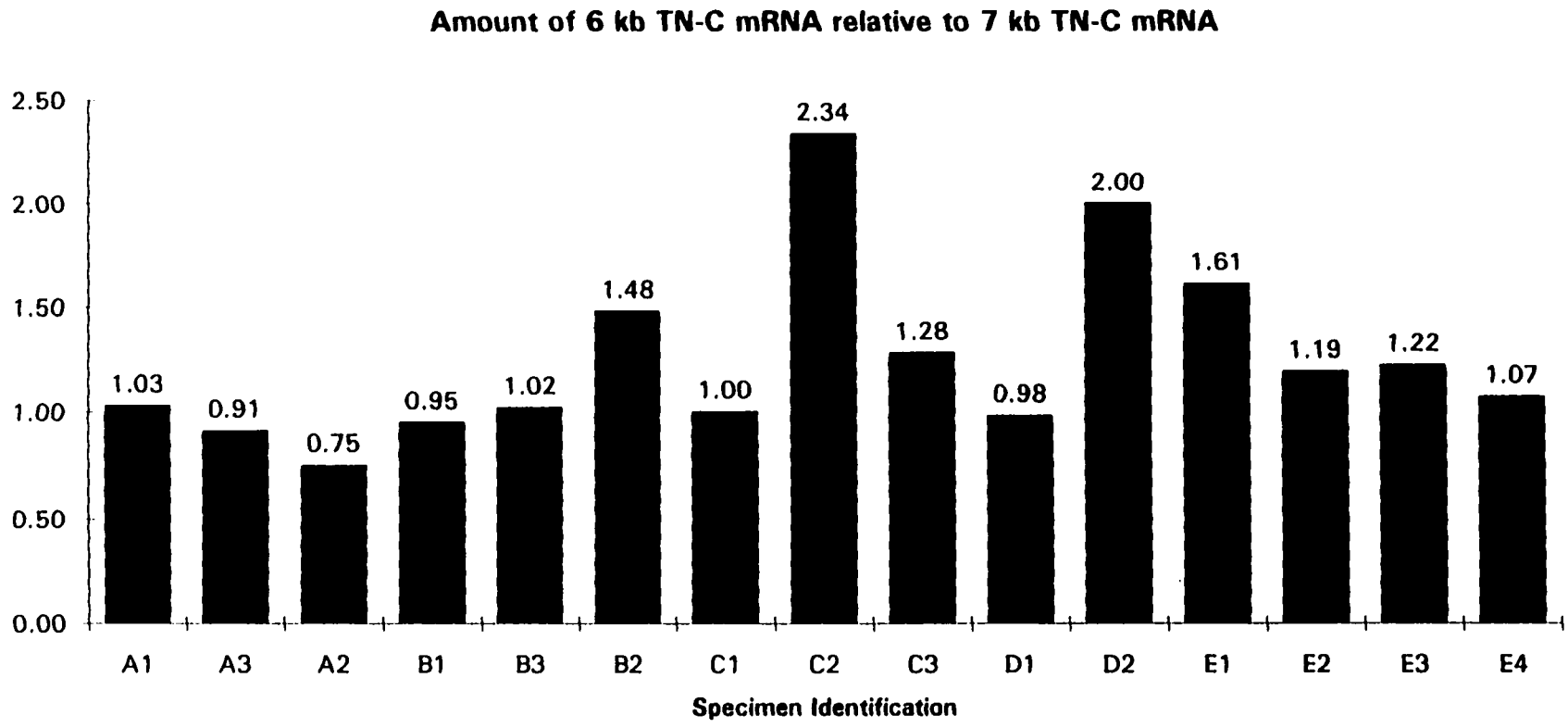
Amount of 6 kb TN-C mRNA relative to 7 kb TN-C mRNA
2.50
2.00
1.50
1.00
0.50
0.00
1.03
0.91
0.75
0.95
1.02
1.48
1.00
2.34
1.28
0.98
2.00
1.61
1.19
1.22
1.07
A1
A3
A2
B1
B3
B2
C1
C2
C3
D1
D2
E1
E2
E3
E4
Specimen Identification

**Figure 3.7 (Continued) Ratio of 6 kb TN-C transcript relative to 7 kb transcript increases at morphognetic initiation**

The average ratio of 6 kb to 7 kb transcript for specimens from Figure 3.7A, categorized according to immunomorphological profile. Error bars indicate standard error of the mean.

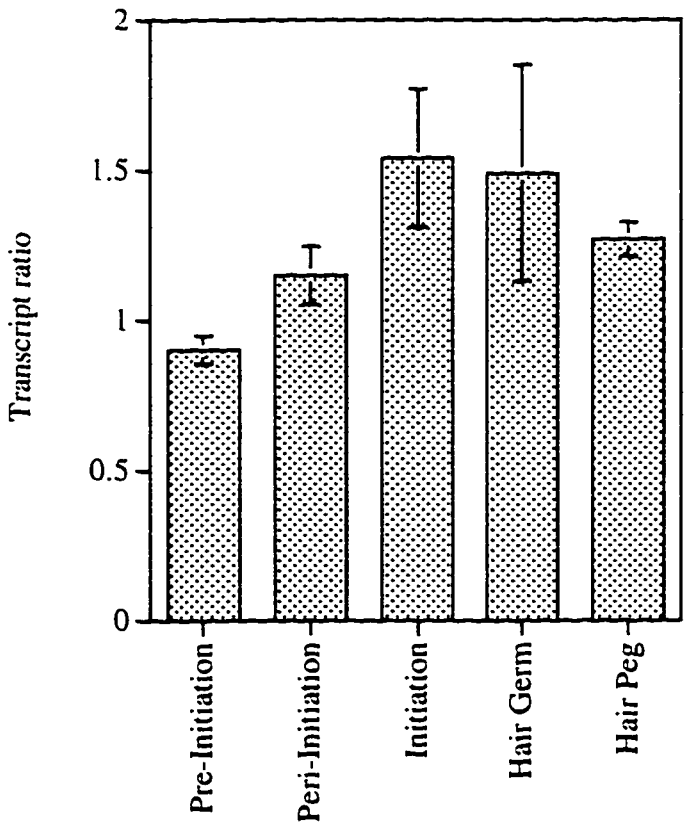
Transcript ratio
2
1.5
1
0.5
0
Pre-Initiation
Peri-Initiation
Initiation
Hair Germ
Hair Peg

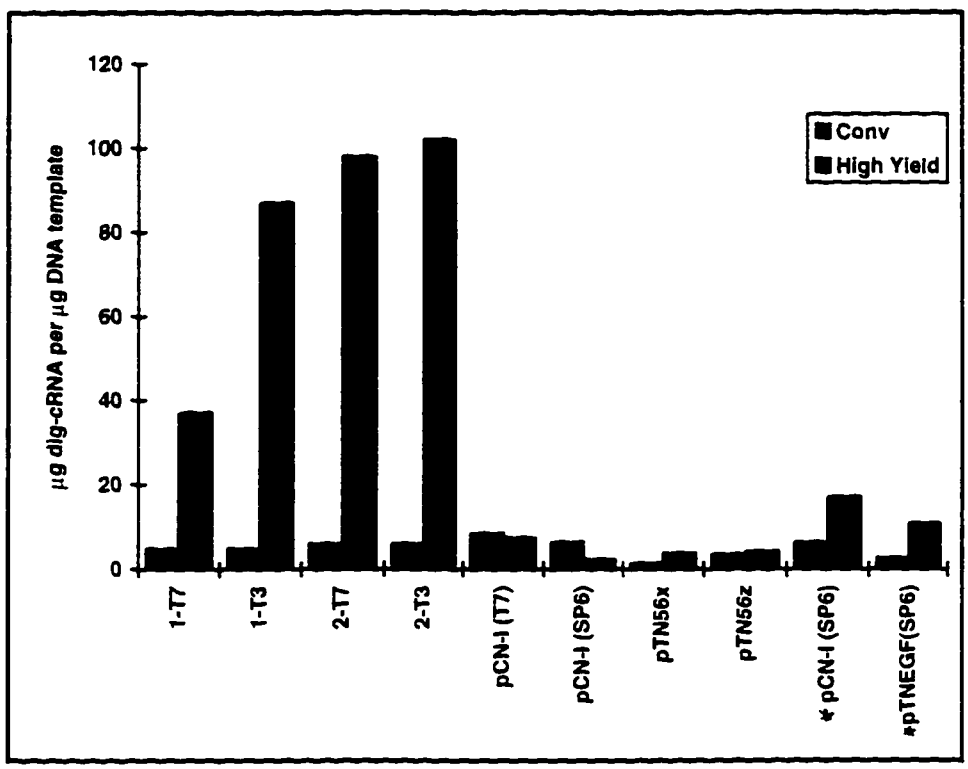


**Figure 3.8 Quantitative comparison of digoxigenin-cRNA yields from conventional and high yield reactions**

Plasmid constructs 1, 2, pCN-I, pTN56 and pTNEGF were used as templates for conventional and high yield transcription reactions indicated in Table 3.2. Yields plotted here were determined spectrophotometrically. Two additional reactions (*) were conducted using a lower concentration of digoxigenin-11-UTP.

**Figure 3.8 (Continued) Northwestern blot comparing digoxigenin-cRNA probes transcribed under conventional and high yield reaction conditions**
Digoxigenin-cRNA transcripts from conventional (Conv) or high yield (HY) reactions were purified by spin-column chromatography (SC) or ammonium acetate precipitation (AA), separated on a 1.2% denaturing agarose gel and blotted to nitrocellulose for immunodetection with alkaline phosphatase-conjugated anti-digoxigenin. Transcripts representing non-specific initiation are indicated (* and **).

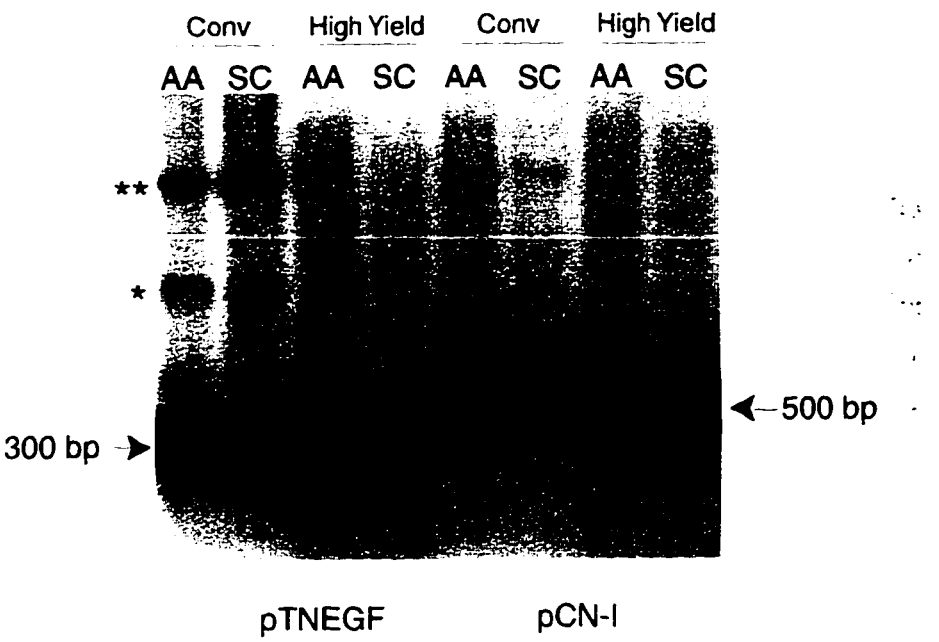
Conv
High Yield
Conv
High Yield
AA
SC
AA
SC
AA
SC
AA
SC
**
*
300 bp
500 bp
pTNEGF
pCN-I

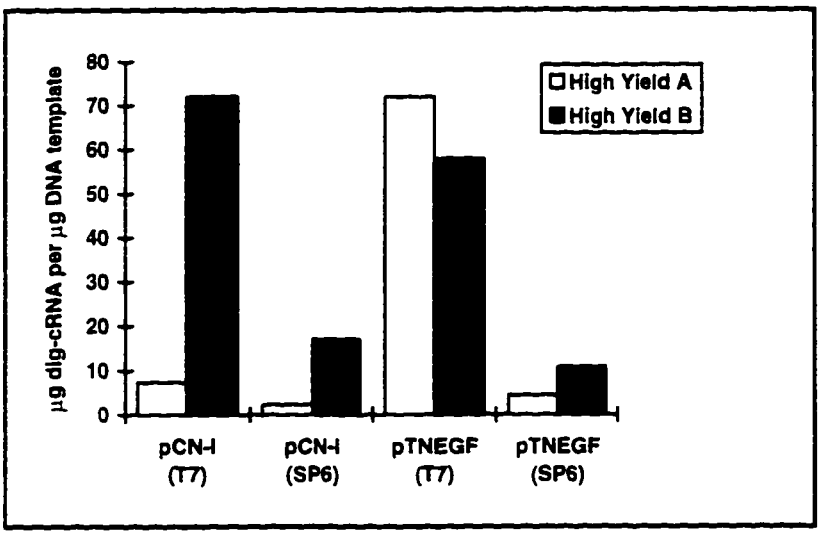


**Figure 3.9 Effect of digoxigenin concentration and incubation temperature on high yield transcription of digoxigenin-cRNA**

High yield T7 and SP6 RNA polymerase transcription reactions were conducted using 3mM digoxigenin-11-UTP concentration and 37 °C incubation temperature (clear bars) or 2 mM digoxigenin-11-UTP and 42°C incubation temperature (gray bars) and yields were quantitated spectrophotometrically for pTNEGF and pCN-I template DNA.

**Figure 3.10 Expression of Type I Collagen mRNA in fetal human skin during hair follicle morphogenesis**

Light micrographs of tissue *in situ* hybridization using a digoxigenin-labeled anti-sense Type I Collagen probe in sections of fetal human skin containing follicles at the pre-germ (* in **A**), hair germ (**B**), hair peg (**C**) and bulbous hair peg (**D**) stages of development. A control section incubated with the sense strand probe (**E**) contains a bulbous hair peg follicle (arrowheads). At all stages, strong hybridization signal was detected in cells of the developing dermis and in follicle-specific cells of the dermal condensation (large arrow in B,C,D). A weaker signal was present in epithelial cells at the base of the hair peg and bulbous hair peg (small arrow in D). Bar, 30 μm.

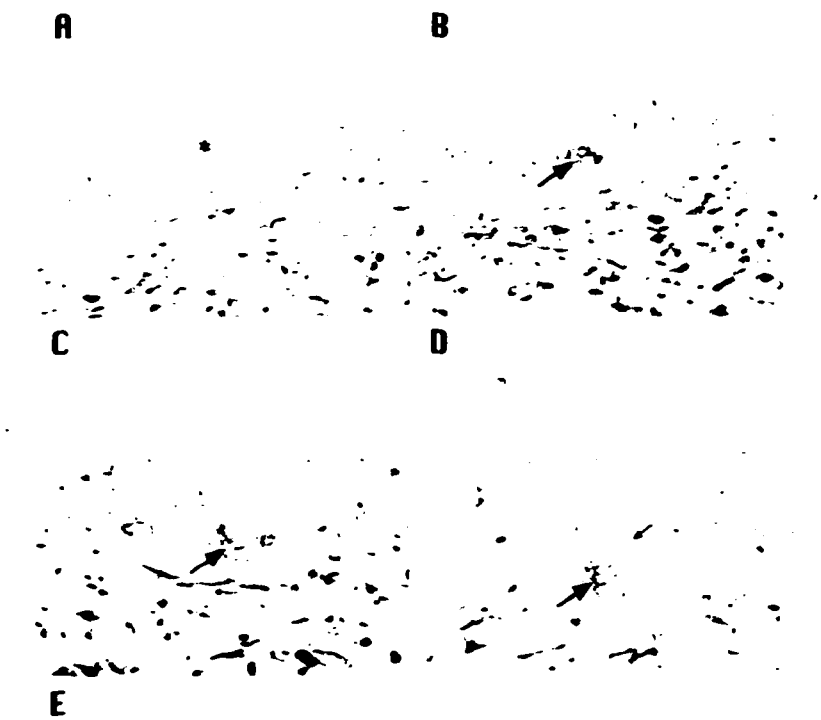
A
B
C
D
E

**Figure 3.11 Patterned expression of TN-C transcript in human hair follicle development**

Light micrographs of tissue *in situ* hybridization using the digoxigenin-labeled TN56 anti-sense probe in sections of fetal human skin. Hybridization signal for TN-C was detected in a cluster of epidermal cells (**A**), and not in cells of the subjacent mesenchyme. At the pre-germ stage (**B**) hybridization was also observed in the cytoplasm of mesenchymal cells of the dermal condensation (arrows indicate invaginated follicle and positive dermal condensation cells). Cells of the hair germ follicle epithelium contained TN-C mRNA (**C, D**), as did those of the dermal condensation (*). Note the segregation of TN-C positive cells to the region of transition from follicle to interfollicular epithelium. Intense labeling was noted in the outer layer of follicle epithelial cells and those of the dermal condensation at the hair peg (**E**) and bulbous hair peg (**F**) stages of development. Note the absence of TN56 hybridization at the follicle base and in the central cord of cells. A control section incubated with the sense strand probe (**E**) contains a hair peg follicle (arrowheads). Abbreviations: **e**, epidermis; **d**, dermis; Bar, 40 μm.

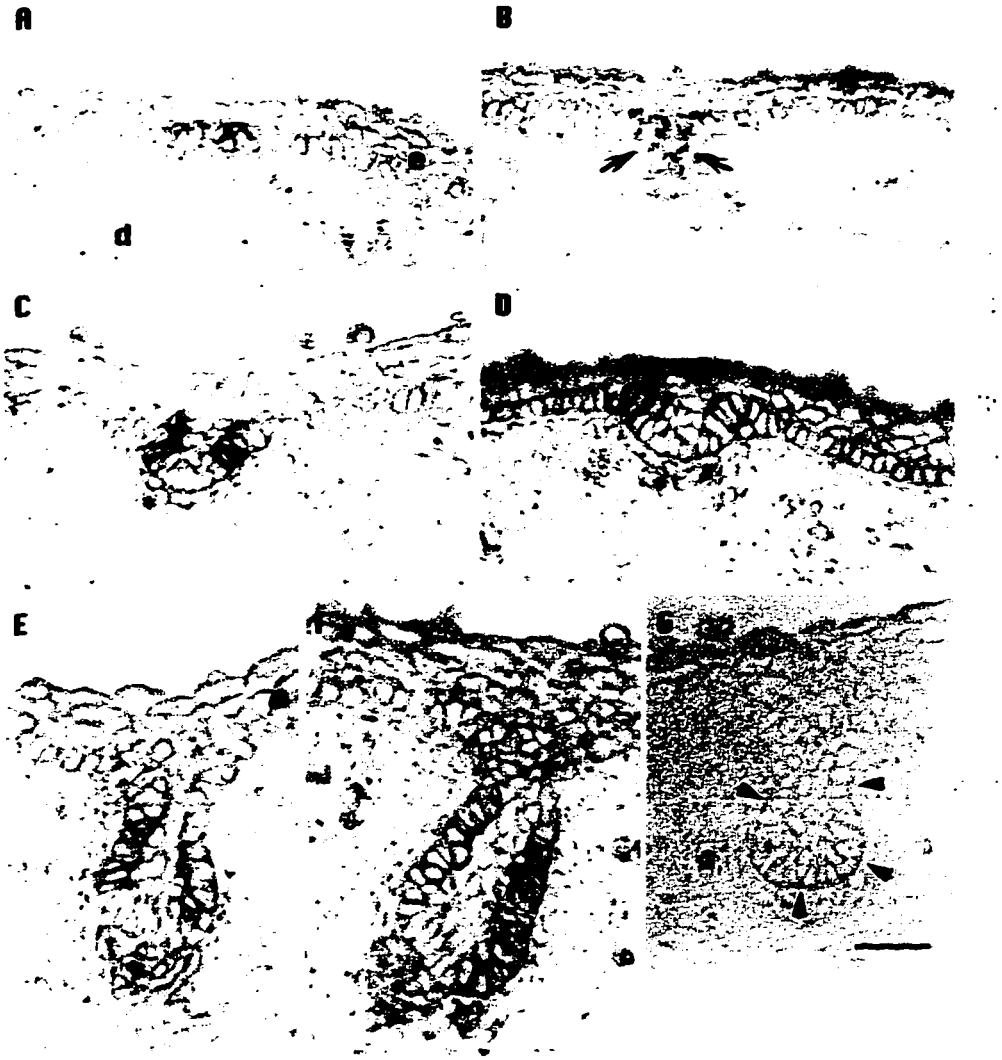
A
B
d
C
D
E
F

**Figure 3.12 Double-label immunostaining for Ki-67 proliferation antigen and TN-C in fetal human skin**

Light micrographs illustrating cell proliferation (dark brown nuclear signal) in the epidermis and mesenchyme of a pre-initiation specimen of 10 weeks EGA (**A**), and mitotic activity in relation to TN-C immunostaining (golden-brown signal) for skin specimens containing initiating (**B**), pre-germ (**C**), hair germ (**D**), hair peg (**E**) and bulbous hair peg (**F**) follicles. Sections were counter-stained with methyl green. A-E: bar= 45 μm; F: bar= 70 μm.


A
B
C
D
E
F

**Figure 3.13 Double-label detection of TN-C transcript and Ki-67 proliferation antigen in fetal human skin**

Light micrographs of human fetal skin sections which were subjected to *in situ* hybridization with digoxigenin-labeled anti-sense (**A-C**) or sense (**D**) TN56 probes and then immunostained with MIB-1 antibody (**A-C**), or with secondary antibody only (**D**). The brownish-purple cytoplasmic staining represents TN-C transcript, and the reddish-pink nuclear label is due to MIB-1 antibody binding. Single-labeled cells expressing TN-C were found in the pre-germ follicle (follicle indicated by * in (**A**)), and double-labeled cells were present in the hair germ follicle (**A** and **B**). A tangential section of a hair peg follicle (**C**) shows double-labeled cells in the outer layer of the follicle epithelium, but not in the core of the follicle. Cells at the base appear to be double-labeled due to the thickness and tangetial plane of section. Cells of the dermal condensation were single-labeled for TN-C transcript only (arrow in C). Bar, 40 μm.

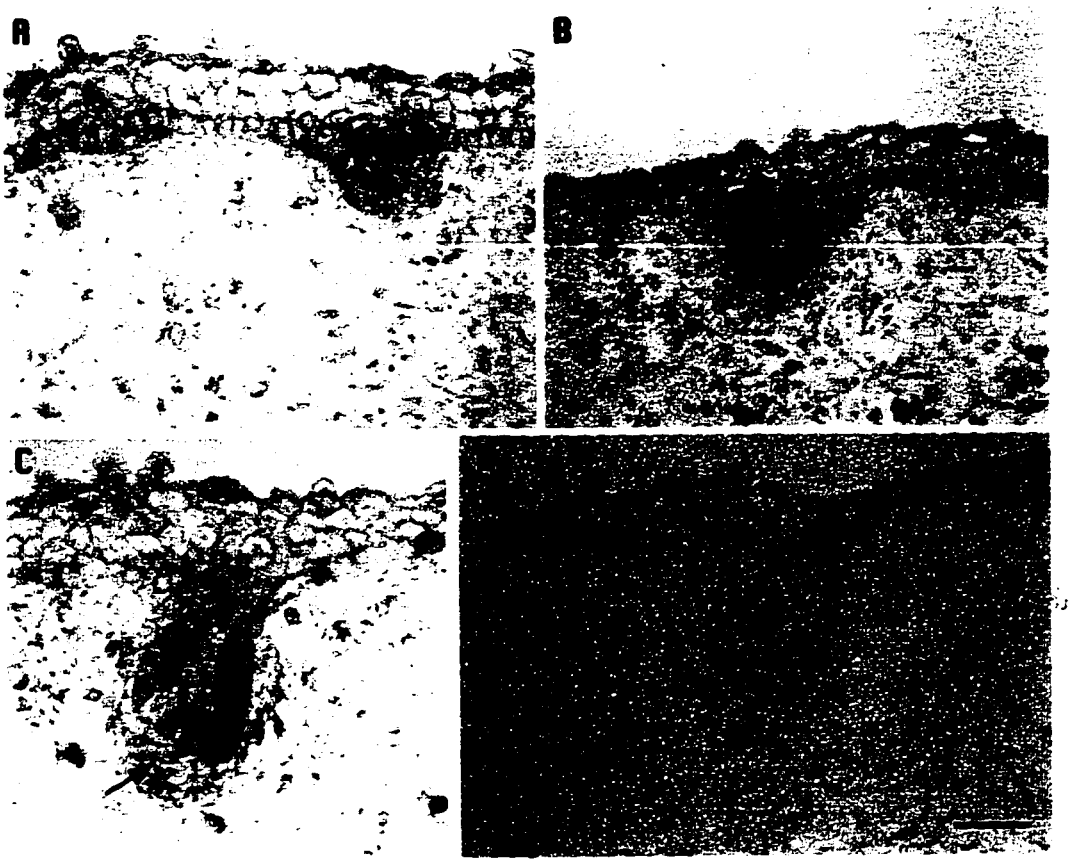
A
B
C

# CHAPTER IV

## TENASCIN-C, VERSICAN AND HYALURONAN: PARTNERS IN THE EXTRACELLULAR MATRIX OF DEVELOPING HUMAN HAIR FOLLICLES?

### INTRODUCTION

Results presented in earlier chapters have shown that during hair follicle morphogenesis, the extracellular matrix protein TN-C is present specifically in the basement membrane zone (BMZ) of the developing follicle, and TN-C mRNA is found in epithelial cells and mesenchymal cells immediately adjacent to the BMZ. While TN-C is purported to disrupt cell adhesion and promote cell migration *in vitro* and *in vivo* (Chiquet-Ehrismann, 1991; Kaplony et al., 1991; Chiquet-Ehrismann, 1993; Hahn et al., 1995), its function at the dermal-epidermal junction during follicle histogenesis is unknown. Both tissues represent potential sources of the TN-C at their interface, and likewise, cells of both tissues are positioned to interact with, and potentially respond to, this extracellular matrix molecule. Cells are proposed to respond to TN-C directly, by binding of TN-C through a cell surface receptor, or indirectly, by binding of TN-C to a receptor ligand such that the receptor-ligand interaction is perturbed or even prevented (Prieto et al., 1993). Numerous cell-surface proteins with previously identified ligands have now been demonstrated to bind TN-C. The current list includes several members of the integrin receptor family, the neuronal transmembrane protein contactin/F11, and a growing number of extracellular matrix and cell surface-associated proteoglycans (Prieto et al., 1993; Sriramarao et al., 1993; Chung and Erickson, 1994; Vaughan et al., 1994).

Integrin-mediated binding of TN-C was suggested initially by experiments in which cell adhesion to the carboxy-terminal portion of chick TN-C was inhibited by a synthetic oligopeptide containing the amino acid sequence arginine-glycine-aspartic acid (RGD) (Friedlander et al., 1988). This was reinforced when cDNA sequence analysis predicted a tri-peptide RGD integrin binding motif in the third fibronectin-III repeat of TN-C, the amino acid sequence of which is evolutionarily conserved between human and chick (Pearson et al., 1988; Nies et al., 1991; Siri et al., 1991). The epithelial integrin dimers $\alpha 2\beta 1$ and $\alpha 9\beta 1$, and the integrin $\alpha v\beta 3$, have since been reported to mediate cell binding to TN-C, although only $\alpha 2\beta 1$ utilizes the RGD sequence (Bourdon and Ruoslahti, 1989; Prieto et al., 1993; Sriramarao et al., 1993; Yokosaki et al., 1994). The absence of $\beta 3$

subunit in human fetal epidermis excludes αvβ3 as a possible tenascin receptor in follicle morphogenesis (Hertle et al., 1991). The same authors reported that although the β1 subunit was constitutively present, α2 was distributed heterogeneously and appeared "patchy" at approximately the same developmental time as placodes of TN-C are detected in the BMZ. This indicated that the α2β1 integrin might be a candidate to mediate epidermal cell binding of TN-C. Moreover, antibodies to either TN-C or β1 integrin, added separately to embryonic chick skin explants, disrupted feather follicle morphogenesis *in vitro*, suggesting that an interaction between the two proteins may be involved in avian morhogenesis of cutaneous appendages (Jiang and Chuong, 1992). In addition to regulating cell morphology by serving as a transmembrane link between extra- and intracellular structural elements, integrin receptors are directly related to cytoplasmic signal transduction pathways, altering transcriptional activity and dramatically affecting primary cell processes such as migration, proliferation and differentiation (reviewed in Dedhar, 1995; Edwards and Streuli, 1995). One goal of the present study, then, was to examine the expression of the integrin subunits α2 and β1 in fetal human skin specimens of initiation age.

As discussed in Chapter II, proteoglycans represent yet another class of molecules with TN-C binding activity. In the initial purification of TN-C from myotendinous junctions of embryonic chicks, the protein was found in close association with a large chondroitin sulfate proteoglycan (Chiquet and Fambrough, 1984). Similarly, the proteoglycan CTB co-localized with TN-C in the avian central nervous system, and also co-purified with TN-C, contaminating the preparation of TN-C used for antibody production (Hoffman and Edelman, 1987; Hoffman et al., 1988; Hoffman et al., 1990). More recently, TN-C binding activity was demonstrated for phosphacan, a proteoglycan isolated from rat central nervous system (Grumet et al., 1994). This is of particular interest because phosphacan is analagous to the extracellular portion of a transmembrane receptor tyrosine phosphatase, RPTP-β, which is found in the human central nervous system and is expected to affect cytoplasmic signal transduction through its phosphatase activity (Barnea et al., 1994). Proteoglycans with TN-C binding activity, then, are associated with the cell membrane and with the extracellular matrix, and TN-C could potentially affect cell behavior either directly or indirectly, depending upon the proteoglycan and extracellular matrix profile of a given cell.

Versican is a large CSPG which is a member of the group of aggregating proteoglycans involved in organizing extracellular matrix and modulating cell adhesion (reviewed in Margolis and Margolis, 1994). It is expressed in the stratum basalis, the proliferative compartment of the epidermis, and in the dermis of adult human skin, as well as in the dermal papillae of developing murine hair follicles (Zimmermann et al., 1994; du Cros et al., 1995). The avian homolog of versican, PG-M, is co-distributed with TN-C during feather follicle morphogenesis, and versican and TN-C are co-localized in rat brain (Perides et al., 1993; Yamagata et al., 1993). Tenascin-C is one member of a growing family of proteins which are related structurally but represent distinct gene products (reviewed in Erickson, 1993; Chiquet-Ehrismann et al., 1994). The family includes the neural protein TN-R (restrictin; J160/180), which was demonstrated recently to overlap with versican *in vivo* and to bind versican *in vitro* (Aspberg et al., 1995). It is possible, then, that versican might interact with TN-C as well, and, because a CSPG of unknown identity overlaps with TN-C in the follicle BMZ (presented in Chapter II), it was important to examine the distribution of versican specifically to determine if it is co-distributed with TN-C and could potentially interact with TN-C during the morphogenetic process of follicle development.

A distinguishing property of the aggregating proteoglycans, such as versican, is their ability to bind hyaluronan (HA), a highly hydrated, polyanionic long chain carbohydrate present in the extracellular matrix (reviewed in Margolis and Margolis, 1994). A primary function of hyaluronan is thought to be the maintenance of extracellular space for diffusion of soluble factors and facilitation of cell movement (reviewed in Laurent and Fraser, 1992). Hyaluronan-dependent cell migration *in vitro* is mediated by the transmembrane receptor, RHAMM, which stands for Receptor for Hyaluronan-Mediated Motility (Savani et al., 1995), and cell adhesion to hyaluronan involves the cell surface adhesion molecule CD44 (reviewed in Underhill, 1992). A lack of hyaluronan has been proposed to contribute to the formation of the dermal condensation in murine follicle morphogenesis (Underhill, 1993). Heparin is structurally similar to HA, and is bound by the fifth FN-III repeat of TN-C, making it plausible that TN-C binds HA as well (Marton et al., 1989; Weber et al., 1995). Indeed, biochemical characterization of avian TN-C suggested an association between TN-C and a large hyaluronidase-sensitive molecule which was not identified but may have been hyaluronan (Hoffman et al., 1988).

Since the presence of either versican or HA in regions of the follicle where TN-C is localized offers a potential mechanism for indirect modulation of cell adhesion or migration through one of the HA receptors (CD44 or RHAMM), and since the interaction of TN-C with either an integrin receptor or a transmembrane phosphatase represents a path by which TN-C might affect intracellular signal transduction, the goal of the present study was to examine the expression of these macromolecules to determine if they coincide with that of TN-C during the morphogenetic period of hair follicle development in fetal human skin.

## EXPERIMENTAL PROCEDURES

*Antibodies and reagents*

Purified human tenascin and monoclonal antibodies P1E6 and P4C10, to $\alpha_2$ and $\beta_1$ integrin subunits, respectively, were purchased from Gibco Life Technologies (Gaithersburg, MD). A monoclonal antibody to RPTP-B was graciously provided by Dr. Joseph Schlessinger (New York University Medical Center). Polyclonal antibody VC-3, against recombinant human versican core protein, was the generous gift of Dr. Richard LeBaron (University of Texas, San Antonio), and the biotinylated hyaluronan probe was kindly given by Dr. Charles Underhill (Georgetown University). Chondroitin ABC lyase, *streptomycces* hyaluronidase, chondroitin sulfate glycosaminoglycan, and fucose were purchased from Sigma (St. Louis, MO), and laminin was from Collaborative Research Products. Dr. Susan Potter-Perigo (University of Washington) generously provided preparations of radio-labeled versican and small dermatan sulfate proteoglycan purified from cultured human smooth muscle cells.

*Immunofluorescent antibody staining and double labeling*

For double-labeled immunofluorescent detection of TN-C and versican, 6 μm cryosections were rinsed in PBS, fixed for 5 min. in 4% paraformaldehyde, washed in TBS, and equilibrated in acetate buffer for chondroitin ABC lyase digestion, as described in Chapter II. Following enzymatic treatment, sections were washed in TBS, non-specific antibody binding was blocked for 30 minutes with normal horse and normal goat serum, and monoclonal antibody BC-4 and polyclonal antibody VC-3 (diluted 1:800) were combined in 1% BSA in TBS, and applied to sections for 1 hour. After washing in TBS, sections were incubated for 30 minutes with a mixed solution of secondary antibodies containing FITC-conjugated anti-rabbit secondary diluted 1:100 (Cappel, Organon

Teknika Corporation, Durham, NC) and biotinylated anti-mouse secondary (used as described previously). Sections were washed briefly and incubated with avidin-Texas Red (Molecular Probes, Eugene, OR) before a final wash in TBS and coverslipping with Vectashield mounting medium (Vector Laboratories, Burlingame, CA). The protocol was modified slightly so that the avidin-Texas Red conjugate could be used to visualize the biotinylated hyaluronan probe (diluted to 4 μg/ml) in the simultaneous detection of TN-C and hyaluronan. Sections were prepared as above, except that enzymatic treatment was omitted, and bound Mab BC-4 was detected using FITC-conjugated anti-mouse antibody (Cappel) which resulted in a comparatively weaker signal relative to that obtained with the biotin-avidin-Texas Red combination. Fluorescently labeled sections were viewed and photographed using a Zeiss Axioskop equipped with epifluorescence imaging capability.

*Gel mobility shift assay*

Binding interactions of purified TN-C with purified proteoglycan (either versican or biglycan-enriched small proteoglycans) were examined using a gel mobility shift assay described by Camejo et al (Camejo et al., 1993). Briefly, a fixed amount of purified $^{35}SO_4$-labeled proteoglycan ($6 \times 10^{-7}$ μmol of versican, or $6.8 \times 10^{-6}$ μmol small dermatan sulfate proteoglycan) was mixed with increasing amounts of TN-C (or laminin) in a 20 μl reaction volume containing physiologically balanced sample buffer (10 mM HEPES, pH 7.4, 140 mM NaCl, 5 mM $CaCl_2$ and 2 mM $MgCl_2$) and, in some cases, either 7 mM EDTA, or an 10-fold molar excess of fucose or chondroitin sulfate glycosaminoglycan. Samples were incubated for 45 minutes at 20°C followed by 60 min at 37°C, after which they were mixed with 2 μl loading buffer (containing 10% glycerol and bromophenol blue) and loaded on a horizontal 0.7 % low melting point agarose gel (NuSeive, FMC Biomedicals) which was pre-equilibrated in running buffer containing 10 mM HEPES, pH 7.2, 2 mM $CaCl_2$ and 4 mM $MgCl_2$. Samples were electrophoresed for 3 hours at a constant 60 volts at 4°C after which the gel was fixed for 1-2 hours in 0.1 % cetyl-pyridium-chloride (in 30 % isopropanol and 10 % acetic acid) and allowed to air-dry before autoradiographic detection of labeled proteoglycans.

## EXPERIMENTAL RESULTS

### *$\alpha_2\beta_1$ integrin is present in fetal epidermis at hair follicle initiation*

Parallel sections of specimens containing either initiating follicles (defined by placodes of TN-C) or follicles at the hair germ stage were immunostained for the $\alpha_2$ and

$\beta_1$ integrin subunits (Figure 4.1). Immunostaining of the basal epidermal layer with P1E6 antibody against the $\alpha 2$ subunit was continuous, and no "patchy" expression was observed in specimens which contained TN-C foci. After initiation, all cells of the follicle hair germ were positive for $\alpha 2$. In parallel sections stained for the $\beta_1$ integrin subunit, immunoreactivity was observed on cells of the basal and intermediate epidermal layers. Strong labeling was observed on profiles in the developing dermis, most likely developing microvasculature, and mesenchymal cells were weakly labeled by the $\beta_1$ antibody. The pattern was preserved at the hair germ stage. The distribution of $\beta_1$ is similar to what Hertle and colleagues found, but the $\alpha 2$ pattern is partially in contrast to their findings, where about 50 % of the specimens had a heterogeneous distribution of $\alpha 2$ (Hertle et al., 1991). Thus, $\alpha_2\beta_1$ integrin is already present on basal epidermal cells when TN-C is deposited in the BMZ. This does not exclude, and in fact supports the hypothesis that selective expression of TN-C may interfere with the binding of $\alpha_2\beta_1$ to its normal ligand, thereby disrupting cell adhesion and contributing to morphogenetic initiation.

***RPTP-β is not detected in fetal human skin***

The distribution of the tyrosine phosphatase RPTP-β was examined in a developmental series of fetal skin sections incubated with an antibody to RPTP-β and compared to control sections of fetal human retina and adult human cerebellum. While immunolabeling was detected along radial processes in fetal retina and adult cerebellum, fetal human skin sections were not labeled at any age (data not shown). This suggests that RPTP-β is not present in fetal skin, a finding which is not entirely unexpected since RPTP-β/phosphacan has been characterized in the developing central nervous system (Canoll et al., 1993; Levy et al., 1993).

***Versican and hyaluronan overlap with TN-C during hair follicle morphogenesis***

A developmental series of fetal human skin sections was double-labeled so that the distribution patterns of versican and hyaluronan (HA) could be examined in relation to that of TN-C. Prior to the initiation of follicles and the expression of TN-C, labeling for versican and HA was widespread in the developing dermis (not shown). At the follicle pre-germ stage, when TN-C was restricted to the follicle BMZ, heterogeneous labeling of HA was observed throughout the dermal extracellular matrix (Figure 4.2A,B). Overlapping labeling of HA and TN-C was present in the follicle BMZ, indicated by the

yellow signal obtained with a double-exposure micrograph (Figure 4.2C). Parallel sections double-labeled for TN-C and versican revealed widespread versican immunoreactivity in the fetal dermis, and co-localization with TN-C in the follicle BMZ. Versican immunostaining of mesenchymal tissue was primarily associated with the extracellular matrix, as indicated by immunonegative regions which corresponded to cellular profiles. Weak double-labeling delineated the boundaries of follicle epithelial cells, indicating that the comparatively limited extracellular space between epidermal cells contains versican and TN-C alike.

During follicle elongation into the dermis (hair germ stage), overlapping TN-C and HA labeling was observed in the follicle BMZ and the condensed mesenchyme, while HA alone was abundant in the interfollicular dermis (Figure 4.3). An adjacent section from the same specimen revealed a co-distribution of versican and TN-C in the condensed mesenchyme, with versican immunoreactivity extending into the interstitial regions of the developing dermis.

Later during follicle elongation, TN-C immunostaining was present in the follicle BMZ, in a fibrillar pattern in the extracellular matrix of the follicle sheath, and in association with follicle epithelial cells situated at the externo-lateral position, approximately in the proliferative zone identified by MIB-1 antibody staining (Figure 4.4). Abundant versican immunoreactivity was detected in the extracellular matrix of intrafollicular regions, and coincided with TN-C in the extracellular matrix of the condensed mesenchyme and in the follicle BMZ. Excepting those cells at the follicle base, versican immunostaining also delineated cells of the follicle epithelium at this stage of morphogenesis.

The early stage of follicle differentiation is characterized by the widened, bulbous appearance of the base of the developing appendage. In this phase, TN-C was present in the follicle BMZ, the matrix of the follicle sheath and the dermal condensation (Figure 4.5). Borders of follicle epithelial cells were stained weakly, excluding those at the widened base which were immunonegative. Versican co-localized with TN-C in the follicle epithelium, the follicle BMZ and sheath, and the dermal condensation. Single-labeling for versican extended into the dermis. A double exposure micrograph of TN-C and HA illustrates that these two molecules were distributed together in follicle sheath and follicle BMZ, where versican was also localized. Follicle epithelial cells were positive for HA, with decreased signal intensity on cells at and near the follicle base.

Double fluorescent detection of versican and HA in a slightly more differentiated follicle (note the invaginating base of the follicle) revealed overlapping labeling in the interstitial dermis, and the follicle-specific BMZ, sheath, and epithelium (Figure 4.5). Versican and HA both were reduced in the dermal condensation, relative to the follicle sheath, although the very center of the dermal condensation was labeled strongly for both. The follicle sheath, follicle BMZ and the center of the dermal condensation were regions of overlapping staining for TN-C, HA and versican, as seen by comparing a double exposure of a section labeled with anti-TN-C and biotinylated HA probe to TN-C and versican double exposure (compare Figure 4.5C and D). The cell-associated epithelial labeling observed at earlier stages persisted at this stage, although a striking feature of the differentiating follicle was the apparent absence of versican, HA and TN-C from the follicle base, the region containing cells which later differentiate to form the hair fiber.

This series of micrographs demonstrates that although TN-C is more resticted temporally and spatially than either versican or HA, the three molecules overlap in follicle-associated mesenchyme, BMZ and epithelium during follicle morphogenesis, and they are uniformly excluded from the presumptive hair fiber producing region of the developing follicle.

***TN-C binds versican under physiological conditions***

The overlapping distribution of versican and TN-C in fetal human skin, together with evidence that the two molecules may be associated non-covalently, prompted a search for binding interactions between TN-C and versican. Preliminary analysis was conducted using a gel mobility shift assay, a technique used widely to characterize DNA-protein binding interactions which has recently been modified to examine proteoglycan-lipoprotein interactions (Camejo et al., 1993). An autoradiograph from a single experiment is shown in Figure 4.6A, in which a purified preparation of $^{35}SO_4$-labeled versican was incubated with range of up to 2-fold molar excess of unreduced (hexameric) TN-C under physiological buffer conditions, and analyzed for electrophoretic mobility. Versican migrated freely into the gel in the absence of TN-C. At a molar ratio of TN-C to versican of 0.25 or less, versican mobility was unchanged, while at a molar ratio of 0.5 or above, the mobility of radio-labeled versican was retarded such that it remained at or near the gel origin. This indicates not only that purified TN-C and versican interact to form an

aggregated complex of high molecular weight, but the molar ratios suggest further that a single TN-C hexabrachion binds two versican molecules.

To examine the specificity of the interaction between TN-C and versican, as well as to investigate potential binding mechanisms, a series of control experiments was conducted, the results of which are shown in Figure 4.6B. Laminin is a heterotrimeric glycoprotein with molecular mass approximately equivalent to that of the TN-C hexabrachion, and is a major component of basal laminae, including the basement membrane of fetal human skin where TN-C is found (Fine et al., 1984; Kleinman and Weeks, 1989). The same molar amount of laminin was substituted for TN-C, and analyzed for binding to versican in the mobility shift assay. Although radiolabeled versican remained at the origin, free versican migrated well into the gel, even in the presence of a 12-fold molar excess of laminin (lane 5), suggesting that there is no binding interaction between laminin and versican and indicating that versican binds TN-C specifically. The reason for the signal at the origin is unclear at this time, but possible explanations being examined are that either purified versican has self-aggregating properties, or the versican preparation may be contaminated by bound hyaluronan, or even TN-C, which was not removed during purification.

The glycosaminoglycan chains of proteoglycans carry a high density of negative charges, raising the possibility that the association of TN-C with versican is due to non-specific charge interactions. This possibility was examined in part by substituting, in place of versican, an equimolar amount of glycosaminoglycan, covalently associated with the small, leucine-rich dermatan sulfate proteoglycans biglycan and decorin, both of which are present in fetal human skin (Bianco et al., 1990). There was no shift in the mobility of the small proteoglycan, even at the highest levels of TN-C (lane 24), indicating that TN-C associates with versican specifically.

Because the binding of versican to TN-R/restrictin is calcium-dependent, and is mediated by the lectin-binding domain of versican (Aspberg et al., 1995), the same parameters were examined for involvement in the interaction of versican with TN-C. Results are included in lanes 6-18 in Figure 4.6B. For comparison, part of the experiment shown in Figure 4.6A was repeated and is pictured in lanes 15-18 in Figure 4.6B. Although radiolabeled versican remained at the origin in all samples (discussed above), free versican migrated well into the gel in lanes 15 and 16 (0 and 0.25 molar ratio of hexabrachion) but not in lanes 17 and 18 (0.5 and 1-fold molar excess of hexabrachion).

The presence in the incubation buffer of either 7 mM EDTA (lanes 6-8), or a 10-fold excess of fucose, the lectin bound preferentially by the lectin-binding domain of versican (lanes 9-11), caused versican to migrate freely into the gel at the same molar ratios of hexabrachion where versican mobility was retarded (compare lanes 7-8 and 10-11 with 17 -18 and also 0.5 and 1-fold excess in Figure 4.6A). Formation of the aggregated complex of TN-C and versican was also prevented by the presence of a 10-fold excess of free chondroitin sulfate glycosaminoglycan (lanes 12-14, compare lanes 13-14 with 17-18). Taken together, these results suggest that interaction of versican and TN-C is calcium-dependent, may be mediated by the lectin-binding domain of versican and is influenced by the presence of chondroitin sulfate glycosaminoglycan chains as well.

## DISCUSSION

The extracellular matrix protein TN-C has a restricted distribution in association with developing hair follicles in fetal human skin, and its expression is correlated with mitotic activity in the follicle epithelium, but not in the adjacent, follicle-specific mesenchyme (Chapters II and III). Temporal regulation of alternatively spliced transcript and protein forms of TN-C was observed as well. While its function in this developmental system is uncharacterized, TN-C interacts with other molecules in the extracellular environment such as fibronectin, and the alternatively spliced region disrupts focal adhesion contacts, suggesting that TN-C modulates cell behavior *in vitro* by affecting adhesive and non-adhesive interactions (reviewed in Erickson, 1994; Hoffman et al., 1994). Consequently, the focus of the current research was to examine the spatio-temporal distributions of some of these TN-C-binding proteins, to determine if they coincide with the pattern of TN-C expression in human hair follicle morphogenesis. The results demonstrate that in fetal human skin, $\alpha 2\beta 1$ integrin, versican and HA, but not RPTP-$\beta$, are more widely expressed, temporally and spatially, than is TN-C. Thus, although there are other extracellular molecules, such as collagen Types I and III, or adhesion molecules, such as E-cadherin, which are absent or diminished from regions of TN-C immunostaining (Smith et al., 1986), all of the proteins examined here, except RPTP-$\beta$, coincide with the distribution of TN-C during hair follicle morphogenesis.

The distribution of $\alpha 2\beta 1$ integrin in fetal human skin on basal epidermal cells was almost exactly in agreement with the findings of Hertle and colleagues (Hertle et al., 1991). A primary motivation for including this receptor in the present study was the

anticipation of a spatial correlation between focal deposits of TN-C in the BMZ and the heterogeneous distribution of the α2 subunit of the α2β1integrin, reported by Hertle and colleages (Hertle et al., 1991). Nothing of this pattern was found, however, and the α2 and β1 subunits both were continuously and ubiquitously distributed on basal epidermal cells prior to TN-C expression. This suggests, as discussed in Chapter III, that the spatially limited distribution of TN-Cs in the BMZ may be morphogenetically relevant, perhaps causing localized modulation of α2β1-dependent adhesion of basal epidermal cells, and thereby influencing morphogenetic initiation.

The lack of immunostaining for the transmembrane protein RPTP-β during hair follicle morphogenesis, when control sections of cerebellum and fetal retina were immunoreactive, suggests that this ligand for TN-C is absent from fetal human skin. Since RPTP-β was isolated from neuronal tissues originally, and was not found outside the central nervous system, its absence in fetal skin does not come as a total surprise. There is always the possibility, however, that the antigen is present but is masked from immunodetection. On the other hand, the lack of immunostaining with an antibody to a neurally-derived protein does not preclude the existence of a non-neuronal form of RPTP-β in fetal human skin. Moreover, since RPTP-β is only one member of an emerging sub-class of receptor-type phosphatases, distinguished from other sub-classes by the presence of a carbonic anhydrase domain in the extracelllular portion of the molecule, still another possibility exists that some other member of the sub-class will be found to bind TN-C and perhaps overlap with TN-C outside the central nervous system (Barnea et al., 1993; Borges, 1995). Tenascin-C distribution is restricted spatially and temporally, often in association with cytokine-rich areas of active tissue remodeling in development and pathogenesis, and the possibility that TN-C acts through a phosphatase receptor and impinges on kinase-activated cytoplasmic signal transduction pathways (mediated by growth factor receptors, for example), holds great potential for explaining the role of TN-C in cell migration and proliferation. Thus, despite the apparent lack of RPTP-β in fetal human skin, future research should nevertheless include analysis of the distribution patterns and TN-C-binding activity of related receptor tyrosine phosphatase family members.

The widespread distribution of HA in the dermis of fetal human skin is similar to its distribution in developing mouse skin (Underhill, 1993). In relation to follicle morphogenesis, however, a subtle difference was noted in the HA staining of the dermal

condensation. Hyaluronan was not detected in the dermal condensation of developing mouse follicles, leading Underhill to hypothesize, and partly demonstrate, that its absence causes a decrease in intercellular distance, allowing cells in this region to achieve a higher population density, thus driving formation of the dermal condensation (Underhill, 1993). The dermal condensation of developing human follicles contained hyaluronan at all morphogenetic stages, although it was diminished relative to the interstitial dermis, suggesting that a similar mechanism could operate in human follicle morphogenesis as well.

In contrast to the interspecies similarity of HA distribution during follicle morphogenesis, the expression pattern of versican in fetal human skin was suprisingly and significantly different from that observed in mouse (du Cros et al., 1995). Whereas versican was expressed nearly ubiquitously in fetal human dermis, consistent with its distribution in adult dermis (Zimmermann et al., 1994), and was enriched in the follicle BMZ and the extracellular matrix of the condensed mesenchyme, in mouse skin, versican was present in the dermal papillae of differentiating follicles only, and was not detected in the follicle sheath or the interstitial dermis at all (du Cros et al., 1995). The VC-3 antibody against recombinant human versican used in the current study was also included in the investigation by du Cros and colleagues, making this discrepancy all the more perplexing (du Cros et al., 1995). The difference in versican immunostaining may reflect species-specific patterning of versican distribution, or it may indicate species-specific expression of the alternatively spliced glycosaminoglycan-containing exon which contains the VC-3 epitope (Ito et al., 1995; Zako et al., 1995).

Although both versican and HA were widely distributed in the developing dermis, they were co-localized with the more restricted TN-C in the condensed mesenchyme associated specifically with the developing follicle. Like TN-$C_L$, HA is expressed in conjunction with neural crest cell migration, as well as in other areas of active tissue remodeling during development (Tan et al., 1987; Mackie et al., 1988; Laurent, 1989), and the migration of smooth muscle cells *in vitro* is mediated by HA and its transmembrane receptor, RHAMM (Savani et al., 1995). Versican, which binds HA and is thought to contribute to macromolecular organization of the extracellular matrix, has been implicated in limb bud morphogenesis (Shinomura et al., 1990), and has also been suggested to modulate cell adhesion and migration, through currently unknown mechansims (Yamagata et al., 1989; Yamagata et al., 1993). Results from Chapter III,

combined with those obtained by Wessells and Roessner (1965), indicate that during follicle elongation, population growth in the associated mesenchyme is mediated by cell migration from the surrounding dermis, and not by proliferation within the follicle sheath. This suggests that the anti-adhesive extracellular matrix molecules TN-C, versican and hyaluronan, co-distributed in this compartment, may function to facilitate cell migration into, or within, the follicle sheath.

Versican and hyaluronan were distributed more widely in association with epidermally-derived cells of the follicle, but overlapped with TN-C in the follicle BMZ and in the outer layer of epithelial cells, identified by MIB-1 as a proliferative region (Chapter III). The three molecules were uniformly excluded from the non-proliferative region at the flattened base of the follicle, where staining of the BMZ was also diminished. This implies that, in contrast to the mesenchymally-derived follicle sheath, the expression of TN-C, versican and HA in the epithelial compartment is associated with mitotic activity, a possibility supported by numerous reports linking each of the three molecules separately to increased cell proliferation (Chiquet-Ehrismann et al., 1986; Gatchalian et al., 1989; Laurent, 1989; Wight et al., 1989; Schalkwijk et al., 1991; Schalkwijk et al., 1991; Schonherr et al., 1991; End et al., 1992; Zimmermann et al., 1994).

The observation that the distributions of a potentially interactive pair of proteins, TN-C and versican, overlap in specific regions of developing hair follicles prompted preliminary experiments to analyze the binding interactions of human TN-C and human versican. Although TN-C bound versican under physiological buffer conditions, the concentrations of versican and TN-C in fetal human skin are unknown, making it difficult to evaluate whether the experimental binding interaction occured at physiologically relevant concentrations of each protein. Immunolabeling of fetal skin suggests that versican is present in vast excess of TN-C, conditions which were reflected in the assay used here. With respect to TN-C, its concentration in adult human skin is estimated at 0.4 μg/ml, although the authors discuss that this is an underestimate, since some TN-C remained in the tissue after biochemical extraction for quantitative analysis of TN-C (Lightner et al., 1989). Moreover, although it is not quantitative, TN-C immunostaining of fetal skin is consistently more intense than that observed in adult skin (data not shown) indicating that TN-C concentrations may be significantly higher in developing skin. These observations suggest that, athough the 25 μg/ml concentration at which TN-C bound versican in the current report was 100-fold higher than its concentration estimated for

adult skin, the disparity between experimental and physiological concentrations may not be a concern. It is also worth noting that versican, as well as TN-C, is subject to alternative splicing and extensive post-translational modifications (Ito et al., 1995; Zako et al., 1995), processes which are regulated in a cell-specific manner. The TN-C and versican reagents used in this study were purified from human glioma and human smooth muscle cells, respectively, and may differ from the molecular forms expressed in fetal skin, perhaps compromising the binding interaction observed *in vitro*. Important aspects of future experiments will be the thorough characterization of the interaction between TN-C and versican, the determination of their physiological concentrations in fetal skin (and other regions of overlapping expression), and the purification of reagents from tissue relevant sources such as skin fibroblasts.

The binding interaction observed between TN-C and versican raises important questions. What regions of the respective proteins mediate binding, and what, if any, is the functional significance of such an interaction? With respect to the first question, clues to the potential interactive domain(s) are already available in the literature. From the TN-C perspective, Hoffman and colleagues mapped the CTB proteoglycan binding region of avian TN-C to the distal of two TN-C fragments generated by peptidase digestion (Hoffman et al., 1990), the region later found to contain FN-III repeats and the alternatively spliced domain (Jones et al., 1989). The availability of recombinant expression proteins containing selected combinations of TN-C FN-III domains should make it relatively straightforward to conduct competition studies and pinpoint the precise region (or regions) of TN-C which bind versican (Aukhil et al., 1993; Erickson, 1993). This approach has already been used successfully to identify the integrin- and heparin-binding domains of TN-C (Prieto et al., 1993; Yokosaki et al., 1994; Weber et al., 1995). With respect to the region of versican which mediates binding to TN-C, Aspberg et al. reported that binding of the tenascin family member, TN-R (restrictin), was calcium-dependent, and mediated by the lectin-binding domain situated near the carboxy terminus of versican, at the opposite end of the molecule from the HA-binding domain (Zimmermann and Ruoslahti, 1989; LeBaron et al., 1992; Aspberg et al., 1995). The results obtained here indicate that the same parameters are involved in binding of versican to TN-C, since versican in the presence of TN-C migrated freely into the gel with either EDTA or excess fucose. Furthermore, a 10-fold excess of free chondroitin sulfate glycosaminoglycan prevented the TN-induced shift in the mobility of versican, suggesting

that not only does the interaction of the two proteins depend upon divalent cations and involve the lectin-binding region of versican, but chondroitin sulfate glycosaminoglycan chains may contribute to the binding as well. This last observation is contrary to results obtained by Hoffman and colleagues, who reported that chondroitin sulfate glycosaminoglycan chains did not have a role in the interaction of CTB (the avian CSPG) with TN-C (Hoffman et al., 1988). The different results may be attributed to the different approaches used to examine the role of glycosaminoglycans. While Hoffman and associates pre-treated the purified proteins with chondroitin ABC lyase to remove the glycosaminoglycans prior to assaying for binding, an excess of free chondroitin sulfate glycosaminoglycans (derived from shark cartilage) was used to compete with intact human versican in the current study. It will be important to resolve this disparity, not only by enzymatic treatment of versican prior incubation with TN-C in the gel mobility shift assay,not only by enzymatic treatment of versican prior incubation with TN-C in the gel mobility shift assay, but also by repeating the competition assay with free chondroitin sulfate glycosaminoglycan derived from the same source as purified versican. .

Even without more detailed information pertaining to the binding sites of TN-C and versican, it is attractive to speculate as to the functional significance of such an interaction. The stoichiometry predicted by the preliminary gel shift assay indicates that a single TN-C hexabrachion binds two versican molecules. Assuming that this is correct, and that versican has an elongated or rod-shaped conformation resulting from the highly charged glycosaminoglycan chains attached to the central portion of the core protein, and assuming further that the proteins interact via the regions discussed above, one would predict that an interaction of TN-C and versican could impart a macromolecular organization to the extracellular matrix, wherein TN-C hexabrachions effectively cross-link HA polymers through versican bridges which extend from the distal arm of the TN-C hexabrachion to HA, which is bound near the N-terminus of versican). A diagram illustrating how these three molecules might interact is shown in Figure 4.7.

If hexabrachions of TN-C do in fact bind versican and interact with HA indirectly, as proposed above, one would expect that TN-C would also be enriched in proteoglycan aggregate, a macromolecular complex containing primarily HA and versican, or aggrecan, which is isolated by density gradient centrifugation from tissue extracts or cell culture medium and is considered to represent the functional organization of extracellular matrix *in vivo*. In a preliminary investigation, TN-C was detected by immunoblot analysis of

aggregate isolated from cultured human smooth muscle cells (data not shown), suggesting that this model may be correct. It will be essential, however, to use other methods, such as immunoprecipitation, for example, to confirm that TN-C is associated specifically with the complex. An even more important task will be to isolate aggregative complex from fetal human skin and assay for the presence of TN-C, versican and hyaluronan.

**Figure 4.1 Distribution of alpha-2 and beta-1 integrin subunits during initiation and early elongation stages of human hair follicle morphogenesis**

Light micrographs showing the distribution of alpha-2 (**A**, **C**) and beta-1 (**B**, **D**) integrin subunits at 10.5 (A, B) and 11.5 (C, D) weeks EGA. Abbreviations: **e**, epidermis; **d**, dermis; **hg**, hair germ; **bv**, blood vessel. Bar, 40 μm.

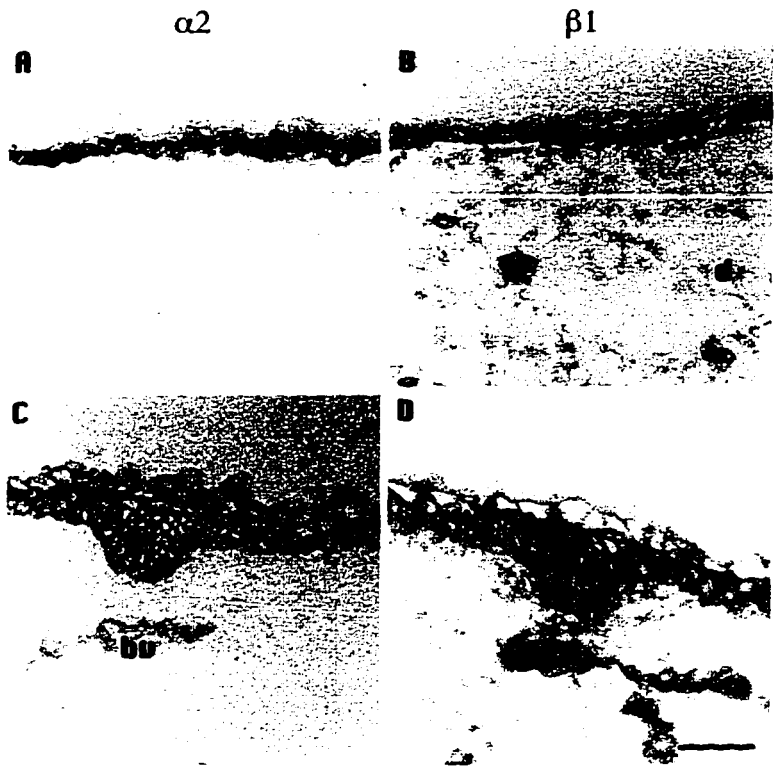
α2
β1
A
B
C
D
bu

**Figure 4.2 Distribution of TN-C, HA and versican in the follicle pre-germ**

*Fluorescence micrographs of 10.5 week EGA fetal skin double labeled for TN-C and hyaluronan* (**A-C**) *or TN-C and versican* (**D-F**). Intense immunolabeling for TN-C, (FITC-conjugated secondary antibody), was found in the BMZ of the pre-germ (**A**), while the biotinylated probe for HA, (detected with avidin-Texas Red and photographed with the rhodamine filter), showed that HA was ubiquitously distributed in the ECM of the developing dermis (**B**). A double-exposure with FITC and rhodamine filters revealed overlapping immunostaining for TN-C and HA in the BMZ (yellow color) (**C**). In an adjacent section, strong labeling of TN-C (detected with a biotinylated secondary antibody and avidin-Texas Red) was found in the BMZ and extended into the mesenchyme (**D**), and versican (FITC-conjugated secondary antibody) was distributed in the extracellular matrix of the dermis (**E**). TN-C and versican were co-distributed in the BMZ of the follicle pre-germ, and the ECM of the condensed mesenchyme (**F**). Abbreviations: **TN-C**, tenascin-C; **HA**, hyaluronan; **VC**, versican; **e**, epidermis; **d**, dermis; *, indicates follicle pre-germ; **cm**, condensed mesenchyme. Bar, 40 μm.

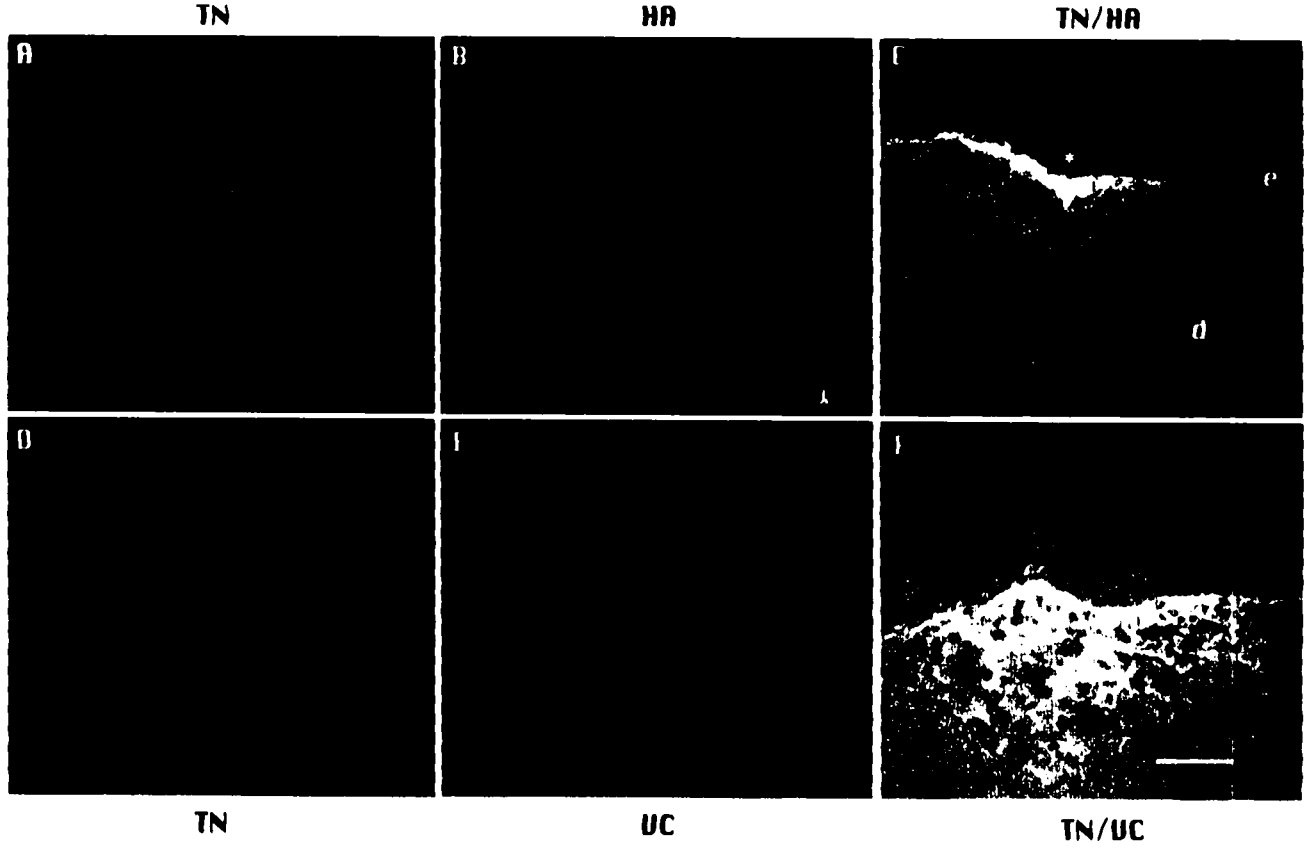
TN
HA
TN/HA
A
B
C
D
E
F
TN
UC
TN/UC

**Figure 4.3 Distribution of TN-C, HA and versican in the follicle hair germ**

Fluorescence light micrographs of fetal skin sections double-labeled for TN-C and hyaluronan (**A-C**), or TN-C and versican (**D**). TN-C was present in the BMZ and condensed mesenchyme of the follicle hair germ (**A**). HA was observed in the BMZ and the dermal extracellular matrix (**B**), and co-localized with TN-C in the BMZ and the condensed mesenchyme, and to a lesser exttent in the follicle BMZ (arrow) (**C**). A double exposure of hyaluronan (rhodamine filter) and versican (FITC filter) showed overlapping distribtuion in the ECM of the dermis, and to a lesser extent in the BMZ of the hair germ follicle. **TN-C**, tenascin-C; **HA**, hyaluronan; **VC**, versican; **hg**, hair germ. Bar, 45 μm.

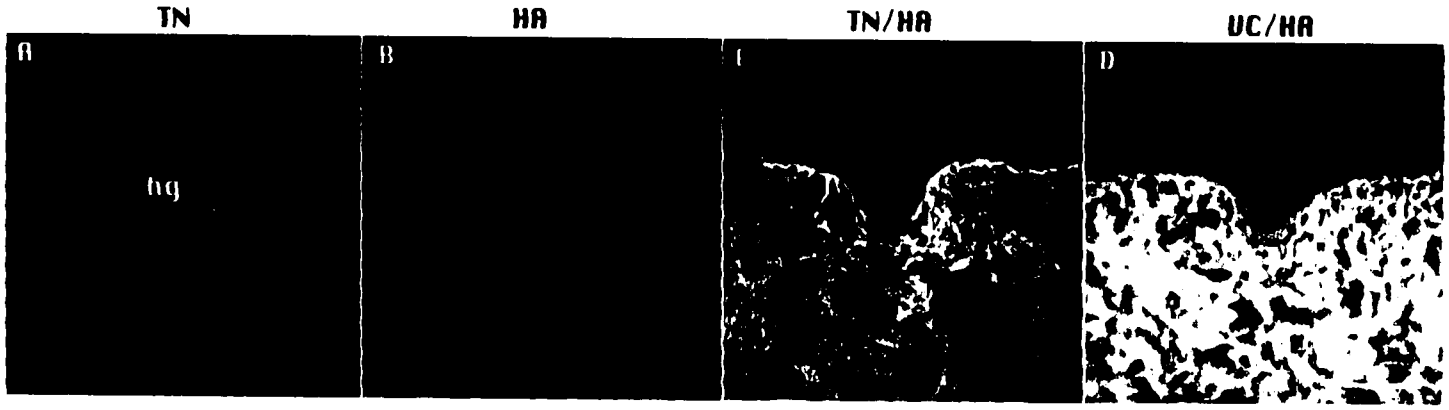
TN
HA
TN/HA
UC/HA
A
hg
B
C
D

**Figure 4.4 Distribution of TN-C and versican in the hair peg follicle**

Fluorescence light micrographs of fetal skin sections double labeled for TN-C (Texas Red) and versican (FITC). Intense labeling for TN-C was present in the follicle-specific mesenchyme (*) and the follicle BMZ, with weak labeling of selected cells in the follicle epithelium (**A**). Versican, widely distributed in the dermal ECM, was enriched in the follicle specific ECM (*) and was present at low levels in the follicle epithelium (**B**). Double-labeling for TN-C and versican was localized to the follicle BMZ, the condensed mesenchyme and a some cells in the posterior wall of the follicle epithelium (arrow) (**C**). Bar, 40 μm.

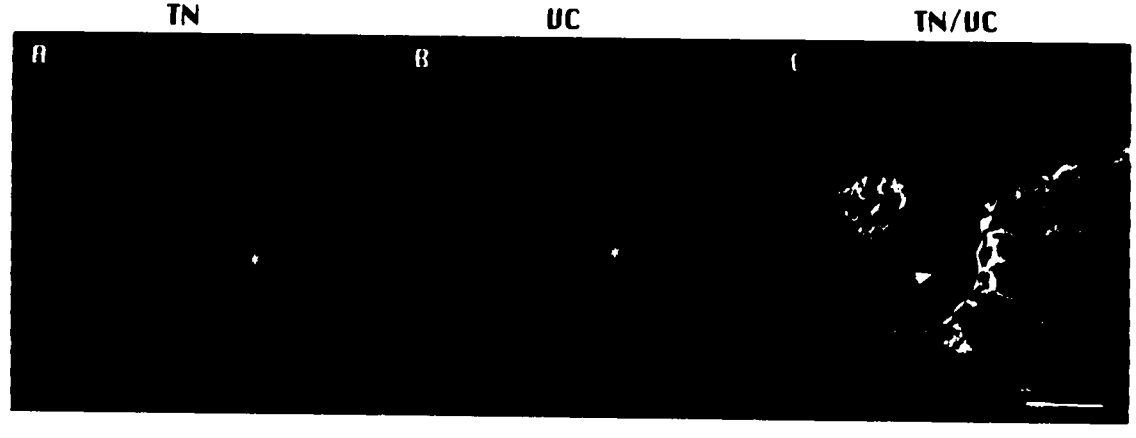
TN
UC
TN/UC
A
B
C

**Figure 4.5 Distribution of TN-C, versican and HA in the differentiating hair follicle**

Double immunofluorescent labeling for TN-C and versican (**A-C**), TN-C and hyaluronan (**D, H**) or versican and hyaluronan (**E-G**). TN-C immunostaining (Texas Red) was enriched in the follicle sheath and the follicle BMZ and outlined cells of the follicle epithelium (**A**), as did immunolabeling for versican (FITC) (**B**), where it overlapped with TN-C (**C**). The same regions were double-labeled for TN-C (FITC) and HA (Texas Red) (**D**). Note the absence of TN-C, versican and HA near the follicle base (*) and diminished HA in the basally situated BMZ and the dermal condensation (arrow and arrowhead, respectively, in **D**). Labeling for versican (FITC) (**E**) and HA (Texas Red) (**F**) co-localized throughout the ECM of the follicle sheath, the follicle BMZ, the dermis, and to a lesser extent in the follicle epithelium (**G**). Note areas of diminished staining at the base of the follicle and in the dermal condensation. The follicle BMZ and condensed mesenchyme contained TN-C (FITC) and HA (Texas Red) as shown by the yellow color in a double-exposure in (**H**), while the presumptive matrix (*) and dermal condensation were mostly negative. Bar, 45 μm.

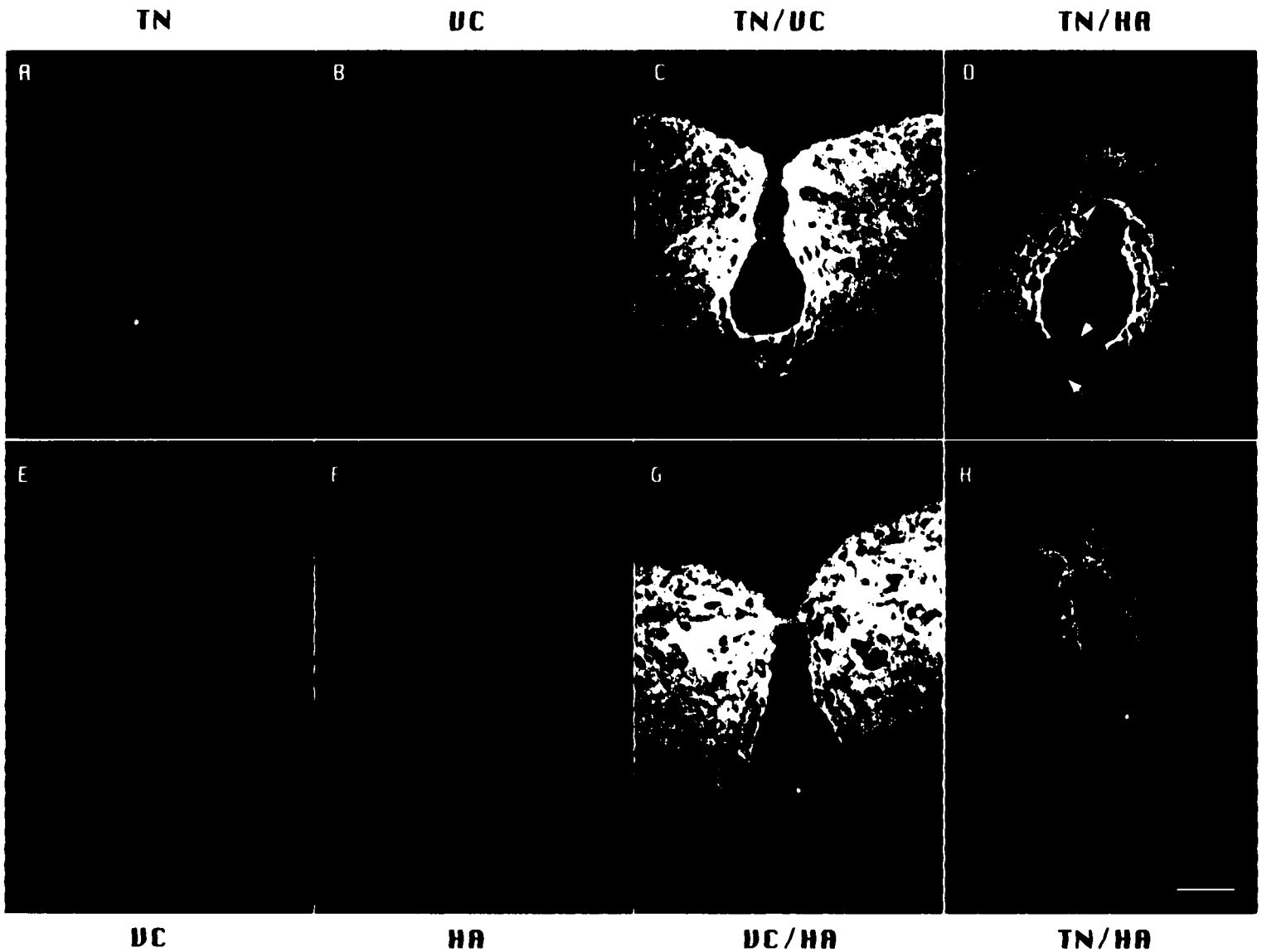
TN
UC
TN/UC
TN/HA
A
B
C
D
E
F
G
H
UC
HA
UC/HA
TN/HA

**Figure 4.6 Interactions of TN-C and versican in gel mobility shift assay**
(**A**) Purified, $^{35}SO_4$-labeled versican was incubated with between 0 and 2 μg of TN-C and subjected to electrophoretic and autoradiographic analysis for detection of changes in mobility. Free versican (**VC**) migrated well into the gel at less than 0.25 μg added TN-C. In the presence of 0.5 μg of TN-C or higher, a radio-labeled complex presumed to contain TN-C was retained near the origin (**O**) of the gel. (**B**) Purified $^{35}SO_4$-labeled versican (lanes 1-18) or small dermatan sulfate proteoglycans (lanes 19-24) was incubated with purified laminin (lanes 1-5) or TN-C (lanes 6-24) under various conditions prior to electrophoresis and autoradiographic exposure. **Lanes 1-5**: Unrestricted migration of $^{35}SO_4$-labeled versican in the presence of 0, 0.25, 0.5, 1 and 2-fold molar excess of laminin (lanes 1-5, respectively). **Lanes 6-8**: 0 (lane 6), 0.5 (lane 7), and 1-fold (lane 8) molar excess of TN-C added to $^{35}SO_4$-labeled versican in the presence of 7 mM EDTA did not alter the mobility of free versican. **Lanes 9-11**: 0, 0.5 and 1-fold molar excess of TN-C added to $^{35}SO_4$-labeled versican in the presence of 10-fold molar excess of fucose did not affect versican mobility. **Lanes 12-14**: No shift in versican mobility was detected when 0, 0.5, and 1-fold molar excess of TN-C was added in the presence of 10-fold molar excess of free chondroitin sulfate glycosaminoglycan. **Lanes 15-18**: 0, 0.25, 0.5, and 1-fold molar excess of TN-C added to $^{35}SO_4$-labeled versican (compare with the same amounts of TN-C in Panel A). The mobility of versican was shifted in lanes 17 and 18. **Lanes 19-24**: An equivalent molar amount of glycosaminoglycan covalently attached to the small dermatansulfate proteoglycans was incubated with 0, 0.12, 0.25, 0.5, 1, and 2 μg TN-C and no change was observed in electrophoretic mobility of the free proteoglycan (**DSPG**). The concentrations of versican and small proteoglycans were determined by Alcian blue staining in comparison to calibrated standards. Molar equivalencies were calculated using molecular weights of approximately $1.45 \times 10^3$ kD for versican, $1.58 \times 10^2$ kD for the small proteoglycan preparation, $1.68 \times 10^3$ kD for the native TN-C hexabrachion, and $55\times 10^3$ kD for the free chondroitin sulfate glycosaminoglycan.

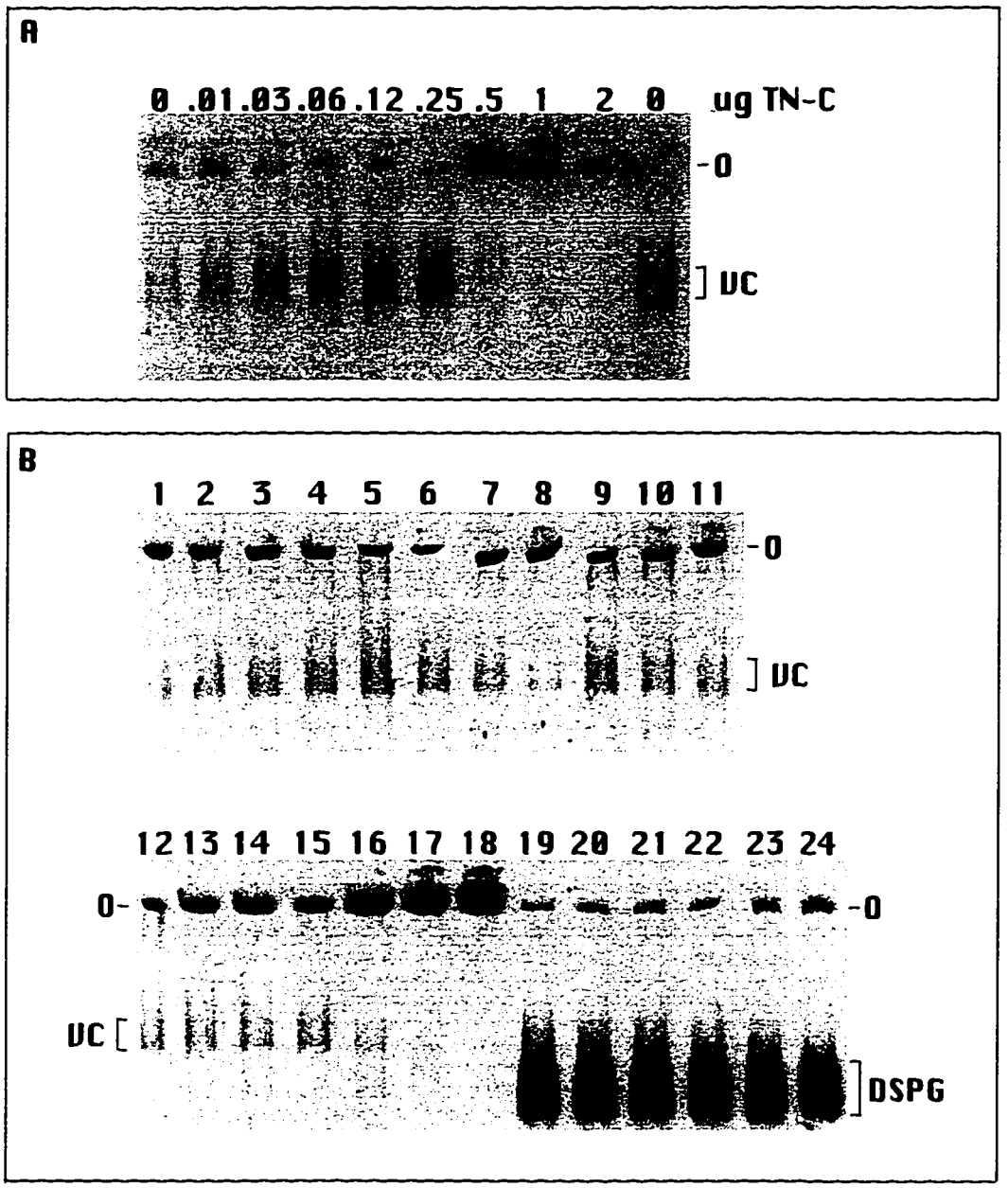
A
0 .01 .03 .06 .12 .25 .5 1 2 0 ug TN-C
-O
] UC
B
1 2 3 4 5 6 7 8 9 10 11
-O
] UC
12 13 14 15 16 17 18 19 20 21 22 23 24
O-
-O
UC [
] DSPG

**Figure 4.7 Schematic diagram modeling binding interactions of hexabrachion, versican and hyaluronan**

The TN-C hexabrachion structure is illustrated as it appears in rotary shadowing (Erickson and Inglesias, 1984), and shows six monomeric subunits joined at their N-termini to form a large globular domain (center). The arms of the hexabrachion radiate outward with the thin lines indicating the EGF-like repeats, the thick segments indicating the repeating FN-III units, and the distal globule representing the C-terminal fibrinogen-like region. Binding of the hexabrachion to versican is expected to be mediated through the FN-III repeats. Versican is illustrated as a link between the hexabrachion and hyaluronan (thin line). Binding to TN-C probably involves the lectin-like region at the C-terminus of versican, and binding of versican to hyaluronan is mediated by the HA-binding region near the N-terminus of versican. For the sake of simplicity, only five chondroitin sulfate glycosaminoglycan chains are indicated, attached to the central region of versican where up to 15 attachment sites have been identified. Although not indicated here, hyaluronan is actually decorated by multiple proteoglycans which are attached non-covalently to the polymer, as is illustrated for versican.

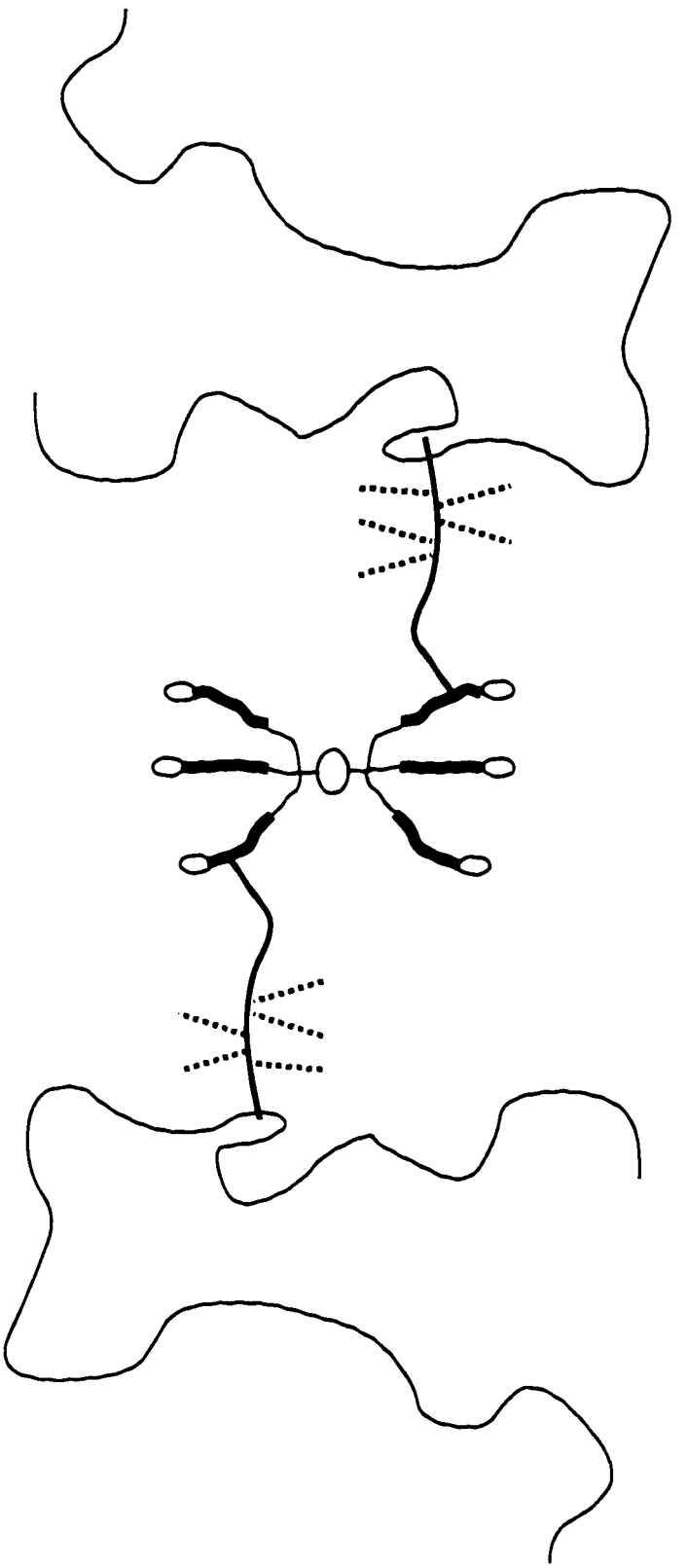

# CHAPTER V

## CONCLUDING REMARKS

Hair follicle morphogenesis is a gradual restructuring of epithelial and mesenchymal tissues to form a mature, fully differentiated pilosebaceous unit. The preceding chapters have detailed the expression patterns of selected substrate and surface adhesion molecules during human hair follicle morphogenesis. When reviewed in sum for each morphogenetic stage, these observations provide valuable insight into the morphogenetic process, and point the direction for future investigations.

Events surrounding follicle initiation have eluded experimental analysis up to now. The observations that, prior to morphogenetic changes, clusters of basal epidermal cells contain TN-C mRNA, and that TN-$C_S$ is selectively deposited in discrete placodes at the epidermal-dermal interface, together offer opportunities not only to examine the functional role of TN-$C_S$, but also to analyze factors governing TN-$C_S$ expression as a means to decipher intercellular signaling events which lead to follicle initiation. For example, because TN-$C_S$ might selectively affect epidermal cell morphology or adhesion, the recombinantly expressed TN-C protein segments developed by Aukhil and colleagues [Aukhil, 1993 #456] could be used to examine the effects of TN-$C_S$ specifically (as opposed to TN-$C_L$) on epidermal cells *in vitro*, while other experiments analyzing the role of transcriptional and post-transcriptional factors regulating TN-$C_S$ expression might help to uncover morphogenetic mediators which trigger follicle initiation. Because of the spatially limited expression and deposition of TN-C, a greater understanding of pattern formation in mammalian skin development is likely to be an inherent result of any experimental approach used.

The early elongation stages of human hair follicle morphogenesis are characterized by the expression of the inflammatory cell adhesion molecule ICAM-1 on epidermally-derived cells of the hair germ. This novel finding has been difficult to explain, in part because ICAM-1 had not previously been associated with morphogenetic processes, and in part because its expression has such precise temporal and spatial limits. More recently, however, ICAM-1 has been reported to mediate hyaluronan uptake by liver endothelial cells (McCourt et al., 1995). Taken together with results presented in Chapter IV demonstrating that HA is present in the follicle epithelium and basement membrane zone,

it suggests that ICAM-1 expression in the developing follicle might be important for HA binding or metabolism. Although the implications for such an interaction are unclear at this point, it is conceivable that ICAM-1 binding of HA mediates invagination or invasion of the epidermal cell cluster into the dermis, similar to the joint functions of HA and RHAMM (Savani et al., 1995).

While epithelial budding and downgrowth have often been likened to invasive behavior in pathogenesis, the upregulation during the invagination phase of follicle morphogenesis of proteins associated with inflammatory conditions (TN-C and ICAM-1), suggests that tissue reorganization at this developmental stage could involve the regulation by morphogenetically active non-inflammatory cell populations of molecules and mechanisms similar to those typically associated with inflammation. In this regard, it is interesting that the epithelial integrin receptor $\alpha V\beta 6$, which binds TN-C, was proposed recently to function in terminating the inflammatory response (D. Sheppard, 1996, public seminar)(Prieto et al., 1993; Weinacker et al., 1995). Although the distribution of this integrin in fetal human skin is unknown, it should be examined in relation to TN-C and ICAM-1 expression during hair follicle morphogenesis, to determine if more parallels exist between morphogenetic and inflammation-associated histological rearrangements.

Results presented in Chapters II, III, and IV suggest collectively that elongation of the developing follicle is characterized by the segregation of follicle epithelial cells into topographic compartments which appear to predict, both spatially and behaviorally, regions in the mature follicle. Cells adjacent to the basal lamina form the outer layer of the developing follicle and will eventually make up the outer root sheath of the adult follicle. This region of the elongating follicle contained actively proliferating cells, as does the outer root sheath in fully differentiated follicles of adult skin. At the same time, a mitotically inactive compartment was observed at the follicle base, apparently corresponding to the presumptive matrix region from which the hair fiber differentiates. Cells in these compartments differed in more than their proliferative activity, with those in the outer layer expressing TN-C mRNA and surrounded by a modest extracellular matrix containing HA, TN-C and versican, while these molecules were strikingly absent from the non-proliferative region at the follicle base. In differentiating murine follicles which have invaginated to enclose the dermal papillae, cells of the presumptive hair matrix express mNotch, the murine homolog of *Drosophila* Notch, a cell surface receptor important in determining cell fate (Kopan and Weintraub, 1993). In the present study, TN-C, HA and

versican were all absent from the region of the presumptive hair matrix at the follicle hair peg stage, while the same cells contained transcript for Type I collagen. These observations indicate that presumptive matrix cells are phenotypically distinct at morphologically earlier developmental stages in developing human hair follicles, and imply that cell fate determination choices may be made very early in the morphogenetic process. Furthermore, an inverse correlation between TN-C and mammary cell differentiation has been demonstrated recently (Jones et al., 1995), suggesting that in the follicle epithelium, where TN-C is expressed in proliferating cells and is absent from cells which are phenotypically distinct, TN-C may function to inhibit differentiation of cells in the outer layer of the elongating follicle.

At all morphogenetic stages, the follicle basement membrane and the extracellular matrix of the follicle-specific mesenchyme contain TN-C, and are enriched in versican and hyaluronan. There is reason to suspect that this co-distribution has functional implications in that the three adhesion modulating molecules (each associated individually with cell migration and proliferation as well) may associate to form a macromolecular complex which uniquely invests the developing epidermal appendage. Such a specialized matrix may be similar to the provisional matrix found in wound healing, and may contribute to the morphogenetic process by facilitating cell movement and tissue restructuring. The formation of this matrix may be tightly regulated, not only by the spatially restricted distribution of TN-C, but also by alternative splicing and post-translational control of TN-C and versican expression. Since both TN-C and versican are substrates for metalloproteinase digestion (Siri et al., 1995; Halpert et al., 1996) the dissolution of the morphogenetic matrix complex may be carefully controlled as well. Moreover, since TN-C and HA interact with several different adhesion molecules at the cell surface, in any given location, the cellular response to the morphogenetic matrix may depend upon the type of cell present and its complement of surface adhesion molecules.

In the preceding chapters, the distribution patterns of several cell adhesion modulating molecules have been examined in association with human hair follicle morphogenesis. Based on their temporal and spatial patterns of expression, some of these, namely TN-C, versican, hyaluronan and ICAM-1, were identified as potential morphogenetic mediators. Although an examination of their functional roles was beyond the scope of this project, it is hoped that the observations presented here will be helpful in designing future experiments which will test the functional relevance of these molecules in

hair follicle morphogenesis, and in this way, contribute to a better overall understanding of the morphogenetic process.

## REFERENCES


Anstrom, J. A., E. J. Mackie and R. P. Tucker (1990). Immunohistochemical localization of a tenascin-like extracellular matrix protein in sea urchin embryos. *Roux's Arch. Devl. Biol.* **199**: 169-173.

Aspberg, A., C. Binkert and E. Ruoslahti (1995). The versican C-type lectin domain recognizes the adhesion protein tenascin-R. *Proc. Natl. Acad. Sci. USA* **92**: 10590-10594.

Aufderheide, E., R. Chiquet-Ehrismann and P. Ekblom (1987). Epithelial-mesenchymal interaction in the developing kidney lead to expression of tenascin in the mesenchyme. *J. Cell Biol.* **105**: 599-608.

Aufderheide, E. and P. Ekblom (1988). Tenascin during gut development: appearance in the mesenchyme, shift in molecular forms, and dependence on epithelial-mesenchymal interactions. *J. Cell Biol.* **107**: 2341-2349.

Aukhil, I., P. Joshi, Y. Yan and H. P. Erickson (1993). Cell- and heparin-binding domains of the hexabrachion arm identified by tenascin expression proteins. *J. Biol. Chem.* **268**(4): 2542-2553.

Balza, E., A. Siri, M. Ponassi, F. Caocci, A. Linnala, I. Virtanen and L. Zardi (1993). Production and characterization of monoclonal antibodies specific for different epitopes of human tenascin. *FEBS* **332**: 39-43.

Banks-Schlegel, S. P. (1982). Keratin alterations during embryonic epidermal differentiation: a presage of adult epidermal maturation. *J. Cell Biol.* **93**: 551-559.

Barnea, G., M. Grumet, P. Milev, O. Silvennoinen, J. B. Levy, J. Sap and J. Schlessinger (1994). Receptor tyrosine phosphatase β is expressed in the gorm of proteoglycan and binds to the extracellular matrix protein tenascin. *J. Biol. Chem.* **269**(20): 14349-14352.

Barnea, G., O. Silvennoinen, B. Shaanan, A. M. Honegger, P. D. Canoll, P. D'eustachio, B. Morse, J. B. Levy, S. Laforgia, K. Huebner, et al. (1993). Identification of a carbonic

anhydrase-like domain in the extracellular region of RPTPγ defines a new subfamily of receptor tyrosine phosphatases. *Mol. Cell. Biol.* **13**(3): 1497-1506.

Bianco, P., L. W. Fisher, M. F. Young, J. D. Termine and P. G. Robey (1990). Expression and localization of the two small proteoglycans biglycan and decorin in developing human skeletal and non-skeletal tissues. *J. Histochem. Cytochem.* **38**: 1549-1563.

Borges, L. G. (1995). Characterization of protein tyrosine phosphatases expressed by vascular cells. Pathology. Seattle, University of Washington.

Borsi, L., E. Balza, P. Castellani, B. Carnemolla, M. Ponassi, G. Querze and L. Zardi (1994). Cell-cycle dependent alternative splicing of the tenascin primary transcript. *Cell Adhes. Comm.* **1**: 307-317.

Borsi, L., B. Carnemolla, G. Nicolo, B. Spina, G. Tanara and L. Zardi (1992). Expression of different tenascin isoforms in normal, hyperplastic and neoplastic human breast tissues. *Int. J. Cancer* **52**: 688-692.

Borsi, L., B. Carnemolla, M. Ponassi and L. Zardi (1993). Steady-state levels of different tenascin mRNAs in various normal human tissues. *Cell Biol. Int.* **17**(3): 325-329.

Bourdon, M. A. and E. Ruoslahti (1989). Tenascin mediates cell attachment through an RGD-dependent receptor. *J. Cell Biol.* **108**: 1149-1155.

Bristow, J., J. K. Tee, S. E. Gitelman, S. H. Mellon and W. L. Miller (1993). Tenascin-X: a novel extracellular matrix protein encoded by the human XB gene overlapping P450c21B. *J. Cell Biol.* **122**(1): 265-278.

Camejo, G., G. Fager, B. Rosengren, E. Hurt-Camejo and G. Bondjers (1993). Binding of low density lipoproteins by proteoglycans synthesized by proliferating and quiescent human arterial smooth muscle cells. *J. Biol. Chem.* **268**(19): 14131-14137.

Canoll, P. D., G. Barnea, J. B. Levy, J. Sap, M. Ehrlich, O. Silvennoinen, J. Schlessinger and J. M. Musacchio (1993). The expression of a novel receptor-type tyrosine phosphatase suggests a role in morphogenesis and plasticity of the nervous system. *Dev. Br. Res.* **75**: 293-298.

Carnemolla, B., L. Borsi, G. Bannikov, S. Troyanovsky and L. Zardi (1992). Comparison of human tenascin expression in normal, Simian-virus-40-transformed and tumor-derived cell lines. *Eur. J. Biochem.* **205**: 561-567.

Carter, W. G. and S. Hakomori (1981). A new cell surface, detergent-insoluble glycoprotein matrix of human and hamster fibroblasts. *J. Biol. Chem.* **256**(13): 6953-6960.

Castellucci, M., I. Classen-Linke, J. Muhlhauser, P. Kaufmann, L. Zardi and R. Chiquet-Ehrismann (1991). The human placenta: a model for tenascin expression. *Histochemistry* **95**: 449-458.

Caterson, B., T. Calabro and A. Hampton (1987). Monoclonal antibodies as probes for elucidating proteoglycan structure and function. Biology of Proteoglycans. T. N. Wight and R. P. Mecham. Orlando, Academic Press, Inc: 1-26.

Chiquet, M. and D. M. Fambrough (1984). Chick myotendinous antigen. II. A novel extracellular glyocoprotein complex consisting of large disulfide-linked subunits. *J. Cell Biol.* **98**: 1937-1946.

Chiquet-Ehrismann, R. (1990). What distinguishes tenascin from fibronectin? *FASEB J.* **4**: 2598-2604.

Chiquet-Ehrismann, R. (1991). Anti-adhesive molecules of the extracellular matrix. *Curr. Op. Cell Biol.* **3**: 800-804.

Chiquet-Ehrismann, R. (1993). Tenascin and other adhesion-modulating proteins in cancer. *Sem. Cancer Biol.* **4**: 301-310.

Chiquet-Ehrismann, R., C. Hagios and K. Matsumoto (1994). The Tenascin Gene Family. *Perspectives on Developmental Neurobiology* **2**(1): 3-7.

Chiquet-Ehrismann, R., P. Kalla, C. A. Pearson, K. Beck and M. Chiquet (1988). Tenascin interferes with fibronectin action. *Cell* **53**: 383-390.

Chiquet-Ehrismann, R., E. J. Mackie, C. A. Pearson and T. Sakakura (1986). Tenascin: an extracellular matrix protein involved in tissue interactions during fetal development and oncogenesis. *Cell* **47**: 131-139.

Chiquet-Ehrismann, R., Y. Matsuoka, U. Hofer, J. Spring, C. Bernasconi and M. Chiquet (1991). Tenascin variants: differential binding to fibronectin and distinct distribution in cell cultures and tissues. *Cell Reg.* **2**: 927-938.

Chomczynski, P. and N. Saachi (1987). Single-step method of RNA isolation by acid guanidinium thiocyanate-phenol-chloroform extraction. *Anal. Biochem.* **162**: 156-159.

Chung, C. Y. and H. P. Erickson (1994). Cell surface annexin II is a high affinity receptor for the alternatively spliced segment of Tenascin-C. *J. Cell Biol.* **126**(2): 539-548.

Chuong, C.-M. (1990). Adhesion molecules (N-CAM and tenascin) in embryonic development and tissue regeneration. *J. Craniofac. Genet. Dev. Biol.* **10**: 147-161.

Chuong, C. M. (1993). The making of a feather: homeoproteins, retinoids and adhesion molecules. *Bioessays* **15**(8): 513-521.

Chuong, C.-M. and H.-M. Chen (1991). Enhanced expression of neural cell adhesion molecules and tenascin (cytotactin) during wound healing. *Am. J. Path.* **138**(2): 427-440.

Chuong, C.-M., H.-M. Chen, T.-X. Jiang and J. Chia (1991). Adhesion molecules in skin development: morphogenesis of feather and hair. *Annals N.Y. Acad. Sci.* **642**: 263-280.

Chuong, C.-M. and G. M. Edelman (1985). Expression of cell-adhesion molecules in embryonic induction. I. Morphogenesis of nestling feathers. *J. Cell Biol.* **101**: 1009-1026.

Clark, E. A., J. A. Ledbetter, R. C. Holly, P. A. Dinndorf and G. Shu (1986). Polypeptides on human B lymphocytes associated with cell activation. *Hum. Immunol.* **16**: 100-113.

Cole, G. J. and M. Burg (1989). Characterization of a heparan sulfate proteoglycan that copurifies with the neural cell adhesion molecule. *Expl. Cell Res.* **182**: 44-60.

Cole, G. J. and L. Glaser (1986). A heparin-binding domain from N-CAM is involved in neural cell-substratum adhesion. *J. Cell Biol.* **102**: 403-412.

Couchman, J. R., B. Caterson, J. E. Christner and J. R. Baker (1984). Mapping by monoclonal antibody detection of glycosaminoglycans in connective tissues. *Nature* **307**: 650-652.

Couchman, J. R., J. L. King and K. J. McCarthy (1990). Distribution of two basement membrane proteoglycans through hair follicle development and the hair growth cycle in the rat. *J. Invest. Dermatol.* **94**: 65-70.

Couchman, J. R. and A. V. Ljubimov (1989). Mammalian tissue distribution of a large heparan sulfate proteoglycan detected by monoclonal antibodies. *Matrix* **9**: 311-321.

Crossin, K. L. (1991). Cytotactin binding: inhibition of stimulated proliferation and intracellular alkalinization in fibroblasts. *Proc. Natl. Acad. Sci. U.S.A.* **88**: 11403-11407.

Crossin, K. L., C.-M. Chuong and G. M. Edelman (1985). Expression sequences of cell adhesion molecules. *Proc. Natl. Acad. Sci. USA* **82**: 6942-6946.

Cunningham, B. A., J. J. Hemperly, B. A. Murray, E. A. Prediger, R. Brackenbury and G. M. Edelman (1987). Neural cell adhesion molecule: structure, immunoglobulin-like domains, cell surface modulation, and alternative RNA splicing. *Science* **236**: 799-806.

Dedhar, S. (1995). Integrin mediated signal transduction in oncogenesis: an overview. *Cancer. Metastasis. Rev.* **14**(3): 165-172.

Detmar, M., S. Tenorio, U. Hettmannsperger, Z. Ruszczak and C. E. Orfanos (1992). Cytokine regulation of proliferation and ICAM-1 expression of human dermal microvascular endothelial cells *in vitro*. *J. Invest. Dermatol.* **98**: 147-153.

Diamond, M. S., D. E. Staunton, S. D. Marlin and T. A. Springer (1991). Binding of the integrin Mac-1 (CD11b/CD18) to the third immunoglobulin-like domain of ICAM-1 (CD54) and its regulation by glycosylation. *Cell* **65**: 961-971.

du Cros, D. L., R. G. LeBaron and J. R. Couchman (1995). Association of versican with dermal matrices and its potential role in hair follicle development and cycling. *J. Invest. Dermatol.* **105**: 426-431.

Dustin, M. L., K. H. Singer, D. T. Tuck and T. A. Springer (1988). Adhesion of T lymphoblasts to epidermal keratinocytes is regulated by interferon τ and is mediated by intercellular adhesion molecule-1 (ICAM-1). *J. Exp. Med.* **167**(4): 1323-1340.

Edelman, G. M. (1984). Cell adhesion and morphogenesis: The regulator hypothesis. *Proc. Natl. Acad. Sci. USA* **81**: 1460-1464.

Edelman, G. M. and F. S. Jones (1992). Cytotactin: a morphoregulatory molecule and a target for regulation by homeobox gene products. *TIBS* **17**: 228-232.

Edwards, G. and C. Streuli (1995). Signalling in extracellular-matrix-mediated control of epithelial cell phenotype. *Biochem. Soc. Trans.* **23**(3): 464-468.

Ekblom, P. and E. Aufderheide (1989). Stimulation of tenascin expression in mesenchyme by epithelial-mesenchymal interactions. *Int. J. Dev. Biol.* **33**: 71-79.

End, P., G. Panayotou, A. Entwistle, M. D. Waterfield and M. Chiquet (1992). Tenascin: a modulator of cell growth. *Eur. J. Biochem.* **209**: 1041-1051.

Erickson, H. P. (1993). Tenascin-C, tenascin-R and tenascin-X: a family of talented proteins in search of functions. *Curr. Op. Cell Biol.* **5**: 869-876.

Erickson, H. P. (1994). Evolution of the tenascin family--implications for function of the C-terminal fibrinogen-like domain. *Perspectives on Developmental Neurobiology* **2**(1): 9-19.

Erickson, H. P. and M. A. Bourdon (1989). Tenascin: an extracellular matrix protein prominent in specialized embryonic tissues and tumors. *Ann. Rev. Cell Biol.* **5**: 71-92.

Erickson, H. P. and J. L. Inglesias (1984). A six-armed oligomer isolated from cell surface fibronectin preparations. *Nature* **311**: 267-269.

Erickson, H. P. and V. A. Lightner (1988). Hexabrachion protein (tenascin, cytotactin, brachionectin) in connective tissues, embryonic brain, and tumors. Advances in Cell Biology. K. R. Miller. London, JAI Press Inc. **2:** 55-90.

Fine, J.-D. and J. R. Couchman (1988). Chondroitin-6-sulfate-containing proteolgycan: a new component of human skin dermoepidermal junction. *J. Invest. Dermatol.* **90**: 283-288.

Fine, J.-D., L. T. Smith, K. A. Holbrook and S. I. Katz (1984). The appearance of four basement membrane zone antigens in developing human fetal skin. *J. Invest. Dermatol.* **83**: 66-69.

Friedlander, D. R., S. Hoffman and G. M. Edelman (1988). Functional mapping of cytotactin: proteolytic fragments active in cell-substrate adhesion. *J. Cell Biol.* **107**: 2329-2340.

Fujita, M., F. Furukawa, K. Fujii, Y. Horiguchi, M. Takeichi and S. Imamura (1992). Expression of cadherin cell adhesion molecules during human skin development: morphogenesis of epidermis, hair follicles and eccrine sweat ducts. *Arch. Dermatol Res.* **284**: 159-166.

Gallin, W. J., C.-M. Chuong, L. H. Finkel and G. M. Edelman (1986). Antibodies to liver cell adhesion molecule perturb inductive interactions and alter feather pattern and structure. *Proc. Natl. Acad. Sci. USA* **83**: 8235-8239.

Gatchalian, C. L., M. Schachner and J. R. Sanes (1989). Fibroblasts that proliferate near denervated synaptic sites in skeletal muscle synthesize the adhesive molecules tenascin (J1), N-CAM, fibronectin, and a heparan sulfate proteoglycan. *J. Cell Biol.* **108**: 1873-1890.

Gerstein, W. (1971). Cell proliferation in human fetal epidermis. *J. Invest. Dermatol.* **57**(4): 262-265.

Gherzi, R., B. Carnemolla, A. Siri, M. Ponassi, E. Balza and L. Zardi (1995). Human tenascin gene. *J. Biol. Chem.* **270**(7): 3429-3434.

Goetinck, P. F. (1991). Proteoglycans in development. *Curr. Top. Devl. Biol.* **25**: 111-131.

Goetinck, P. F. and D. L. Carlone (1988). Altered proteoglycan synthesis disrupts feather pattern formation in chick embryonic skin. *Devl. Biol.* **127**: 179-186.

Grumet, M., P. Milev, T. Sakurai, L. Karthikeyan, M. Bourdon, R. K. Margolis and R. U. Margolis (1994). Interactions with tenascin and differential effects on cell adhesion of neurocan and phosphacan, two major chondroitin sulfate proteoglycans of nervous tissue. *J. Biol. Chem.* **269**(16): 12142-12146.

Hahn, A. W. A., F. Kern, U. Jonas, M. John, F. R. Buhler and T. J. Resink (1995). Functional aspects of vascular tenascin-C expression. *J. Vasc. Res.* **32**: 162-174.

Hardy, M. H. (1992). The secret life of the hair follicle. *Trends Genet.* **8**: 55-61.

Hardy, M. H., I. R. Gibson and U. Vielkind (1992). Changing patterns of cell adhesion molecules during development of hair follicles in mice. *Soc. Dev. Biol. Symp.*: 5.

Heer, A. H., G. M. Keyszer, R. E. Gay and G. S. (1994). Inhibition of RNA polymerases by digoxigenin-labeled UTP. *Biotechniques* **16**(1): 54-5.

Hertle, M. D., J. C. Adams and F. M. Watt (1991). Integrin expression during human epidermal development *in vivo* and *in vitro*. *Development* **112**: 193-206.

Hirai, Y., A. Nose, S. Kobayashi and M. Takeichi (1989). Expression and role of E- and P-cadherin adhesion molecules in embryonic histogenesis. II. Skin morphogenesis. *Development* **105**: 271-277.

Hoffman, S., K. L. Crossin and G. M. Edelman (1988). Molecular forms, binding functions, and developmental expression patterns of cytotactin and cytotactin-binding proteoglycan, an interactive pair of extracellular matrix molecules. *J. Cell Biol.* **106**: 519-532.

Hoffman, S., K. L. Crossin, F. S. Jones, D. R. Friedlander and G. M. Edelman (1990). Cytotactin and cytotactin-binding proteoglycan. *Ann. N. Y. Acad. Sci.* **580**: 288-301.

Hoffman, S., S. L. Dutton, H. Ernst, M. K. Boackle, D. Everman, A. Tourkin and J. D. Loike (1994). Functional characterization of antiadhesion molecules. *Perspectives on Developmental Neurobiology* **2**(1): 101-110.

Hoffman, S. and G. M. Edelman (1987). A proteoglycan with HNK-1 antigenic determinants is a neuron-associated ligand for cytotactin. *Proc. Natl. Acad. Sci. USA* **84**: 2523-2527.

Holbrook, K. A. (1979). Human epidermal embryogenesis. *Int. J. Derm.* **18**: 329-356.

Holbrook, K. A., C. Fisher, B. A. Dale and R. Hartley (1988). Morphogenesis of the hair follicle during the ontogeny of human skin. The Biology of Wool and Hair. G. E. Rogers, P. J. Reis, K. A. Ward and R. C. Marshall. New York, Chapman and Hall: 15-35.

Holbrook, K. A., L. T. Smith, E. D. Kaplan, S. I. Minami, G. P. Hebert and R. A. Underwood (1993). The expression of morphogens during human follicle development *in vivo* and a model for studying follicle morphogenesis *in vitro*. *J. Invest. Dermatol.* **101 Suppl.**: 39S-49S.

Horiguchi, Y., J. R. Couchman, A. V. Ljubimov, H. Yamasaki and J.-D. Fine (1989). Distribution, ultrastructural localization, and ontogeny of the core protein of a heparan sulfate proteoglycan in human skin and other basement membranes. *J. Histochem. Cytochem.* **37**: 961-970.

Hsu, S.-M., L. Raine and H. Fanger (1981). Use of avidin-biotin-peroxidase complex (ABC) in immunoperoxidase techniques: a comparison between ABC and unlabeled antibody (PAP) procedures. *J. Histochem. Cytochem.* **29**(4): 577-580.

Hynes, R. O. (1987). Integrins: a family of cell surface receptors. *Cell* **48**: 549-554.

Hynes, R. O. (1992). Integrins: versatility, moduation, and signaling in cell adhesion. *Cell* **69**: 11-25.

Inaguma, Y., M. Kusakabe, E. J. Mackie, C. A. Pearson, R. Chiquet-Ehrismann and T. Sakakura (1988). Epithelial induction of stromal tenascin in the mouse mammary gland: from embryogenesis to carcinogenesis. *Devl. Biol.* **128**: 245-255.

Ito, K., T. Shinomura, M. Zako, M. Ujita and K. Kimata (1995). Multiple forms of mouse PG-M, a large chondroitin sulfate proteoglycan generated by alternative splicing. *J. Biol. Chem.* **270**(2): 958-965.

Jahoda, C. A. B., K. A. Horne and R. F. Oliver (1984). Induction of hair growth by implantation of cultured dermal papilla cells. *Nature* **311**: 560-562.

Jiang, T.-X. and C.-M. Chuong (1992). Mechanism of skin morphogenesis. I. Analyses with antibodies to adhesion molecules tenascin, N-CAM and integrin. *Devl Biol.* **150**: 82-98.

Jones, F. S., G. Chalepakis, P. Gruss and G. M. Edelman (1992). Activation of the cytotactin promoter by the homeobox-containing gene *Evx-1*. *Proc. Natl. Acad. Sci. U.S.A.* **89**: 2091-2095.

Jones, F. S., S. Hoffman, B. A. Cunningham and G. M. Edelman (1989). A detailed structural model of cytotactin: protein homologies, alternative RNA splicing, and binding regions. *Proc. Natl. Acad. Sci. USA* **86**: 1905-1909.

Jones, P. L., N. Boudreau, C. A. Myers, H. P. Erickson and M. J. Bissell (1995). Tenascin-C inhibits extracellular matrix-dependent gene expression in mammary epithelial cells. *J. Cell Science* **108**: 519-527.

Kallunki, P. and K. Tryggvason (1992). Human basement membrane heparan sulfate proteolgycan core protein: a 467-kD protein containing multiple domains resembling elements of the low density lipoprotein receptor, laminin, neural cell adhesion molecules, and epidermal growth factor. *J. Cell Biol.* **116**(2): 559-571.

Kanno, S. and Y. Fukuda (1994). Fibronectin and tenascin in rat tracheal wound healing and their relation to cell proliferation. *Pathology International* **44**: 96-106.

Kaplony, A., D. R. Zimmermann, R. W. Fischer, B. A. Imhof, B. F. Odermatt, K. H. Winterhalter and L. Vaughan (1991). Tenascin $M_r$ 220 000 isoform expression correlates with corneal cell migration. *Development* **112**: 605-614.

Karelina, T. V., G. I. Goldberg and A. Z. Eisen (1994). Matrilysin (PUMP) Correlates with Dermal Invasion During Appendageal Development and Cutaneous Neoplasia. *J. Invest. Dermatol.* **103**: 482-487.

Kleinman, H. K. and B. S. Weeks (1989). Laminin: structure, functions and receptors. *Curr. Op. Cell Biol.* **1**: 964-967.

Koch, M., B. Wehrle-Haller, S. Baumgartner, J. Spring, D. Brubacher and M. Chiquet (1991). Epithelial synthesis of tenascin at tips of growing bronchi and graded accumulation in basement membrane and mesenchyme. *Expl. Cell Res.* **194**: 297-300.

Kollar, E. J. (1970). The induction of hair follicles by embryonic dermal papillae. *J. Invest. Dermatol.* **55**(6): 374-378.

Konter, U., I. Kellner, E. Klein, R. Kaufmann, V. Mielke and W. Sterry (1989). Adhesion molecules mapping in normal human skin. *Arch. Dermatol Res.* **281**: 454-462.

Kopan, R. and H. Weintraub (1993). Mouse Notch: expression in hair follicles correlates with cell fate determination. *J. Cell Biol.* **121**(3): 631-641.

LaBell, T. (1995). The cDNA sequence, chromosomal location and characterization of two novel cDNAs in humans: thrombospondin 2 and dermal fibroblast heparan sulfate *N*-Deacetylase/*N*-Sulfotransferase. Pathology. Seattle, University of Washington: 96.

Laemmli, U. K. (1970). Cleavage of structural proteins during the assembly of bacteriophage T4. *Nature* **316**: 146-148.

LaFleur, D. W., J. A. Fagin, J. S. Forrester, S. A. Rubin and B. G. Sharifi (1994). Cloning and characterization of alternatively spliced isoforms of tat tenascin. *J. Biol. Chem.* **269**(32): 20757-20763.

Lark, M. W., T.-K. Yeo, M. Henderson, S. Lara, I. Hellstrom, K.-E. Hellstrom and T. N. Wight (1988). Arterial chondroitin sulfate proteoglycan: localization with a monoclonal antibody. *J. Histochem. Cytochem.* **36**: 1211-1221.

Laurent, T. (1989). The Biology of Hyaluronan. *CIBA Found. Symp.* **143**: 1-20.

Laurent, T. C. and J. R. Fraser (1992). Hyaluronan. *FASEB J.* **6**(7): 2397-2404.

LeBaron, R. G., D. R. Zimmermann and E. Ruoslahti (1992). Hyaluronate binding properties of versican. *J. Biol. Chem.* **267**(14): 10003-10010.

Leprini, A., G. Querze and L. Zardi (1994). Tenascin isoforms: possible targets for diagnosis and therapy of cancer and mechanisms regulating their expression. *Perspectives on Developmental Neurobiology* **2**(1): 117-123.

Levy, J. B., P. D. Canoll, O. Silvennoinen, G. Barnea, B. Morse, A. M. Honegger, J. T. Huang, L. A. Cannizzaro, S.-H. Park, T. Druck, et al. (1993). The cloning of a receptor-type protein tyrosine phosphatase expressed in the central nervous system. *J. Biol. Chem.* **268**(14): 10573-10581.

Lightner, V. A., F. Gumkowski, D. D. Bigner and H. P. Erickson (1989). Tenascin/hexabrachion in human skin: biochemical identification and localization by light and electron microscopy. *J. Cell Biol.* **108**: 2483-2493.

Lightner, V. A., J. R. Marks and S. S. McCachren (1994). Epithelial cells are an important source of tenascin in normal and malignant human breast tissue. *Exp. Cell Res.* **210**: 177-184.

Lightner, V. A., C. A. Slemp and H. P. Erickson (1990). Localization and quantitation of hexabrachion (tenascin) in skin, embryonic brain, tumors, and plasma. *Annals N.Y. Acad. Sci.* **580**: 260-275.

Limas, C., A. Bigler, R. Bair, P. Bernhart and P. Reddy (1993). Proliferative activity of urothelial neoplasms: comparison of BrdU incorporation, Ki67 expression, and nucleolar organiser regions. *J. Clin. Pathol.* **46**: 159-165.

Linnala, A., E. Balza, L. Zardi and I. Virtanen (1993). Human amnion epithelial cells assemble tenascins and three fibronectin isoforms in the extracellular matrix. *FEBS* **317**: 74-78.

Lotz, M. M., C. A. Burdsal, H. P. Erickson and D. R. McClay (1989). Cell adhesion to fibronectin and tenascin: quantitative measurements of initial binding and subsequent strengthening response. *J. Cell Biol.* **109**: 1795-1805.

Mackie, E. J. (1988). Induction of tenascin in healing wounds. *J. Cell Biol.* **107**(6): 2757-2767.

Mackie, E. J. (1994). Tenascin in connective tissue development and pathogenesis. *Perspectives on Developmental Neurobiology* **2**(1): 125-132.

Mackie, E. J., T. Scott-Burden, A. W. A. Hahn, F. Kern, J. Bernhardt, S. Regenass, A. Weller and F. R. Buhler (1992). Expression of tenascin by vascular smooth muscle cells. *Am. J. Pathol.* **141**(2): 377-388.

Mackie, E. J., R. P. Tucker, W. Halfter, R. Chiquet-EHrismann and H. H. Epperlein (1988). The distribution of tenascin coincides with pathways of neural crest cell migration. *Development* **102**: 237-250.

Makgoba, M. W., M. E. Sanders, G. E. Ginther Luce, M. L. Dustin, T. A. Springer, E. A. Clark, P. Mannoni and S. Shaw (1988). ICAM-1 a ligand for LFA-1-dependent adhesion of B, T and myeloid cells. *Nature* **331**: 86-88.

Margolis, R. U. and R. K. Margolis (1994). Aggrecan-versican-neurocan family proteoglycans. *Methods. Enzymol.* **245**: 105-126.

Marton, L. S., J. R. Gulcher and K. Stefansson (1989). Binding of hexabrachions to heparin and DNA. *J. Biol. Chem.* **264**(22): 13145-13149.

Matsumoto, K., Y. Saga, T. Ikemura, T. Sakakura and R. Chiquet-Ehrismann (1994). The distribution of tenascin-X is distinct and often reciprocal to that of tenascin-C. *J. Cell Biol.* **125**: 483-493.

McCourt, P. A. G., B. Ek, N. Forsberg and S. Gustafson (1995). Intercellular adhesion molecule-1 is a cell surface receptor for hyaluronan. *J. Biol. Chem.* **269**(48): 30081-30084.

Mercer, B. M., S. Sklar, A. Shariatmadar, M. S. Gillieson and M. E. D'Alton (1987). Fetal foot length as a predictor of gestational age. *Am. J. Obstet. Gynecol.* **156**: 350-355.

Messenger, A. G., K. Elliott, G. E. Westgate and W. T. Gibson (1991). Distribution of extracellular matrix molecules in human hair follicles. *Annals N.Y. Acad. Sci.* **642**: 253-262.

Moolenaar, C. E. C. K., E. J. Muller, D. J. Schol, C. G. Figdor, E. Bock, D. Bitter-Suermann and R. J. A. M. Michalides (1990). Expression of neural cell adhesion molecule-related sialoglycoprotein in small cell lung cancer and neuroblastoma cell lines H69 and CHP-212. *Cancer Res* **50**: 1102-1106.

Morris, W., Ed. (1969). The American Heritage Dictionary of the English Language. Palo Alto, Houghton Mifflin Company.

Murphy-Ullrich, J. E., V. A. Lightner, I. Aukhil, Y. Z. Yan, H. P. Erickson and M. Hook (1991). Focal adhesion integrity is downregulated by the alternatively spliced domain of human tenascin. *J. Cell Biol.* **115**: 1127-1136.

Murray, B. A. (1990). Cell-cell adhesion molecules in vertebrate development. *Sem. Devl Biol.* **1**: 3-14.

Nagase, H. (1994). Matrix Metalloproteinases. Extracellular Matix in the Kidney, Contrib. Nephrol. H. Koide and T. Hayashi. Basel, Karger. **107:** 85-93.

Nanney, L. B., C. M. Stoschek, J. King, L.E., R. A. Underwood and K. A. Holbrook (1990). Immunolocalization of epidermal growth factor in normal developing human skin. *J. Invest. Dermatol.* **94**: 742-748.

Natali, P. G., M. R. Nicotra, A. Bartolazzi, M. Mottolese, N. Coscia, A. Bigotti and L. Zardi (1990). Expression and production of tenascin in benign and malignant lesions of melanocyte lineage. *Int. J. Cancer* **46**: 586-590.

Nelson, W. J., E. M. Shore, A. Z. Wang and R. W. Hammerton (1990). Identification of a membrane-cytoskeletal complex containing the cell adhesion molecule uvomorulin (E-cadherin), ankyrin, and fodrin in Madin-Darby Canine Kidney epithelial cells. *J. Cell Biol.* **110**: 349-357.

Nicolo, G., S. Salvi, G. Oliveri, L. Borsi, P. Castellani and L. Zardi (1990). Expression of tenascin and of the ED-B containing oncofetal fibronectin isoform in human cancer. *Cell Diff. Dev.* **32**: 401-408.

Nies, D. E., T. J. Hemesath, J.-H. Kim, J. R. Gulcher and K. Stefansson (1991). The complete cDNA sequence of human hexabrachion (tenascin). *J. Biol. Chem.* **266**(5): 2818-2823.

Noveen, A., T. X. Jiang, S. A. Ting-Berreth and C. M. Chuong (1995). Homeobox genes Msx-1 and Msx-2 are associated with induction and growth of skin appendages. *J. Invest. Dermatol.* **104**(5): 711-719.

Oliver, R. F. (1967). Ectopic regeneration of whiskers in the hooded rat from implanted lengths of vibrissa follicle wall. *J. Embryol. Exp. Morph.* **17**: 27-34.

Oliver, R. F. (1968). The regeneration of vibrissae--a model for the study of dermal-epidermal interactions. Epithelial-Mesenchymal Interactions. R. Fleischmajer and R. E. Billingham. Baltimore, Williams & Wilkins Co.: 267-279; Chapter 18.

Pearson, C. A., D. Pearson, S. Shibahara, J. Hofsteenge and R. Chiquet-Ehrismann (1988). Tenascin: cDNA cloning and induction by TGF-B. *EMBO J.* 7(10): 2677-2981.

Perides, G., H. P. Erickson, F. Rahemtulla and A. Bignami (1993). Colocalization of tenascin with versican, a hylauronate-binding chondroitin sulfate proteoglycan. *Anat. Embryol.* **188**: 467-479.

Pinkus, H. (1958). Embryology of hair. The Biology of Hair Growth. W. Montagna and R. A. Ellis. New York, Academic Press.

Pog'any, G. and K. G. Vogel (1992). The interaction of decorin core protein fragments with type I collagen. *Biochem. Biophys. Res. Commun.* **189**(1): 165-172.

Prieto, A. L., G. M. Edelman and K. L. Crossin (1993). Multiple integrins mediate cell attachment to cytotactin/tenascin. *P.N.A.S.* **90**: 10154-10158.

Prieto, J., P. G. Beatty, E. A. Clark and M. Patarroyo (1988). Molecules mediating adhesion of T and B cells, monocytes and granulocytes to vascular endothelial cells. *Immunology* **63**: 631-637.

Rettig, W. J., H. P. Erickson, A. P. Albino and P. Garin-Chesa (1994). Induction of human tenascin (neuronectin) by growth factors and cytokines: cell type-specific signals and signalling pathways. *J. Cell Sci.* **107**: 487-497.

Riou, J.-F., D.-L. Shi, M. Chiquet and J.-C. Boucat (1990). Exogenous tenascin inhibits mesodermal cell migration during amphibian gastrulation. *Dev. Biol.* **137**: 305-317.

Rothlein, R., M. Czajkowski, M. M. O'Neill, S. D. Marlin, E. Mainolfi and V. J. Merluzzi (1988). Induction of intercellular adhesion molecule 1 on primary and continuous cell lines by pro-inflammatory cytokines. *J. Immunol.* **141**: 1665-1669.

Rutishauser, U. (1990). Neural cell adhesion molecule as a regulator of cell-cell interactions. Molecular Aspects of Development and Aging of the Nervous System. J. M. Lauder. New York, Plenum Press: 179-183.

Saga, Y., T. Tsukamoto, N. Jing, M. Kusakabe and T. Sakakura (1991). Murine tenascin: cDNA cloning, structure and temporal expression of isoforms. *Gene* **104**: 177-185.

Saga, Y., T. Yagi, Y. Ikawa, T. Sakakura and S. Aizawa (1992). Mice develop normally without tenascin. *Genes Dev* **6**: 1821-1831.

Sage, E. H. and P. Bornstein (1991). Extracellular proteins that modulate cell-matrix interactions. *J. Biol. Chem.* **266**(23): 14831-14834.

Sakai, T., H. Kawakatsu, N. Hirota, T. Yokoyama, T. Takaoka, T. Sakakura and M. Saito (1993). Tenascin expression *in vitro* and *in vivo:* comparison between epithelial and nonepithelial rat cell lines. *Exp. Cell Res.* **206**: 244-254.

Sambrook, J., E. F. Fritsch and T. Maniatis (1989). Molecular Cloning: A Laboratory Manual. Cold Spring Harbor, Cold Spring Harbor Laboratory.

Savani, R. C., C. Wang, B. Yang, S. Zhang, M. G. Kinsella, T. N. Wight, R. Stern, D. M. Nance and E. A. Turley (1995). Migration of bovine aortic smooth muscle cells after wounding injury. The role of hyaluronan and RHAMM. *J. Clin. Invest.* **95**(3): 1158-1168.

Schaeren-Wiemers, N. and A. Gerfin-Moser (1993). A single protocol to detect transcripts of various types and expression levels in neural tissue and cultured cells: in situ hybridization using digoxigenin-labelled cRNA probes. *Histochemistry* **100**(6): 431-440.

Schalkwijk, J., P. M. Steijlen, I. M. J. J. van Vlijmen-Willems, B. Oosterling, E. J. Mackie and A. A. Verstraeten (1991). Tenascin expression in human dermis is related to epidermal proliferation. *Am. J. Path.* **139**: 1143-1150.

Schalkwijk, J., I. van Vlijmen, B. Oosterling, C. Perret, R. Koopman, J. van den Born and E. J. Mackie (1991). Tenascin expression in hyperproliferative skin diseases. *Br. J. Dermatol.* **124**: 13-20.

Schluter, C., M. Duchrow, C. Wohlenberg, M. H. G. Becker, G. Key, H.-D. Flad and J. Gerdes (1993). The cell proliferation-associated antigen of antibody Ki-67: a very large, ubiquitous nuclear protein with numerous repeated elements, representing a new kind of cell cycle-maintaining proteins. *J. Cell Biol.* **123**(3): 513-522.

Schonherr, E., H. T. Jarvelainen, L. J. Sandell and T. N. Wight (1991). Effects of platelet-derived growth factor and transforming growth factor-β 1 on the synthesis of a large versican-like chondroitin sulfate proteoglycan by arterial smooth muscle cells. *J. Biol. Chem.* **266**: 17640-17647.

Sengel, P. (1976). Morphogenesis of Skin. Cambridge, Cambridge University Press.

Sengel, P. (1983). Epidermal-dermal interactions during formation of skin and cutaneous appendages. Biochemistry and Physiology of the Skin. L. A. Goldsmith. New York, Oxford University Press: 102-131.

Sengel, P. (1990). Pattern formation in skin development. *Int. J. Dev. Biol.* **34**: 33-50.

Shames, R. B., A. G. Jennings and R. H. Sawyer (1991). Expression of the cell adhesion molecules, L-CAM and N-CAM during avian scale development. *J. Exp. Zool.* **257**: 195-207.

Shames, R. B., A. G. Jennings and R. H. Sawyer (1991). The initial expression and patterned appearance of tenascin in scutate scales is absent from the dermis of the scaleless (sc/sc) chicken. *Devl. Biol.* **147**: 174-186.

Shepard, T. H. (1975). Normal and abnormal growth patterns. Growth and development of the human embryo and fetus. Endocrine and Genetic Dieseases of Childhood and Adolescence. L. I. Gardner. Philadelphia, W.B. Saunders Co.: 1-8.

Shinomura, T., K. L. Jensen, M. Yamagata, K. Kimata and M. Solursh (1990). The distribution of mesenchyme proteoglycan (PG-M) during wing bud outgrowth. *Anat. Embryol.* **181**: 227-233.

Siri, A., B. Carnemolla, M. Saginati, A. Leprini, G. Casari, F. Baralle and L. Zardi (1991). Human tenascin: primary structure, pre-mRNA splicing patterns and localization of the epitopes recognized by two monoclonal antibodies. *Nucl. Acids Res.* **19**(3): 525-531.

Siri, A., V. Knauper, N. Veirana, F. Caocci, G. Murphy and L. Zardi (1995). Different susceptibility of small and large human tenascin-C isoforms to degradation by matrix metalloproteinases. *J. Biol. Chem.* **270**(5): 8650-8654.

Smith, L. T., K. A. Holbrook and J. A. Madri (1986). Collagen types I, III, and V in human embryonic and fetal skin. *Am. J. Anat.* **175**: 507-521.

Sriramarao, P. and M. A. Bourdon (1993). A novel tenascin type III repeat is part of a complex of tenascin mRNA alternative splices. *Nucl. Acids Res.* **21**(1): 163-168.

Sriramarao, P., M. Mendler and M. A. Bourdon (1993). Endothelial cell attachment and spreading on human tenascin is mediated by $\alpha 2\beta 1$ and $\alpha\varpi\beta 3$ integrins. *J. Cell Sci.* **105**: 1001-1012.

Takeichi, M. (1988). The cadherins: cell-cell adhesion molecules controlling animal morphogenesis. *Development* **102**: 639-655.

Tan, S.-S., K. L. Crossin, S. Hoffman and G. M. Edelman (1987). Asymmetric expression in somites of cytotactin and its proteoglycan ligand is correlated with neural crest cell distribution. *Proc. Natl. Acad. Sci. U.S.A.* **84**: 7977-7981.

Taylor, H. C., V. A. Lightner, W. F. J. Beyer, D. McCaslin, G. Briscoe and H. P. Erickson (1989). Biochemical and structural studies of tenascin/hexabrachion proteins. *J. Cell. Biochem.* **41**: 71-90.

Thesleff, I., E. Mackie, S. Vainio and R. Chiquet-Ehrismann (1987). Changes in the distribution of tenascin during tooth development. *Development* **101**: 289-296.

Thesleff, I., A. Vaahtokari and A.-M. Partanen (1995). Regulation of organogenesis. Common molecular mechanisms regulating the development of teeth and other organs. *Int. J. Dev. Biol.* **39**: 35-50.

Towbin, H., T. Stachelin and J. Gordon (1979). Electrophoretic transfer of proteins from polyacrylamide gels to nitrocellulose sheets: procedure and some applications. *Proc. Natl. Acad. Sci. U.S.A.* **76**: 4350-4354.

Tucker, R. P. (1991). The sequential expression of tenascin mRNA in epithelium and mesenchyme during feather morphogenesis. *Roux's Arch. Devl. Biol.* **200**: 108-112.

Underhill, C. (1992). CD44: the haluronan receptor. *J Cell Sci* **103**: 293-298.

Underhill, C. B. (1993). Hyaluronan is inversely correlated with the expression of CD44 on the dermal condensation of the embryonic hair follicle. *J. Invest. Dermatol.* **101**: 820-826.

Vainio, S. and I. Thesleff (1992). Sequential induction of syndecan, tenascin and cell proliferation associated with mesenchymal cell condensation during early tooth development. *Differentiation* **50**: 97-105.

van Weerden, W. M., E. P. C. M. Moerings, A. van Kreuningen, F. H. de Jong, G. J. van Steenbrugge and F. H. Schroder (1993). Ki-67 expression and BrdUrd incorporation as markers of proliferative activity in human prostate tumour models. *Cell Prolif.* **26**: 67-75.

Vaughan, L., S. Huber, M. Chiquet and K. H. Winterhalter (1987). A major, six-armed glycoprotein from embryonic cartilage. *EMBO J.* **6**(2): 349-353.

Vaughan, L., A. H. Zisch, P. Weber, L. D'Allesandri, P. Ferber, G. David, D. R. Zimmermann and K. H. Winterhalter (1994). Cellular receptors for tenascin. *Extracellular Matrix in the Kidney, Contrib Nephrol* **107**: 80-84.

Ventimiglia, J. B., C. J. Wikstrand, L. E. Ostrowski, M. A. Bourdon, V. A. Lightner and D. D. Bigner (1992). Tenascin expression in human glioma cell lines and normal tissues. *J Neuroimmunol* **36**: 41-55.

Voss, B., Glossl, Z. Cully and H. Kresse (1986). Immunocytochemical investigation on the distribution of small chodroitin sulfate-dermatan sulfate proteoglycan in the human. *J. Histochem. Cytochem.* **34**: 1013-1019.

Weber, P., D. R. Zimmermann, K. H. Winterhalter and L. Vaughan (1995). Tenascin-C binds heparin by its fibronectin type III domain five. *J. Biol. Chem.* **270**(9): 4619-4623.

Weinacker, A., R. Ferando, M. Elliott, J. Hogg, J. Balmes and D. Sheppard (1995). Distribution of integrins alpha v beta 6 and alpha 9 beta 1 and their known ligands, fibronectin and tenascin, in human airways. *Am. J. Respir. Cell Mol. Biol.* **12**(5): 547-556.

Weller, A., S. Beck and P. Ekblom (1991). Amino acid sequence of mouse tenascin and differential expression of two tenascin isoforms during embryogenesis. *J. Cell Biol.* **112**: 355-362.

Wessells, N. K. (1965). Morphology and proliferation during early feather development. *Devl. Biol.* **12**: 131-153.

Wessells, N. K. and K. D. Roessner (1965). Nonproliferation in dermal condensations of mouse vibrissae and pelage hairs. *Devl. Biol.* **12**: 419-433.

Westgate, G. E., A. G. Messenger, L. P. Watson and W. T. Gibson (1991). Distribution of proteoglycans during the hair growth cycle in human skin. *J. Invest. Dermatol.* **96**: 191-195.

Wheelock, M. J., C. A. Buck, K. B. Bechtol and C. H. Damsky (1987). Soluble 80-kd fragment of Cell-CAM 120/80 disrupts cell-cell adhesion. *J. Cell. Biochem.* **34**: 187-202.

Wight, T. N., S. Potter-Perigo and T. Aulinskas (1989). Proteoglycans and vascular cell proliferation. *Am. Rev. Respir. Dis.* **140**: 1132-1135.

Willing, M. C., D. H. Cohn, B. Starman, K. A. Holbrook, C. R. Greenberg and P. H. Byers (1988). Heterozygosity for a large deletion in the alpha 2(I) collagen gene has a dramatic effecton type I collagen secretion and produces perinatal lethal osteogenesis imperfecta. *J. Biol. Chem.* **263**: 8398-8404.

Wolpert, L. (1994). Positional information and pattern formation in development. *Dev. Genet.* **15**(6): 485-490.

Yamagata, M., S. Saga, M. Kato, M. Bernfield and K. Kimata (1993). Selective distribution of proteoglycans and their ligands in pericellular matrix of cultured fibroblasts. *J. Cell Sci.* **106**: 55-65.

Yamagata, M., S. Suzuki, S. K. Akiyama, K. M. Yamada and K. Kimata (1989). Regulation of cell-substrate adhesion by proteoglycans immobilized on extracellular substrates. *J. Biol. Chem.* **264**(14): 8012-8018.

Yeo, T.-K., S. Macfarlane and T. N. Wight (1992). Characterization of a chondroitin sulfate proteoglycan synthesized by monkey arterial smooth muscle cells in vitro. *Connect. Tissue Res.* **27**: 265-277.

Yokosaki, Y., E. L. Palmer, A. L. Prieto, K. L. Crossin, M. A. Bourdon, R. Pytela and D. Sheppard (1994). The integrin alpha 9 beta 1 mediates cell attachment to a non-RGD site in the third fibronectin type III repeat of tenascin. *J. Biol. Chem.* **269**(43): 26691-6.

Young, S. L., L.-Y. Chang and H. P. Erickson (1994). Tenascin-C in rat lung: distribution, ontogeny and role in branching morphogenesis. *Dev. Biol.* **161**: 615-625.

Zagzag, D., D. R. Friedlander, D. C. Miller, J. Dosik, J. Cangiarella, M. Kostianovsky, H. Cohen, M. Grumet and M. A. Greco (1995). Tenascin Expression in Astrocytomas Correlates with Angiogenesis. *Cancer Res.* **55**: 907-914.

Zako, M., T. Shinomura, M. Ujita, K. Ito and K. Kimata (1995). Expression of PG-M(V3), an alternatively spliced form of PG-M without a chondroitin sulfate attachment region in mouse and human tissues. *J. Biol. Chem.* **270**(8): 3914-3918.

Zimmermann, D. R., M. T. Dours-Zimmermann, M. Schubert and L. Bruckner-Tuderman (1994). Versican is expressed in the proliferating zone in the epidermis and in association with the elastic network of the dermis. *J. Cell Biol.* **124**(5): 817-825.

Zimmermann, D. R. and E. Ruoslahti (1989). Multiple domains of the large fibroblast proteoglycan, versican. *EMBO J.* **8**(10): 2975-2981.

# ELIZABETH DANFORD KAPLAN

## PERSONAL

Birthdate: March 29, 1960 — Birthplace: Racine, WI
Married to John F. Kaplan, LCDR, United States Coast Guard

## EDUCATION

University of Washington, Seattle, WA — 1990 to 1996
Department of Biological Structure
Uniformed Services University of the Health Sciences (USUHS) — 1988-1990
Bethesda, MD
Department of Anatomy
Mount Holyoke College, South Hadley, MA — May 1982
A.B. Degree in Mathematics

## EXPERIENCE

**University of Washington** — 1990
Teaching Assistant: Microscopic Anatomy
**USUHS** — 1989-1990
Teaching Assistant: Gross Anatomy
Teaching Assistant: Microscopic Anatomy
**USUHS** — 1986-1988
Research associate: worked with Dr. David Beebe to screen chicken genomic and cDNA libraries for IGF-1 which had been implicated in avian lens development..
**Massachusetts Institute of Technology** — 1984-1986
Research Technician: Worked with Dr . Roland Siezen in the laboratory of Dr. George Benedek to develop liquid chromatographic procedures to chronicle ontogenetic and pathologic changes in crystallin proteins from human, bovine, rat, dogfish and codfish lenses.
**University of Washington** — 1982-1984
Research Technician: Worked with Dr. John Clark to analyze calcium-induced cataract formation in bovine and rabbit lenses.
**Université de Paris-sud, Orsay, France** — Jan to April, 1984
Researcher: Worked with Drs. Mireille Delaye, Anette Tardieu and John Clark as part of an international collaborative project researching structural components of calcium-induced cataracts in bovine lenses. Funded in part by National Institutes of Health.

## AWARDS

Molecular and Cellular Biology Training Grant #GM-07270-20 — 9/15/93 to 12/15/95
Dermatology Training Grant NIH#2T32AR07019-16 — 5/1/91 to 4/30/92

## PUBLICATIONS

Kaplan, ED and Holbrook, KA, (1994) Dynamic Expression Patterns of Tenascin, Proteoglycans and Cell Adhesion Molecules During Human Hair Follicle Morphogenesis. Dev Dynamics 199: 141-155.

Holbrook, KA, Smith, LT, Kaplan, ED, Minami, SI, Hebert, GP and Underwood, RA (1993) The Expression of Morphogens During Human Follicle Development *in vivo* and a Model for Studying Follicle Morphogenesis *in vitro*. J Invest Dermatol *101*: 39S-49S.

Thomson, JA, Siezen, RJ, Kaplan, ED, Messmer, M and Chakrabarti, B (1989) Comparative Studies of $\beta_s$-crystallins from human, bovine, rat and rabbit lenses. Cur Eye Res 8: 139-149.

Siezen, RJ, Coppin, CM, Kaplan, ED, Dwyer, D and Thomson, JA (1989) Oxidative

Modifications to Crystallins Induced in Calf Lenses In Vitro by Hydrogen Peroxide. Exp Eye Res 48: 225-235.

Siezen, RJ and Kaplan, ED (1988) Optimal resolution of eye lens γ-crystallins by cation-exchange HPLC on Synchropak CM300. J Chromatog 444: 239-250.

Clark, JI, Danford-Kaplan, ME and Delaye, M (1988) Calcium Decreases Transparency of Homogenate from Lens Cortex and has no Effect on Nucleus. Exp Eye Res 47: 447-455.

Siezen, RJ, Wu, E, Kaplan, ED, Thomson, JA and Benedek, GB (1988) Rat Lens γ-Crystallins. Characterizations of the Six Gene Products and their Spatial and Temporal Distribution Resulting from Differential Synthesis. J Mol Biol 199: 475-490.

Siezen, RJ, Thomson, JA, Kaplan, ED and Benedek, GB (1987) Human lens γ-crystallins: isolation, identification and characterization of the expressed gene products. Proc Natl Acad Sci. USA 84: 6088-6092.

Delaye, M, Danford-Kaplan, ME, Clark, JI, Krop, B, Gulik-Drzywicki, T and Tardieu, A (1987) Effect of Calcium on the Calf Lens Cytoplasm. Exp Eye Res 44: 601-616.

Siezen, RJ, Kaplan, ED and Anello, RD (1985) Superior resolution of γ-crystallins from microdissected eye lens by cation-exchange high-performance liquid chromatography. Biochem Biophys Res Comm 127: 153-160.

Danford, ME and Clark, JI (1985) Low temperature and acrylamide inhibit lens opacification caused by calcium. Ophthal Res 17: 246-250.

**ABSTRACTS**

Kaplan, ED and Wight, TN (1994) Differential expression of TN isoforms during human skin development. ASCB Abstracts 5 (Suppl):178a.

Kaplan, ED and Holbrook, KA (1992) Tenascin and chondroitin sulfate proteoglycans undergo developmental changes during human hair follicle morphogenesis. Soc Dev Biol, Molecular Basis of Morphogenesis, 51st Annual Symposium: 10.

Kaplan, ED and Holbrook, KA (1992) Patterned distribution of tenascin and proteoglycans during human hair follicle morphogenesis. J Cellular Biochem 16F (Suppl): 187.

Kaplan, ED, Underwood, RA and Holbrook, KA (1991) Cell aggregation in follicle morphogenesis during fetal skin development. Anat Rec 229: 47a.

Kaplan, ED and Siezen, RJ (1988) Optimal resolution of eye lens γ-crystallins by cation-exchange HPLC on Synchropak CM300. Invest Ophthalmol Vis Sci 29: 185.

Beebe, D, St.John, C, Gross, A, Cerrelli, S, Li, X and Kaplan, E (1988) Lentropin activity is present in mammalian vitreous humor. Invest Ophthalmol Vis Sci 29: 425.

Beebe, DC, Parmalee, JT, Cerrelli, S and Kaplan, ED (1987) Intra- and extracellular control of lens fiber cell differentiation in the chicken embryo. Invest Ophthalmol Vis Sci 28: 13.

Siezen, RJ, Hom, C, Kaplan, ED, Thomson, JA and Benedek, GB (1987) Heterogeneity of γ-crystallins from spiny dogfish. Invest Ophthalmol Vis Sci 28: 387.

Thomson, JA, Kaplan, ED, Wu, E, Siezen, RJ and Benedek, GB (1986) Missing link between phylogeny and ontogeny of the monomeric crystallins. Invest Ophthalmol Vis Sci 27: 214.

Coppin, CM, Kaplan, ED, Thomson, JA, Siezen, RJ and Benedek, GB (1986) Specificity of initial hydrogen peroxide damage to crystallins in calf lenses. Invest Ophthalmol Vis Sci 27: 278.

Clark, JI and Danford, ME (1984) Calcium decreases transparency of homogenate from lens cortex and has no effect on nucleus. Invest Ophthalmol Vis Sci 25: 48.

Danford, ME and Clark, JI (1984) Calcium induced opacification in lens cell homogenate. Anat Rec 208: 41A-42B.

**MEMBERSHIPS**

Society of Investigative Dermatology
American Association for the Advancement of Science